

DTIC.

**DEVELOPMENT OF AN  
INUNDATION MAPPING CAPABILITY USING  
HIGH RESOLUTION FINITE ELEMENT MODELLING**

by

**C.SMITH, P.D.BATES and M.G.ANDERSON**

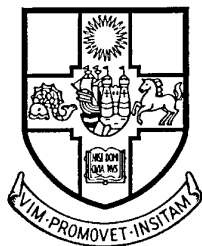
**Final Technical Report  
May 1997**

United States Army

European Research Office of the U.S.Army  
London, England

CONTRACT NUMBER: N681710-94-C-9109  
R & D 7301-EN-01

Professor M.G.Anderson



University of Bristol, England

DTIC QUALITY INSPECTED 4

Approved for Public Release: distribution unlimited

19970728 164

## Acknowledgements

The authors acknowledge support from the USACE Remote Sensing and Geographic Information Systems Center, CRREL, New Hampshire, in particular the specific contribution from Dr. Tim Pangburn and Dr. Ike McKim.

The majority of this project was undertaken when Dr. Ed Link was Director of CRREL and his support and encouragement are acknowledged with gratitude.

**Table of Contents**

Acknowledgements	i
Table of Contents	ii
List of Figures	iv
List of Tables	vii
<b>1 INTRODUCTION</b>	<b>1</b>
1.1 OBJECTIVES OF THE STUDY	1
1.2 BACKGROUND INFORMATION	1
1.3 KEY FEATURES OF THE STUDY	3
<b>2 THE TELEMAC MODELLING SYSTEM</b>	<b>4</b>
2.1 TELEMAC-2D	6
2.1.1 SHALLOW WATER EQUATIONS	6
2.1.2 SOLVING THE EQUATIONS	7
2.1.3 BOUNDARY CONDITIONS	9
2.1.4 PHYSICAL PARAMETER OPTIONS	9
2.1.4.1 Bottom Friction	9
2.1.4.2 Turbulence Representation	10
2.1.4.3 Other Physical Parameters	10
2.1.5 WETTING AND DRYING ZONES	10
2.2 POST-PROCESSING OF RESULTS	11
2.3 SUMMARY OF THE TELEMAC-2D SYSTEM	11
<b>3 THE MISSOURI RIVER MODEL</b>	<b>13</b>
3.1 PRODUCING THE FINITE ELEMENT MESH	13
3.2 BATHYMETRIC DATA	15
3.3 BOUNDARY CONDITION SPECIFICATION	16
3.4 PHYSICAL PARAMETER SPECIFICATION	16
3.5 CREATING THE INITIAL CONDITIONS	16
3.6 THE MODEL RUN	16
3.7 SUMMARY OF MODEL APPLICATION	17
<b>4 SENSITIVITY ANALYSIS</b>	<b>18</b>
4.1 BACKGROUND TO THE SENSITIVITY ANALYSIS	18
4.2 RESULTS OF THE SENSITIVITY ANALYSIS	20
4.3 CONCLUSIONS OF THE SENSITIVITY ANALYSIS	26

<b>5 COMPARISON OF MODEL PREDICTIONS TO OBSERVED DATA</b>	<b>27</b>
<b>5.1 EVENT 1 (6TH JUNE 1994)</b>	<b>29</b>
5.1.1 INTERNAL STAGE DATA	29
5.1.2 SATELLITE IMAGERY	31
5.1.3 SUMMARY OF EVENT 1	40
<b>5.2 EVENT 2 (25TH JUNE 1994)</b>	<b>40</b>
<b>5.3 EVENT 3 (26TH JUNE 1984)</b>	<b>41</b>
<b>5.4 EVENT 4 (8TH FEBRUARY 1991)</b>	<b>50</b>
<b>5.5 EVENT 5 (13TH - 14TH JUNE 1994)</b>	<b>54</b>
<b>5.6 SUMMARY OF THE COMPARISON TO OBSERVED DATA</b>	<b>56</b>
<b>6 MESH RESOLUTION COMPARISON</b>	<b>57</b>
6.1 COMPARISON TO OBSERVED DATA	58
6.2 SUMMARY	65
<b>7 BATHYMETRIC DATA REQUIREMENTS</b>	<b>66</b>
7.1 COMPARISON TO OBSERVED DATA	67
7.2 SUMMARY	67
<b>8 CONCLUDING REMARKS</b>	<b>74</b>
<b>9 REFERENCES</b>	<b>76</b>

## List of Figures

Figure 1-1a) Location and (b) detail of the study reach of the Missouri River, USA. The modelled reach is from Gavins Point Dam to Maskell and includes the gauging stations at Yankton and Gayville.	2
Figure 2-1 The TELEMAC-2D modelling system (after Hervouet and Lang, 1995).	5
Figure 2-2 The geometry notation used in TELEMAC-2D (After Hervouet and Van Haren, 1995).	8
Figure 2-3 Partially dry elements: (a) the real situation, (b) element remaining fully wet introducing spurious momentum terms, (c) element exclusion method and (d) TELEMAC-2D method keeping the element partially dry (after Price, 1997).	12
Figure 3-1 The boundary delineation of the Missouri River model.	13
Figure 3-2 Finite element meshes of the Missouri River from Gavins Point Dam to Maskell, (a) low resolution Mesh 1 and (b) high resolution Mesh 2.	14
Figure 3-3 An example portion of the models bathymetric representation. This section is immediately upstream of Yankton.	15
Figure 4-1 Inundation Extent change with (a) bed friction and (b) velocity diffusivity for both high and low resolution meshes.	20
Figure 4-2 Sensitivity analysis plots for water surface against bed friction at (a) Yankton and (b) Gayville and against velocity diffusivity at (c) Yankton and (d) Gayville.	22
Figure 4-3 Change in velocity at Gayville as (a) bed friction and (b) velocity diffusivity varies for both high and low resolution meshes.	23
Figure 4-4 Difference surfaces created by subtracting the results of the lowest friction run ( $n=0.01$ ) from the highest friction run ( $n=0.04$ ) for (a) water depth and (b) velocity.	24
Figure 4-5 Sensitivity analysis plots showing results for all node points for differences between high and low friction runs for (a) velocity difference against water depth in the low friction run and (b) velocity difference against water depth difference.	26
Figure 5-1 Linear sensitivity of water surface elevation to bed friction at the two gauge sites, Yankton and Gayville.	29
Figure 5-2 Downstream section of the reach showing the elevations of the river bed, observed water surface and predicted water surface (using a bed friction of $n = 0.025$ ) at the 4 gauges.	30
Figure 5-3 Locations of the six sites to be used in the comparison of model predictions with satellite imagery.	32
Figure 5-4a Comparison of Landsat TM image and 4 alternative model predictions with different bed friction (Manning's 'n') values at site 1 for event 1.	34
Figure 5-4b Comparison of Landsat TM image and 4 alternative model predictions with different bed friction (Manning's 'n') values at site 2 for event 1.	35
Figure 5-4c Comparison of Landsat TM image and 4 alternative model predictions with different bed friction (Manning's 'n') values at site 3 for event 1.	36
Figure 5-4d Comparison of Landsat TM image and 4 alternative model predictions with different bed friction (Manning's 'n') values at site 4 for event 1.	37
Figure 5-4e Comparison of Landsat TM image and 4 alternative model predictions with different bed friction (Manning's 'n') values at site 5 for event 1.	38
Figure 5-4f Comparison of Landsat TM image and 4 alternative model predictions with different bed friction (Manning's 'n') values at site 6 for event 1.	39
Figure 5-5 An overlay of the model prediction of flow field boundary onto the Landsat TM image for a region around Goat Island (including sites 5 and 6) for event 1.	40
Figure 5-6a Comparison of Landsat TM image and 4 alternative model predictions with different bed friction (Manning's 'n') values at site 1 for event 3.	43
Figure 5-6b Comparison of Landsat TM image and 4 alternative model predictions with different bed friction (Manning's 'n') values at site 2 for event 3.	44

Figure 5-6c Comparison of Landsat TM image and 4 alternative model predictions with different bed friction (Manning's 'n') values at site 3 for event 3.	45
Figure 5-6d Comparison of Landsat TM image and 4 alternative model predictions with different bed friction (Manning's 'n') values at site 4 for event 3.	46
Figure 5-6e Comparison of Landsat TM image and 4 alternative model predictions with different bed friction (Manning's 'n') values at site 5 for event 3.	47
Figure 5-6f Comparison of Landsat TM image and 4 alternative model predictions with different bed friction (Manning's 'n') values at site 6 for event 3.	48
Figure 5-7 Validation of the flow processes occurring around the James River Island during event 3. The satellite image (a) shows the flow from the James River splitting around the island and the model simulation of this event (b) agrees with this.	49
Figure 5-8 Comparison of SPOT image to model predictions for event 4 at (a) site 2 and (b) site 3.	51
Figure 5-8 Comparison of SPOT image to model predictions for event 4 at (c) site 4 and (d) site 6.	52
Figure 5-8 Comparison of SPOT image to model predictions for event 4 at (e) site 5.	53
Figure 5-9 Observed and predicted, for several bed friction values, water surface elevations at (a) Yankton and (b) Gayville over the duration of dynamic event 5.	55
Figure 6-1 Comparison of a section of the model bathymetries in the (a) low and (b) high resolution meshes.	57
Figure 6-2a Comparison of Landsat TM image to 4 alternative model predictions with different values of bed friction (Manning's 'n') on the high resolution mesh (mesh 2) for event 1 at site 1.	59
Figure 6-2b Comparison of Landsat TM image to 4 alternative model predictions with different values of bed friction (Manning's 'n') on the high resolution mesh (mesh 2) for event 1 at site 2.	60
Figure 6-2c Comparison of Landsat TM image to 4 alternative model predictions with different values of bed friction (Manning's 'n') on the high resolution mesh (mesh 2) for event 1 at site 3.	61
Figure 6-2d Comparison of Landsat TM image to 4 alternative model predictions with different values of bed friction (Manning's 'n') on the high resolution mesh (mesh 2) for event 1 at site 4.	62
Figure 6-2e Comparison of Landsat TM image to 4 alternative model predictions with different values of bed friction (Manning's 'n') on the high resolution mesh (mesh 2) for event 1 at site 5.	63
Figure 6-2f Comparison of Landsat TM image to 4 alternative model predictions with different values of bed friction (Manning's 'n') on the high resolution mesh (mesh 2) for event 1 at site 6.	64
Figure 7-1 Impact of degrading the number of cross sections used on the model bathymetry. The spacing degrades from 150 m to 1200 m across the range illustrated.	66
Figure 7-2a Comparison of the Landsat TM image to model predictions with the 4 levels of model bathymetry used for event 1 at site 1. The bathymetries were created by varying the spacing of cross sections used from 150 m to 1200 m.	68
Figure 7-2b Comparison of the Landsat TM image to model predictions with the 4 levels of model bathymetry used for event 1 at site 2. The bathymetries were created by varying the spacing of cross sections used from 150 m to 1200 m.	69
Figure 7-2c Comparison of the Landsat TM image to model predictions with the 4 levels of model bathymetry used for event 1 at site 3. The bathymetries were created by varying the spacing of cross sections used from 150 m to 1200 m.	70
Figure 7-2d Comparison of the Landsat TM image to model predictions with the 4 levels of model bathymetry used for event 1 at site 4. The bathymetries were created by varying the spacing of cross sections used from 150 m to 1200 m.	71

*Figure 7-2e Comparison of the Landsat TM image to model predictions with the 4 levels of model bathymetry used for event 1 at site 5. The bathymetries were created by varying the spacing of cross sections used from 150 m to 1200 m.* \_\_\_\_\_ 72

*Figure 7-2f Comparison of the Landsat TM image to model predictions with the 4 levels of model bathymetry used for event 1 at site 6. The bathymetries were created by varying the spacing of cross sections used from 150 m to 1200 m.* \_\_\_\_\_ 73

## List of Tables

<i>Table 1-1 Gauge station location and data availability.</i>	<i>1</i>
<i>Table 3-1 Comparison of the attributes of the two meshes used to model the Missouri River in this report.</i>	<i>14</i>
<i>Table 4-1 The simulations carried out for the sensitivity analysis. The figures in bold are the parameter values held constant whilst the other is varied.</i>	<i>19</i>
<i>Table 4-2 Values of Manning's n for various channel types (after Bathurst, 1988).</i>	<i>19</i>
<i>Table 5-1 The flow records to be simulated.</i>	<i>28</i>
<i>Table 5-2 Comparison of observed and predicted water surface elevations at Yankton and Gayville on 8th February 1991.</i>	<i>50</i>
<i>Table 5-3 Observed and predicted changes in water surface elevation over dynamic event 5.</i>	<i>54</i>
<i>Table 6-1 Comparison of the calibrated results from the two meshes.</i>	<i>58</i>
<i>Table 7-1 Water surface elevations at Yankton and Gayville for simulations with the various levels of bathymetric data supplied to the model.</i>	<i>67</i>



## **1. Introduction**

### **1.1 Objectives of the study**

- *To produce a state of the art numerical model of a large reach of the Missouri River, capable of simulating high resolution spatially/temporally distributed results of water depth and velocity.*
- *To investigate model behaviour through a sensitivity analysis.*
- *To compare model predictions to multiple types of measured data, internal to the model domain, in order to assess model performance and the utility of the validation data.*
- *To investigate the impact of varying levels of bathymetric data and mesh resolutions on the model predictions.*

### **1.2 Background Information**

The reach of the Missouri River being used for this modelling study is that from Gavins Point Dam, South Dakota, to the gauging station at Maskell, Nebraska (Figure 1.1). The reach covers river miles 811 to 776 making it 35 miles or 55 km long. The channel varies in width between 300m and 1200m. The channel slope is very low, dropping only about 12 metres along its 55 km length, giving a gradient of 0.02%. The bed material in this channel is sand which is fairly mobile but the channel banks have been strengthened or stabilised along much of the reach. There are several islands along the reach several of which are permanent. There is one major tributary, the James River, that joins the main stem at river mile 800 adjacent to the James River Island.

The flow out of Gavins Point Dam is regulated to minimise the risk of flooding downstream, hence the reach being modelled is very unlikely to attain out of bank conditions. The flow in the James River is however naturally variable. The model of this system can therefore remain as channel only. River flow data is available at several points along the reach on an hourly basis. Table 1.1 shows the data availability and gauge locations (also Figure 1.1).

**Table 1-1 Gauge station location and data availability.**

Gauging Station	Distance from top of reach (km)	Data Available
Gavins Point Dam, SD.	0	Flow rate
Yankton, SD.	7.5	Flow rate and Stage
Gayville, SD.	21.5	Stage
Maskell, Neb.	55	Stage
Scotland, SD.	53 km up James River from confluence	Flow rate and Stage

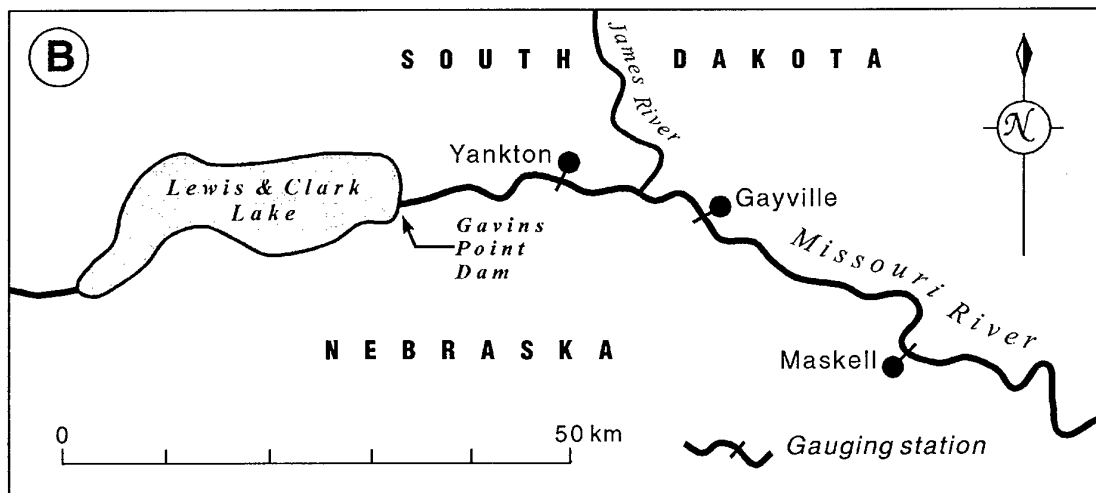
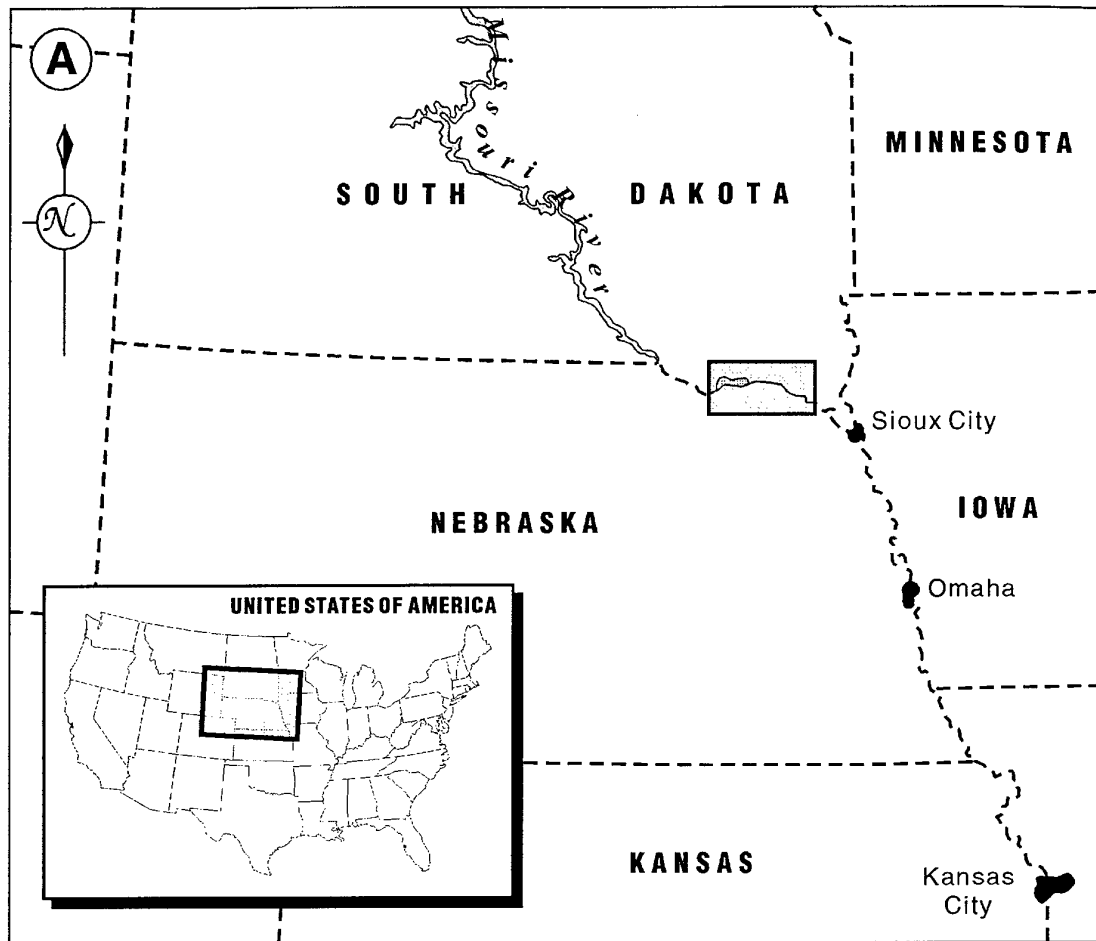


Figure 1-1a) Location and (b) detail of the study reach of the Missouri River, USA. The modelled reach is from Gavins Point Dam to Maskell and includes the gauging stations at Yankton and Gayville.

The flow from the James River gauge at Scotland, South Dakota, is routed using a simple one-dimensional kinematic wave model to the required location on the main model input boundary when necessary.

The hydraulic model used in this study is TELEMAC-2D. This is a high resolution space/time distributed hydraulic model using finite element methodology. The model is potentially capable of fulfilling all the objectives of this study. The model is described in some detail in section 2.

### **1.3 Key Features of the study**

- *The application of a state of the art two-dimensional finite element code for modelling large scale fluvial hydraulics on the Missouri River.*
- *The use of a high resolution model, in both space and time, along with wetting and drying algorithms for representing moving flow field boundaries allows dynamic inundation predictions.*
- *For the first time model predictions are validated on this scale in both time and space using multiple data sources. The data sources are internal stage data at two sites, supplied by the USACE Missouri River District (MRD), and satellite imagery, supplied by the Remote Sensing and Geographic Information Systems Center at USACE Cold Regions Research and Engineering Laboratory (CRREL).*
- *The strength of model validation is graded depending on the data source and model prediction.*
- *The influence of bathymetric data on the model predictions is studied for its potential in aiding future data collection strategy.*

## **2. The TELEMAC modelling system**

The TELEMAC system has been developed by the Département Laboratoire National d'Hydraulique (LNH) at Electricité de France, Direction des Études et Recherches (EDF-DER). LNH was formed in 1946 to undertake studies for EDF's hydroelectric power projects and to solve the hydraulic engineering problems of the Maritime Ports and Waterways Authority. Since 1965 the role of LNH has changed somewhat. About 70% of LNH's work is now directly for the benefit of EDF, split between hydraulics inside power station machinery and the study of environmental problems in rivers, seas and the atmosphere brought about through the siting of such plants. The rest of LNH's work is on behalf of other organisations.

The TELEMAC system therefore follows a line of hydraulic simulation codes originating from LNH for the study of environmental problems, such as flooding resulting from a dam break or thermal emission into a river or estuary. TELEMAC was developed from the ULYSSE code, a 2D finite difference system (Ulysses being the father of Telemachus in Greek mythology). TELEMAC is now in its second four year development period, each period having a budget of 118 million francs (Hardy, 1997). TELEMAC is a general purpose code that is applicable to many situations beyond the original remit of its design, such as natural floods on rivers.

The TELEMAC system is a series of computer programs utilising finite element techniques for simulating hydraulic situations. The system includes pre- and post-processing components and offers solutions in two- and three-dimensions. It also contains facilities for sediment and contaminant transport (SUBIEF) and sand transport (TSEF). The full system is further outlined in Figure 2.1. All the components of the system have common file formats and are written in the high level language FORTRAN 77. This enables easy file transfer between components of the system and allows model users to modify parts of the code as desired for specific applications.

The TELEMAC system contains both two- and three-dimensional versions. The three-dimensional version (TELEMAC-3D) has advantages in many applications where vertical velocity variations are important such as small scale and oceanic studies but in large scale fluvial applications depth averaged calculations are adequate. Indeed the equations used in nearly all fluvial hydraulic models derive from the depth averaged equations known as the Shallow Water or St. Venant Equations, TELEMAC-2D being no exception. The third dimension, though initially appealing, would simply add to the computational and data demands. Descriptions of TELEMAC-3D can be found in Hervouet *et al.* (1994), Hervouet and Janin (1994) and Hervouet and Van Haren (1996). TELEMAC-2D is however used throughout the work presented here and is now discussed in more detail.

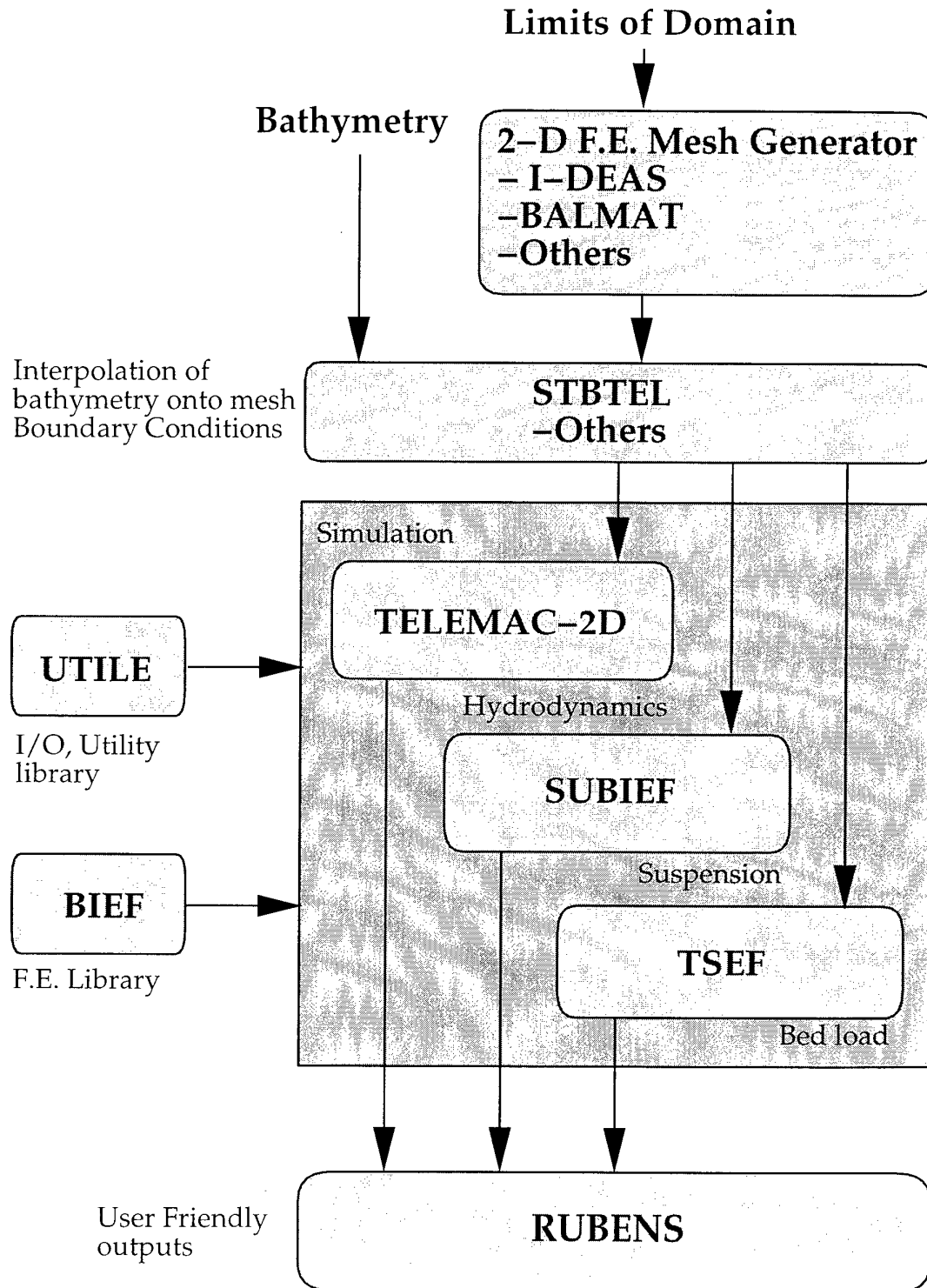


Figure 2-1 The TELEMAC-2D modelling system (after Hervouet and Lang, 1995).

## 2.1 TELEMAC-2D

The main features of TELEMAC-2D are listed by Hervouet *et al.* (1994) as:

- structured or non structured meshing,
- use of Cartesian or spherical co-ordinates,
- subcritical and supercritical regimes (with hydraulic jumps),
- various momentum source terms : bottom friction, wind stress atmospheric pressure, Coriolis force,
- turbulence modelling (k-epsilon model),
- equation on temperature or a substance concentration,
- treatment of tidal flats,
- many types of boundary conditions including free slip condition and incident waves.

Many of these are of minimal importance for fluvial applications but are necessary for the diverse nature of cases that TELEMAC-2D can be applied to. A wide range of test cases are illustrated in the TELEMAC-2D (version 3.0) validation document (Cooper, 1996) prepared to substantiate the explicit claims made about the applicability and accuracy of the computer code. The test cases illustrated range from the Western European Coast and the Mersey estuary UK, to flows around bridge piers and over a weir. On a scale more relevant to this study dam breaks, flow at a river confluence and the simulation of a flood event on the River Culm, UK are also shown. A new version of TELEMAC-2D is released annually. All of the simulation in this report have been carried out using version 3.0, released in 1995.

### 2.1.1 Shallow water equations

TELEMAC-2D solves the shallow water equations (SWE), the depth averaged version of the fully three dimensional Navier Stokes equations of fluid flow. The SWE require that:

- the flow is incompressible
- the water column is well mixed, so that there are no significant density variations in the vertical
- vertical accelerations are negligible (hydrostatic pressure approximation)
- the effective lateral stresses can be represented by an isotropic (usually constant) eddy viscosity
- bed stresses can be modelled using a linear or quadratic friction law.

All of these conditions are commonly met in rivers, estuaries and seas making the choice of these equations over the full three dimensional Navier Stokes equations valid for the applications of the model (Cooper, 1996).

The choice of formulation of the SWE used in TELEMAC-2D is not obvious. A conservative form would seem better but divisions by the water depth are needed to produce the velocity field, hence causing problems in dry areas of the model domain. Hence a non-conservative form is preferred. Moreover numerical stability analysis also favours the non-conservative version of the equations. Using finite element methods mass conservation can be ensured with non-conservative equations. Two versions of these non-conservative equations have been developed, the celerity-velocity version and the depth-velocity version. The depth-velocity version are marginally favoured as they are easier to employ mass-conservation techniques to (Hervouet and Janin, 1994). These equations are shown below:

$$\frac{\partial h}{\partial t} + \mathbf{u} \cdot \text{grad}(\mathbf{h}) + h \cdot \text{div}(\mathbf{u}) = 0 \quad 2.1$$

$$\frac{\partial u}{\partial t} + \mathbf{u} \cdot \mathbf{grad}(\mathbf{u}) + g \frac{\partial h}{\partial x} - \text{div}(\mathbf{v} \cdot \mathbf{grad}(\mathbf{u})) = S_x - g \frac{\partial Zf}{\partial x} \quad 2.2$$

$$\frac{\partial v}{\partial t} + \mathbf{u} \cdot \mathbf{grad}(\mathbf{v}) + g \frac{\partial h}{\partial y} - \text{div}(\mathbf{v} \cdot \mathbf{grad}(\mathbf{v})) = S_y - g \frac{\partial Zf}{\partial y} \quad 2.3$$

where:

- $h$  : water depth
- $u, v$  : velocity components
- $g$  : gravity
- $Zf$  : bottom elevation.
- $S_x, S_y$  : Source/sink terms (bottom friction, wind, etc.)
- $\mathbf{v}$  : eddy viscosity

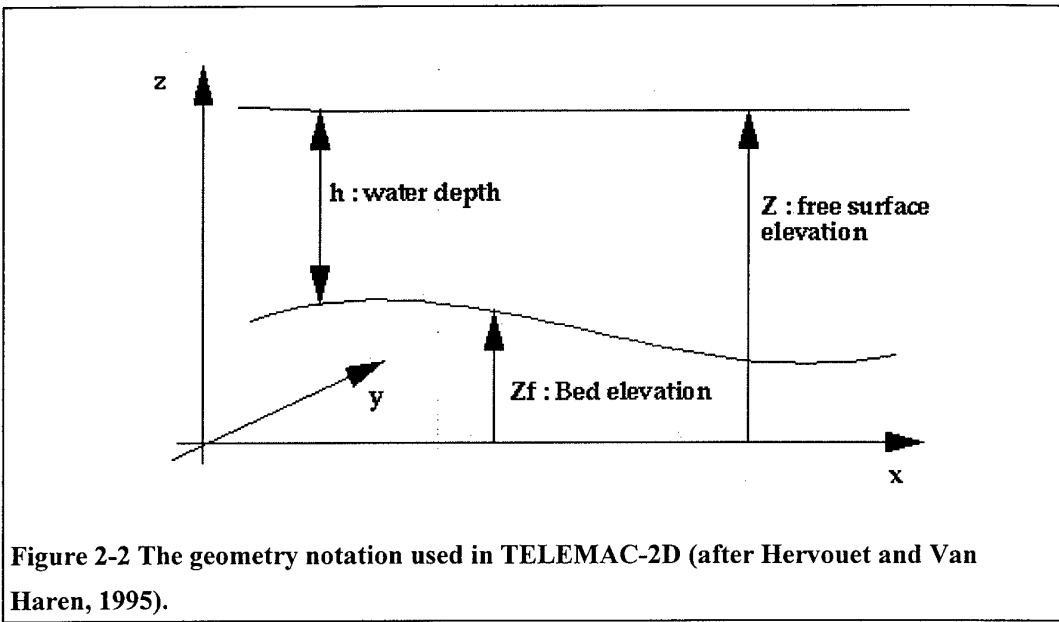
$h, u$  &  $v$  are the unknown variables.

Equation 2.1 being the continuity equation, 2.2 and 2.3 the force-momentum equations. Full derivations can be found in Norton *et al.* (1973).

### 2.1.2 Solving the equations

The TELEMAC system uses finite element methodology to solve the shallow water equations to produce values of water depth ( $h$ ) and two velocity components ( $u$  and  $v$ ) at all points in the model domain. To achieve this the domain must be discretized into a grid or mesh, usually made up of linear triangles (unstructured grid) for flexibility. The mesh is created outside TELEMAC using specialised mesh generation software such as I-DEAS or BALMAT. The mesh is then incorporated with the topographic data to produce a geometry file that is then used in the TELEMAC-2D simulation. The mesh consists of a series of node points, the vertices of the triangles with a elevation ( $z$ ) value, where the equations are solved and the triangles themselves are the elements. The geometry notation used is shown in Figure 2.2.

All three dependant variables ( $h, u$  and  $v$ ) are defined at each point in the domain in terms of linear interpolation functions associated with the value attained at each node. Linear interpolation functions between nodes can be a limitation where the bed gradients are varying rapidly compared to the distance between nodes. Mesh refinement can however be used to overcome this problem in most cases. The time discretization is semi-implicit so a system of  $3N$  simultaneous algebraic equations is obtained, where  $N$  is the number of nodes in the domain (Cooper, 1996). Furthermore TELEMAC-2D employs element by element (EBE) techniques to minimise and simplify computation. More detailed descriptions of finite element methodology can be found in Norton *et al.* (1973) and Pinder and Gray (1977).



Several solution algorithms are available in TELEMAC-2D including (Cooper, 1996):

- a fractional step method using characteristics for the advection terms and a Galerkin method for the propagation and diffusion terms in the equations
- several variants of the Streamline Upwind Petrov Galerkin (SUPG) method (Brooks and Hughes, 1982)
- a hybrid scheme that combines the characteristics and SUPG approaches.

Further details of these options are available in Hervouet and Van Haren (1995).

In the simulations presented later in this report a fractional step method (Marchuk, 1975) is used where the advection terms are solved initially followed by a second step where the propagation, diffusion and source terms are solved. For the advection step the method of characteristics is used for the momentum equation and a SUPG method for advection of  $h$  in the continuity equation, ensuring mass conservation. The use of the semi-implicit SUPG method for the continuity equation achieves unconditional stability (Hervouet and Janin, 1994). The second step of the calculation, propagation, is then solved using a conjugate gradient type method.

The different solution techniques do however produce very similar results when used with on the same simulations with the same mesh. For example Bates *et al.* (1996) show the SUPG and hybrid methods used on a flood event on the River Culm, UK, showing very similar outflow hydrographs and inundation extent.

The Courant number is used as a measure of the quality of the numerical solution. It derives from explicit numerical methods and is calculated thus:

$$C_r = u \frac{\Delta t}{\Delta x} \quad 2.4$$

where (Bates *et al.* 1996):

$C_r$  : Courant number



t : time step  
x : mesh size  
u : flow velocity.

Explicit methods become unstable when  $C_r > 1$ . Although TELEMAC-2D is implicit and theoretically not subject to such constraints the Courant number remains a good measure of the quality of the numerical solution (Hervouet and Janin, 1994; Bates *et al.*, 1996). Hervouet and Janin (1994) suggest that in some cases simulations can be performed with values of the Courant number of up to 50 but this is not advisable.

### 2.1.3 Boundary conditions

There are two main types of boundary condition that can be used, solid boundaries and liquid boundaries. The boundaries described here are round the sides of the model domain and through the bed of the model. All boundary conditions are assigned on a node by node basis. Solid boundaries are no flux (impermeable) and incorporate a friction factor (Hervouet and Van Haren, 1995). Liquid boundaries allow a flux across them. They are more difficult to deal with as they suppose the existence of a fluid area that is not part of the calculation domain but can however influence it. This influence is described through the boundary condition. There are four types of liquid boundary, entry and exit with supercritical flow (Froude number  $> 1$ ) and entry and exit with subcritical flow (Froude number  $< 1$ ). Incident waves and prescribed flowrates can be incorporated through these 4 boundary types. Hervouet and Van Haren (1995) describe these boundary conditions more fully.

### 2.1.4 Physical parameter options

Physical representation of parameters is essential in models such as TELEMAC-2D in order to apply them to different applications. TELEMAC-2D includes numerous physical parameters. The most important are discussed in this section.

#### 2.1.4.1 Bottom friction

There are six options in TELEMAC-2D for representing bed friction, these are:

- No friction
- Linear friction
- Chezy's law
- Strickler's law
- Manning's law
- Nikuradse's law

The applied friction coefficient is converted to force terms in the x and y directions at each computational node which is then fed into the Shallow Water Equations (in the source terms  $S_x$  and  $S_y$  - see section 2.1.1., equations 2.2 and 2.3). In reality the bed friction force is a quadratic function of velocity so the no friction and linear law are rarely used in practical applications (Hervouet and Van Haren, 1996). The Chezy, Strickler and Manning laws are all closely related and utilise the quadratic function mentioned and are all described more fully by Hervouet and Van Haren (1995). Nikuradse's law calculates a Chezy coefficient from the water depth (h) and grain size of the bed material which is then converted into a force term. Which of these laws that is used is not very important as they are very closely related and friction coefficients can easily be converted between them. The choice rests with the model user.

#### 2.1.4.2 Turbulence representation

Turbulence is one of the remaining major unresolved problems in physics. Its importance in hydraulics is well known but its representation in hydraulic models is a different problem. The concern in hydraulic modelling is how turbulence in flow affects the mean structure of the flow. Turbulence modelling is a scientific discipline in itself and the reader is referred to Younis (1996) for a general discussion of turbulence modelling and to Hervouet and Van Haren (1996) for a fuller exposition of turbulence representation in TELEMAC-2D than is possible here. In TELEMAC-2D version 3.0 there are two options for turbulence representation:

- constant viscosity
- k-epsilon model.

The first and simplest is a constant viscosity coefficient, zero-equation turbulence model. The term VELOCITY DIFFUSIVITY is used to set the molecular viscosity, turbulent viscosity and dispersion throughout the model domain. In turbulent flows the turbulent viscosity is dominant and can virtually be equated to the velocity diffusivity value. A constant value of turbulent viscosity over the model domain is often used but is an oversimplification.

The second is the k-epsilon model where the turbulent viscosity is expressed as a function of the turbulent kinetic energy ( $k$ ) and its dissipation rate ( $\epsilon$ ). This two-equation turbulence model is overcomplicated for large scale applications and is computationally intensive.

A third turbulence model, the single-equation Elder's model, has just been introduced into the newest version of TELEMAC-2D (version 3.1). This model separates longitudinal and transverse dispersion terms. It offers improvements on the previous two methods in fluvial applications where such separation is important. Unfortunately this method was not available for the work in this report.

#### 2.1.4.3 Other physical parameters

Several other physical parameters can also be specified in TELEMAC-2D. These include wind stress on the water surface, atmospheric pressure, water temperature and water density. The Coriolis force can also be applied when modelling large areas.

### 2.1.5 Wetting and drying zones

Applications of TELEMAC-2D to river and estuaries generally involve wetting and drying areas of the model domain. For example the tidal simulation in the Mersey estuary and the flood event on the River Culm, both described by Cooper (1996), involve this type of behaviour. The ability of the model to deal with this sort of behaviour is therefore of vital importance but is problematic. The behaviour in the dry zones, where divisions by the water depth ( $h$ ) in the calculations, can cause spurious terms to appear as  $h$  tends towards zero.

Two solutions to this problem are available in TELEMAC-2D, both described in more detail by Hervouet and Van Haren (1995),

- solving the equations everywhere and coping with the spurious terms.
- removing the dry zones from the computational domain.

The first is the simplest but corrections must be applied in the dry zone. In dry areas the water surface gradient becomes that of the bottom topography but this cannot be allowed to act as a driving force in the momentum equation.

The second method removes the dry zone from the computational domain and is often called the "moving boundary technique". In TELEMAC-2D this is achieved efficiently, avoiding the need to redefine the mesh at each time step, by keeping the elements in the mesh but cancelling their existence through the use of an array set to 0 for dry elements and 1 for all others.

Partially dry elements are another important area, especially where the elements are large such as in the Missouri River model. These are coped with in TELEMAC-2D by a sophisticated method that allows the water depth to go to zero within an element. This compares favourably with the usual techniques of keeping the elements fully wet or excluding partially dry elements (Figure 2.3).

## **2.2 Post-processing of results**

After the computations have been completed the numerical results must be converted to a more user friendly visual form. This is done using the graphics visualisation software RUBENS, also written by EDF-DER. RUBENS allows quick, easy and flexible representation of the results in many different forms such as:

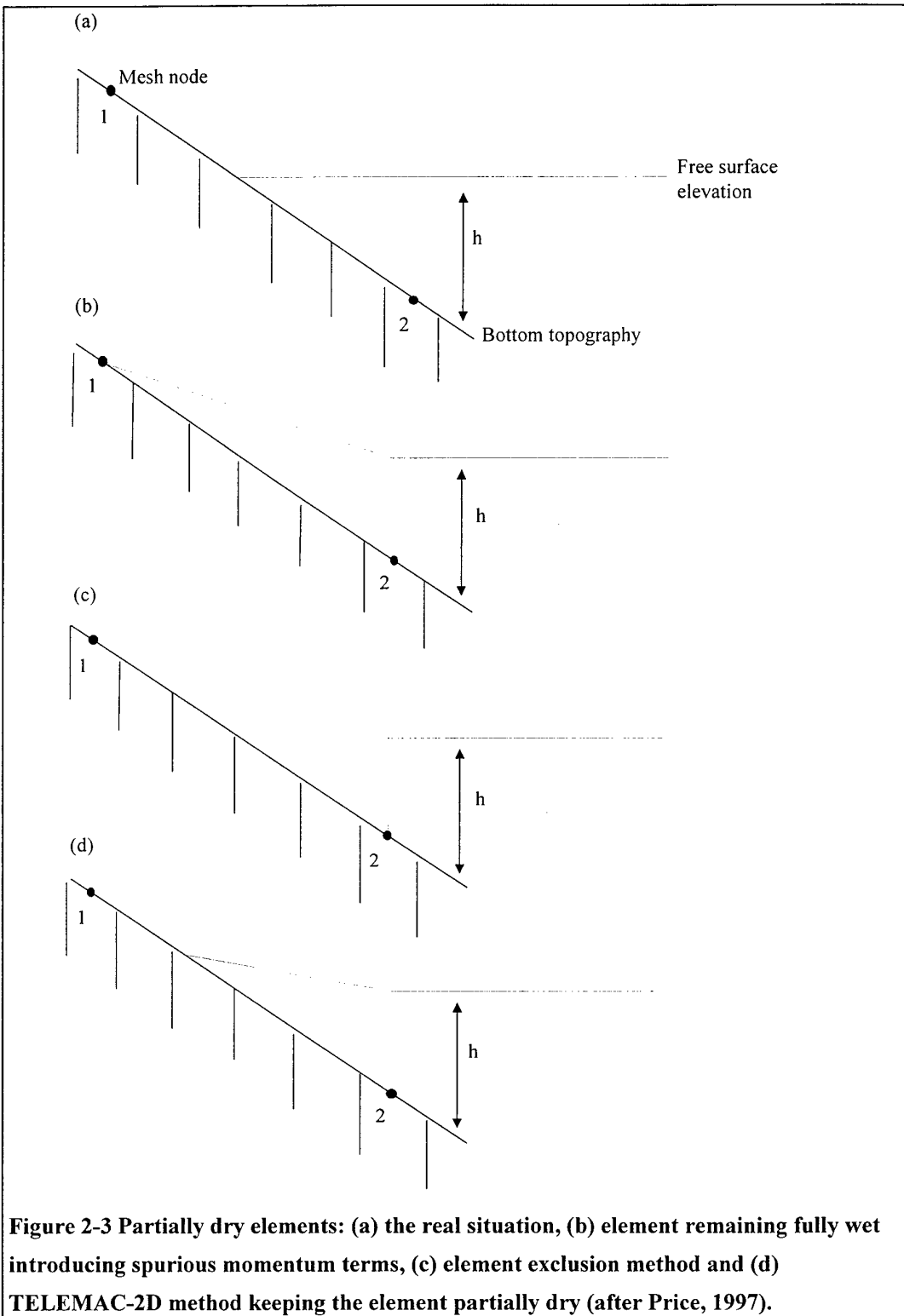
- mesh plots
- vector fields
- contour lines
- coloured surfaces
- space profiles
- time profiles

RUBENS also allows the superposition of measurements and graphics and also the manipulation and processing of the visualised data. Most of the plots of model results in this report are created using the RUBENS software. For more information on RUBENS the reader is referred to Piro (1993).

## **2.3 Summary of the TELEMAC-2D system**

TELEMAC-2D is a high resolution space/time distributed hydraulic model that solves the Shallow Water Equations for fluid flow using finite methodology. The model can be used in a wide variety of scenarios including those involving wetting and drying fronts within the model domain. Bed friction and turbulence are represented in the model through the use of physically based parameters.

TELEMAC-2D can therefore be seen to be well specified for the type of fluvial application that is of interest in this study. The code has been shown to work, through the report of Cooper (1996), in a wide range of cases. Success in any individual situation is however dependant on the data provided, physical and numerical parameters used. How these important factors have been determined in the Missouri River model case is the subject of the next section.



### 3. The Missouri River model

This section looks at how TELEMAC-2D has been applied to the Missouri River between Gavins Point Dam, South Dakota, and Maskell, Nebraska. The theoretical aspects of the model were examined in section 2 but the practical details of applying the model to this specific scenario reach is vital to gain an understanding of the model and its capabilities.

#### 3.1 Producing the finite element mesh

The finite element mesh for the model must be created by first defining the boundary of the model domain and secondly discretizing this area into elements.

The boundary of the 2D model was defined by digitising round the edge of the river as represented on United States Department of the Interior 7.5 minute quadrangle series maps. The use of wetting and drying algorithms in the model enable the flow field boundary to be calculated within this outer boundary thus allowing this boundary to be fairly loosely defined. The digitised boundary was then converted to Universal Transverse Mercator (UTM) metre co-ordinates for compatibility with the metric scale used by TELEMAC-2D. The boundary of the model (with TELEMAC-2D's metric scale), which includes three permanent islands, is shown in Figure 3.1.

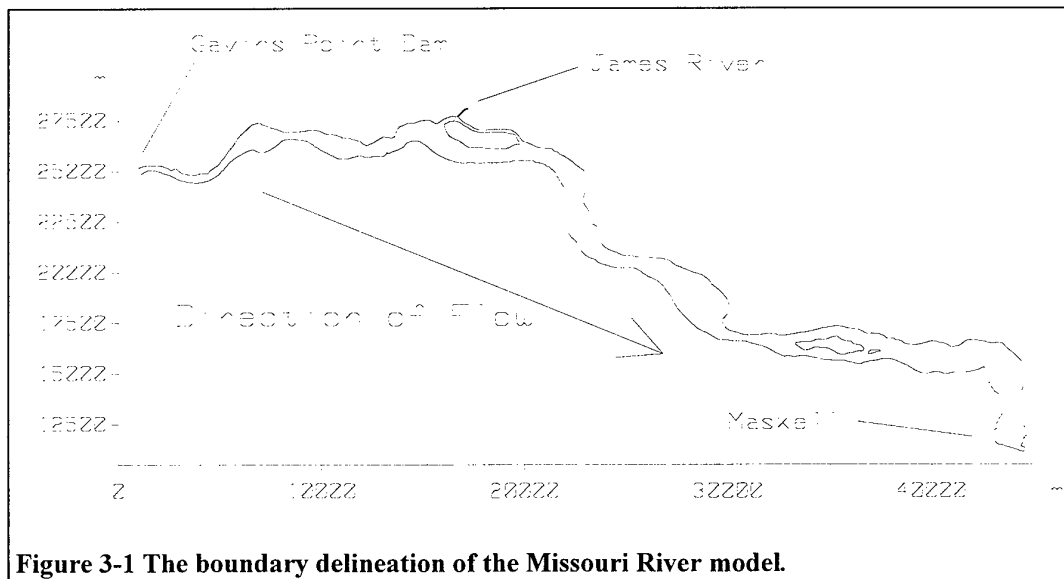


**Figure 3-1 The boundary delineation of the Missouri River model.**

A mesh of triangles or quadrilaterals must be made within the model domain to facilitate the finite element solution technique. The finite element meshes used with the Missouri model were generated inside the prescribed boundary using the mesh generation package BALMAT. The meshes created were made of near equilateral triangles in order to increase the accuracy and minimise mass conservation errors. Two meshes have been created of this reach. The two are shown in Figure 3.2 and their attributes compared in Table 3.1.

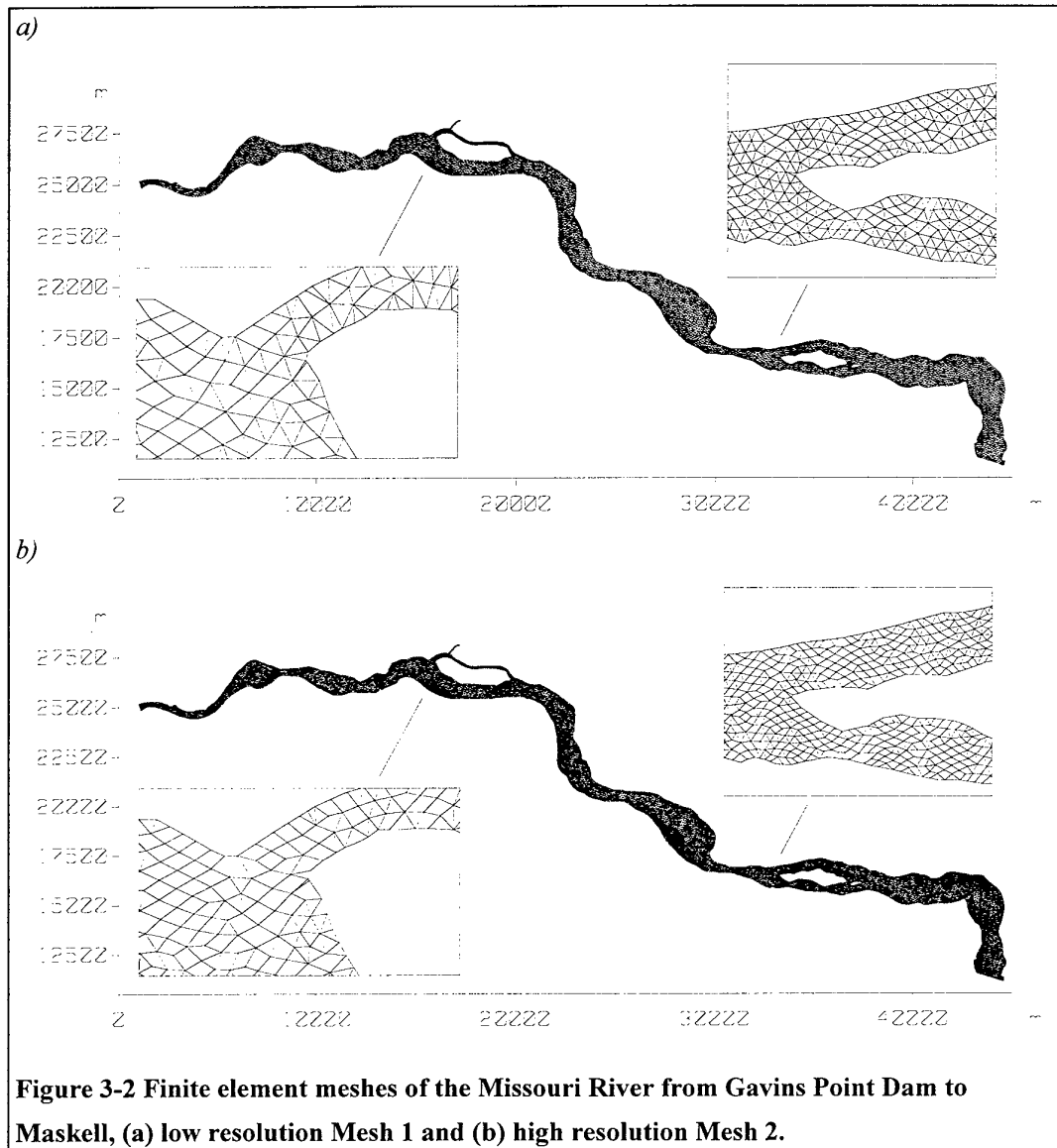


**Figure 3-2 Finite element meshes of the Missouri River from Gavins Point Dam to Maskell, (a) low resolution Mesh 1 and (b) high resolution Mesh 2.**

Mesh 1, the lower resolution mesh, is used for the majority of the simulations in this report. It should be assumed this has been used when looking at results unless otherwise stated. Mesh 2 is only used in the sensitivity analysis (section 4) and section 6 where its performance is compared to that of mesh 1.

**Table 3-1 Comparison of the attributes of the two meshes used to model the Missouri River in this report.**

Attribute	Mesh 1	Mesh 2
Number of Nodes	5969	9213
Number of Elements	10437	16567
Average Element Size (m <sup>2</sup> )	100.77	79.98

### 3.2 Bathymetric Data

The bathymetric data in a 2D hydraulic model is one of the most important factors in attaining high quality simulations. The quantity and quality of the bathymetric data is therefore of utmost significance.

Along this reach of the Missouri River the bathymetry was obtained by the MRD in 1995 by echo sounder surveys of channel cross sections. In total 343 cross sections were available along the 55 km reach creating an average spacing of just over 150m. Each cross section was made up of between 30 and 200 data points, depending on section length. The typical spacing between data points along a section was 6m. All elevation data was converted to metres. Bathymetric data was missing on the cross sections where the bed was above the water surface, such as on sand banks and mud flats. In these regions the topographic elevation was estimated from United States Department of the Interior 7.5 minute quadrangle maps, except on the permanent island in the model where no such data is required.

The bathymetric data must now be applied to the finite element mesh. This is the process of interpolating between topographic data points and assigning elevation (z) values to the nodal points in the mesh. This produces a geometry file for the model simulation. The interpolation is usually carried out using STBTEL, the TELEMAC sub-program. This uses a quad-directional interpolation routine, taking the nearest data point in the four quadrants around each node, weighting for distance from the node and combining to give the nodal elevation. An alternative interpolation routine has been written at Bristol for use with cross sectional data of river channels. This is a linear interpolation down the line of greatest depth between sections and improves the definition of this line in such cases as the Missouri River. A portion of the models topography is shown in Figure 3.3.

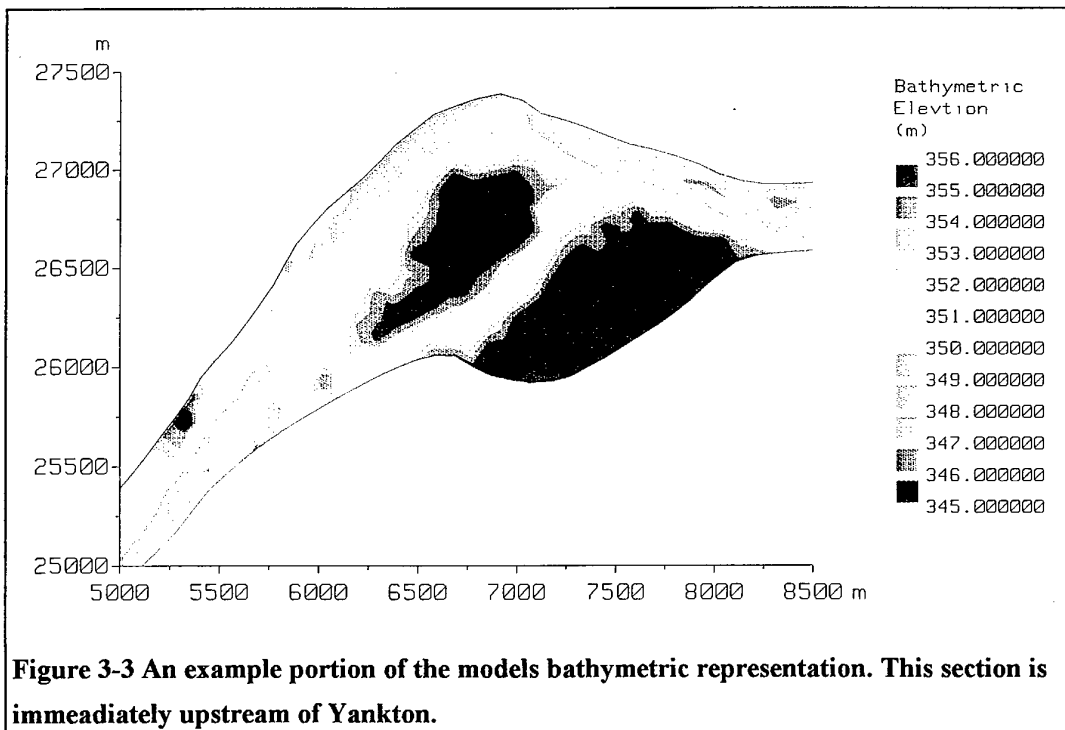


**Figure 3-3** An example portion of the models bathymetric representation. This section is immediately upstream of Yankton.

### **3.3 Boundary Condition Specification**

The boundary conditions of the model are very important to the simulations run. There are several boundaries to each model that must be set with care prior to the model run. These boundaries are divided into two types, liquid boundaries and solid boundaries.

With the Missouri model the liquid boundaries, allowing flow across them, are at the top and bottom ends of the reach and on the James River tributary inflow. Model inflows are prescribed as flowrates, at Gavins Point Dam and from the James River, and outflows as water surface elevations, at Maskell. This produces a well posed problem for fluvial flows according to the theory of characteristics (Hervouet and Van Haren, 1995). All measured flowrates were converted to  $\text{m}^3/\text{s}$  (cumecs) and stage values to metres.

Solid boundaries allow no flux across them. They are found down the sides of the reach and through the bed. The side boundaries in the Missouri model are set as slip boundaries, allowing a velocity along them. This is justified by the size of the elements making flow overly restrained in areas of channel constriction when the more realistic no-slip boundaries are imposed. The flexible boundary of the flow field removes this problem for large portions of the reach where such an argument is irrelevant.

### **3.4 Physical Parameter Specification**

The two most important physical parameters in fluvial hydraulic models are generally agreed to be bed friction and turbulence (Baird and Anderson, 1990; Bates *et al.*, 1992). The theory of the two in TELEMAC-2D has been discussed in section 2.1.4. They are the only two considered in any detail here.

Given the channel only nature of the model and lack of additional information the bed friction and turbulence parameters were defined as constant throughout the entire reach. These are obviously simplifications but should be adequate as a first approximation. The bed friction is always defined using Manning's law enabling the standard Manning's 'n' measure of flow resistance to be used. The turbulence was defined using the zero-equation velocity diffusivity representation.

### **3.5 Creating the initial conditions**

Before any dynamic simulation can take place the model must be run to a position closely resembling those required at the start of the simulation, the initial conditions.

### **3.6 The model run**

The model run is the end product of the modelling process. This run simulates the flow event that is required creating the model predictions. In order to carry out this run all the previously discussed factors must be in place. A geometry file containing the topography and finite element mesh, a boundary condition file, parameter values and the initial conditions file must all be accessed. A time step for the model run must also be set. Given the implicit nature of the



numerical schemes in TELEMAC-2D the size of the time step should be relatively unimportant. It does however influence the Courant number and therefore, despite probably not causing instability, a large time step could undermine the quality of the simulation. With the Missouri River model the time step used is usually 4 seconds creating Courant numbers less than unity.

### ***3.7 Summary of model application***

The application of TELEMAC-2D to the Missouri River between Gavins Point Dam and Maskell has been described in detail. The data sets are all of high quality and the model set up is fairly simple but justifiable. The model is now in a position to be applied.

## 4. Sensitivity Analysis

The first stage in model application is the sensitivity analysis. Sensitivity analysis is a widely used technique in hydrological and hydraulic modelling to determine the impact of changing parameter values and/or input stresses on the model predictions. Virtually every modelling study involves a sensitivity analysis at some stage. It is a technique that is potentially useful in model formulation, model calibration and model verification (McCuen, 1973).

### 4.1 Background to the sensitivity analysis

Howes and Anderson (1988) suggest that a sensitivity analysis can be used to:

- Demonstrate that in response to representative variation of model input and parameter values, theoretically realistic model behaviour is experienced.
- Illustrate the model to be sufficiently sensitive to represent actual variation in the prototype system.
- Identify those model parameters or inputs to which the model is most sensitive.
- Assess model behaviour without recourse to comparisons to field data.

Perhaps more importantly in the case of this model is that sensitivity analysis is very useful for deciding which parameters to adjust during calibration. Adjusting the most sensitive parameters will produce a greater improvements in the predictions for small changes in parameter values, which means that if the initial values were approximately physically realistic then the calibrated ones should be as well. Conversely if the less important parameters are left fixed at incorrect values then the resulting error on model predictions is likely to be small (Troutman, 1985).

Some of the theoretical considerations of sensitivity analysis are now discussed. Sensitivity is defined as the rate of change in one factor with respect to change in another factor. Mathematically it can be derived from a Taylor series expansion of model behaviour and after discarding the non-linear terms the linearized sensitivity ( $S$ ) can be expressed in simple terms as (McCuen, 1973)

$$S = \partial F_o / \partial F_i \quad 4.1$$

where  $F_o$  the model output prediction and  $F_i$  is the model input parameter. In many instances this linear approximation of sensitivity is adequate to describe model behaviour but whether it is appropriate for the Missouri model is unknown at present.

There are two methods for determining the value of the model sensitivity which are (Lane *et al.*, 1994).

- The direct differentiation of the governing equations. This has been demonstrated with simple models, for example Beven (1979) uses this method to assess the sensitivity of the Penman-Monteith evapotranspiration equations and LaVenue *et al.* (1989) use it to help estimate travel time uncertainties in ground water flow. However with complex, distributed models this methodology has not been developed sufficiently and cannot possibly assess the entire complex response of a model such as TELEMAC-2D.
- Factor perturbation approaches can evaluate the sensitivity of the model by incrementing parameter values and assessing the model response. This is the most commonly used form of sensitivity analysis.

Given the problems of direct differentiation in assessing the sensitivity in complex models the parameter perturbation approach is the only one considered in this rest of this section.

Assuming the overall physically based validity of TELEMAC-2D to this type of application the sensitivity analysis of the Missouri River model has one major function. This to set up the basis for the following calibration procedures by determining:

- the relative sensitivity of the different physical parameters,
- the effect of mesh resolution on this.

Once these questions have been resolved the application and calibration of the model can proceed.

The runs carried out in this sensitivity analysis are outlined in Table 4.1. The data from these simulations is enough to fulfil the two aims above. As discussed in the previous section only two physical parameters in the model were varied, bed friction and turbulence representation (velocity diffusivity), both of which were evenly distributed across the domain.

**Table 4-1 The simulations carried out for the sensitivity analysis. The figures in bold are the parameter values held constant whilst the other is varied.**

Parameter Varied	Mesh 1	Mesh 2
Bed Friction (n)	0.01, 0.015, 0.02, <b>0.025</b> , 0.03, 0.035, 0.04	0.01, 0.015, 0.02, <b>0.025</b> , 0.03, 0.035, 0.04
Turbulence (Velocity Diffusivity - m <sup>2</sup> /s)	1, 2, 4	1, 2, 4

The range of bed friction was chosen to represent the very broad range for this channel type, sand-bed with a shallow gradient (0.02% in this case) (Table 4.2). This full range is used here as no further data is available to make a further judgement at this stage and uncertainties in the overall model set-up create the possibility that the values needed to fit the results to the observed are not those that would be selected from the field. The velocity diffusivity values are harder to physically justify given their vastly oversimplified application to the flow. The values chosen are similar to those used in other applications that have performed well, producing realistic output and maintaining model stability.

**Table 4-2 Values of Manning's n for various channel types (after Bathurst 1988).**

Channel Type	Channel Slope (%)	Manning 'n' range
Sand-bed	<0.1	0.01 - 0.04
Gravel-bed	0.05 - 0.5	0.02 - 0.07
Boulder-bed	0.5 - 5	0.03 - 0.2
Steep pool/fall	>5	0.1 - 5

The parameter space was sampled using simple single parameter perturbation techniques. The flow record used for these sensitivity tests is that from around the 6th June 1994 when the river is essentially at a steady state. The results are therefore all steady state values of the variables.

#### 4.2 Results of the sensitivity analysis

The results of the parameter changes are looked at on the inundated area, water depth at Gayville and Yankton, velocity at Gayville and the spatial distribution of differences of water depth and velocity between two runs over the whole domain. At this stage no comparison to observed data is made.

Firstly the relative sensitivity of the two parameters on both meshes is looked at. Figure 4.1 shows the impact of parameter variation on the total percentage inundation extent in the domain. It can clearly be seen from this that the bed friction has a far greater impact than the velocity diffusivity over the ranges tested.

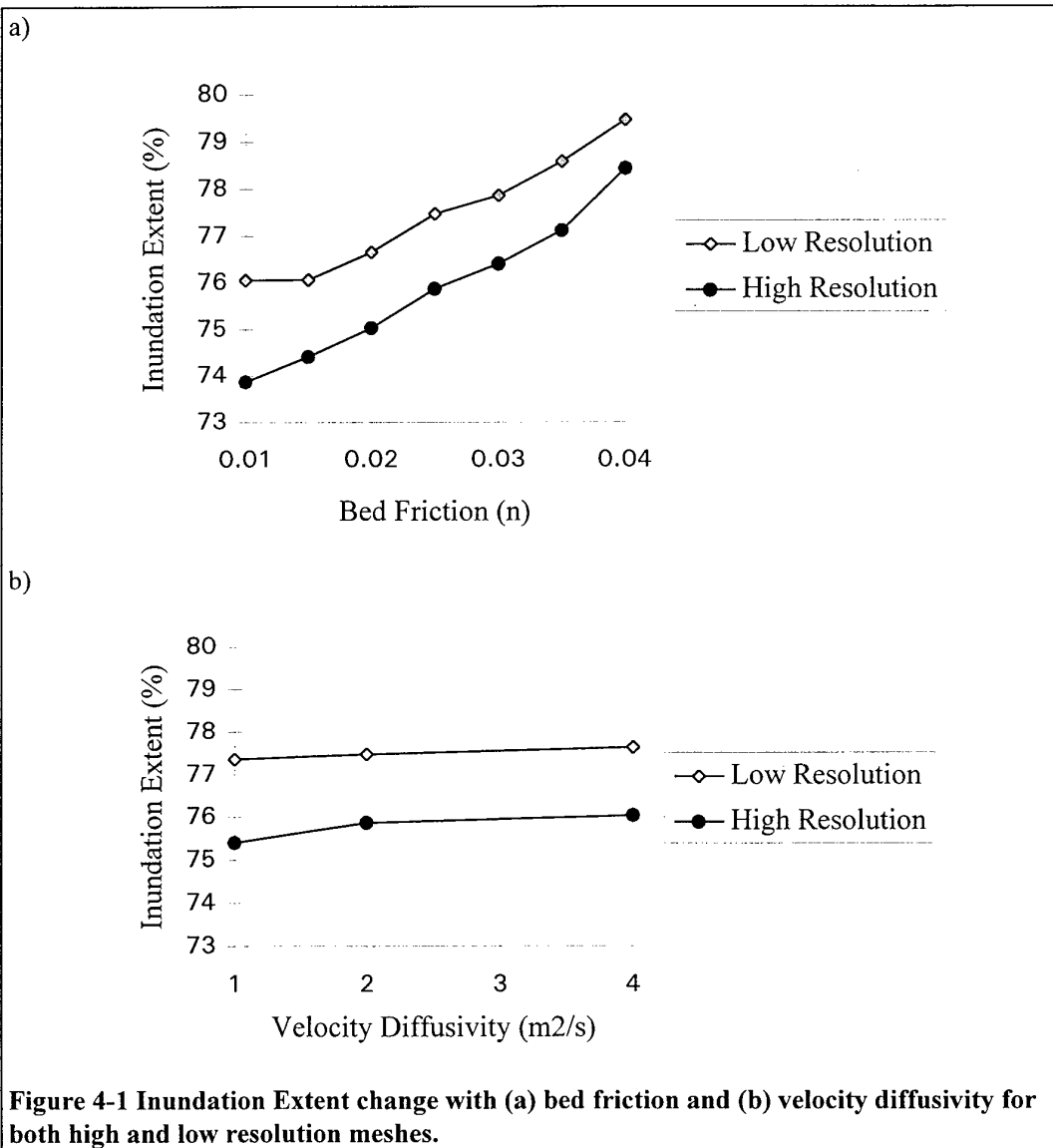
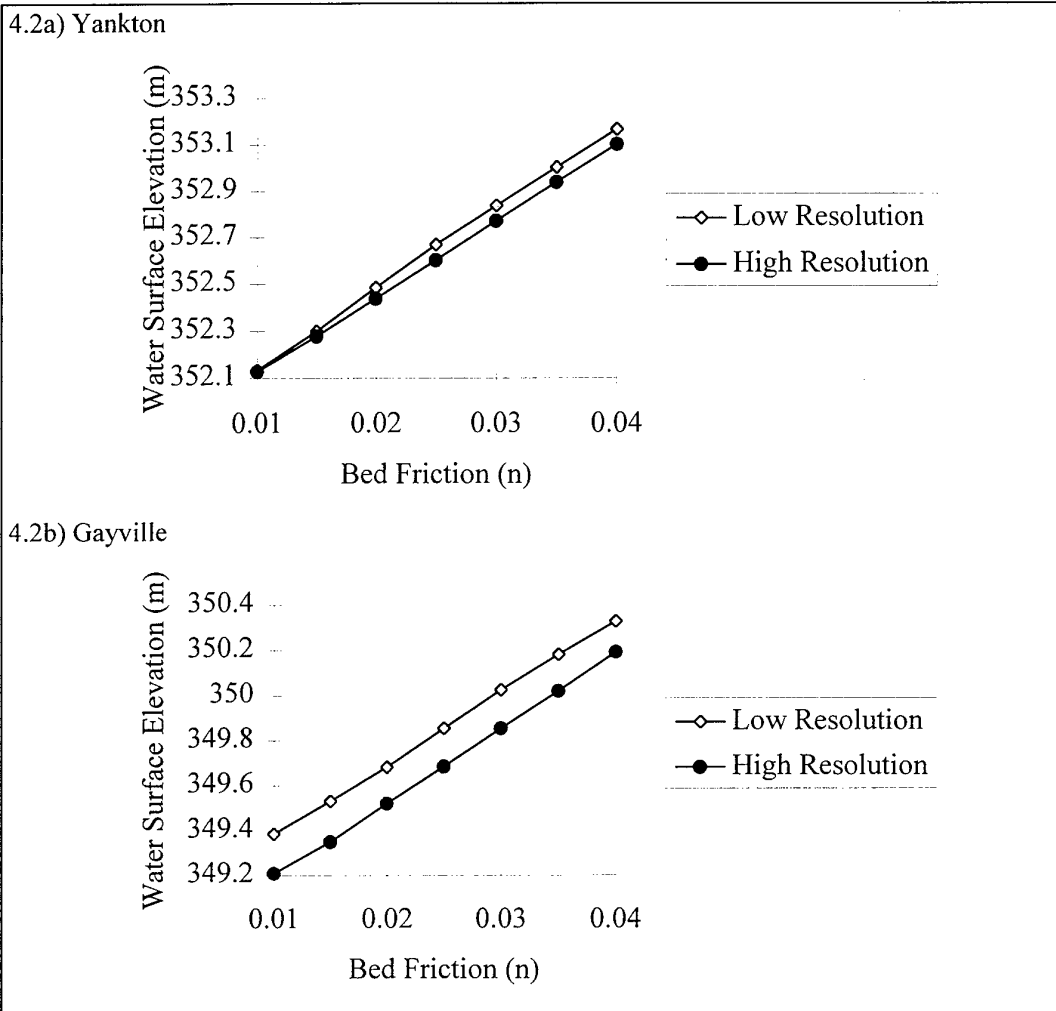
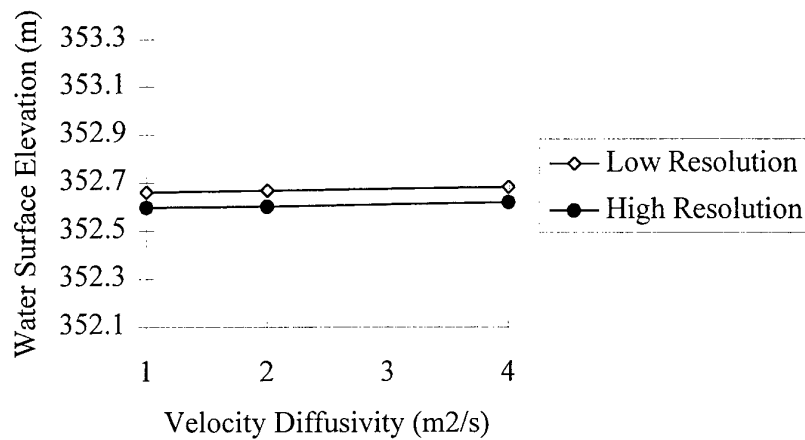


Figure 4.2 shows the impact of both bed friction and velocity diffusivity on the water surface elevation at both gauge stations, Yankton and Gayville, for both mesh resolutions. The results in all cases show that the bed friction has a far greater influence on the water surface elevation than the velocity diffusivity.



4.2c) Yankton



4.2d) Gayville

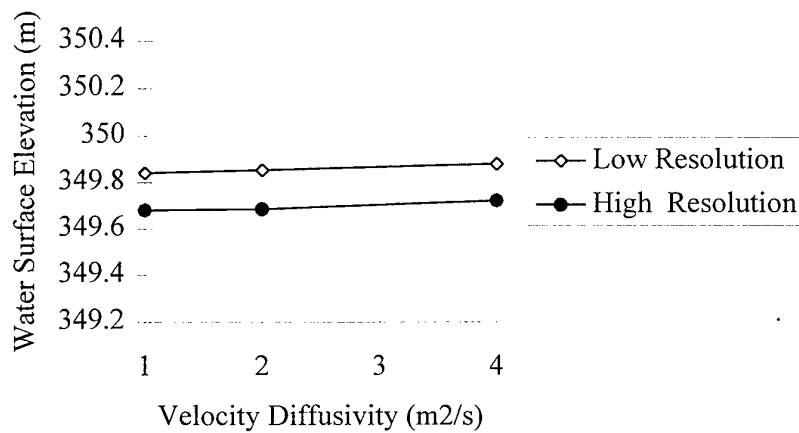
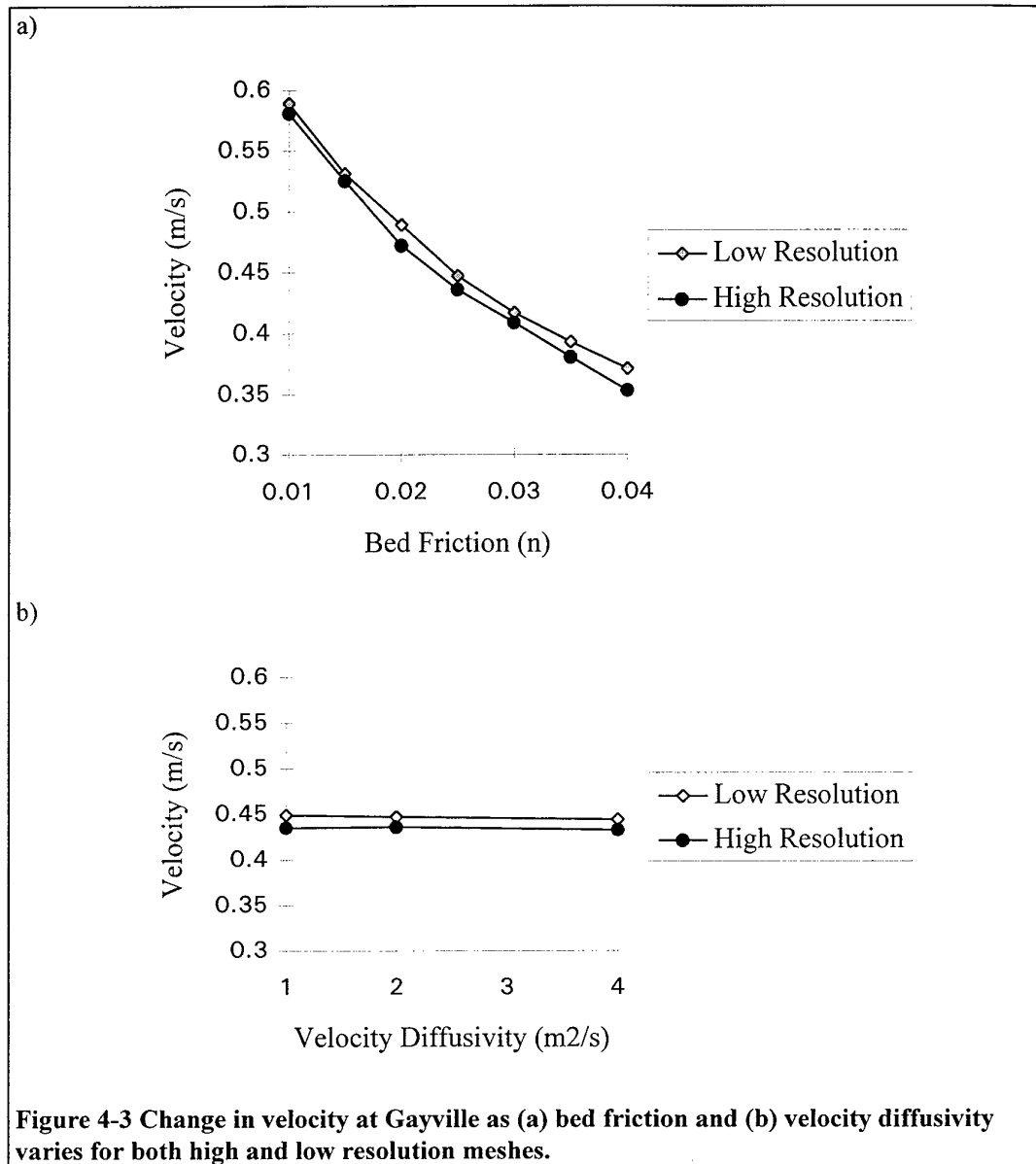


**Figure 4-2 Sensitivity analysis plots for water surface against bed friction at (a) Yankton and (b) Gayville and against velocity diffusivity at (c) Yankton and (d) Gayville.**

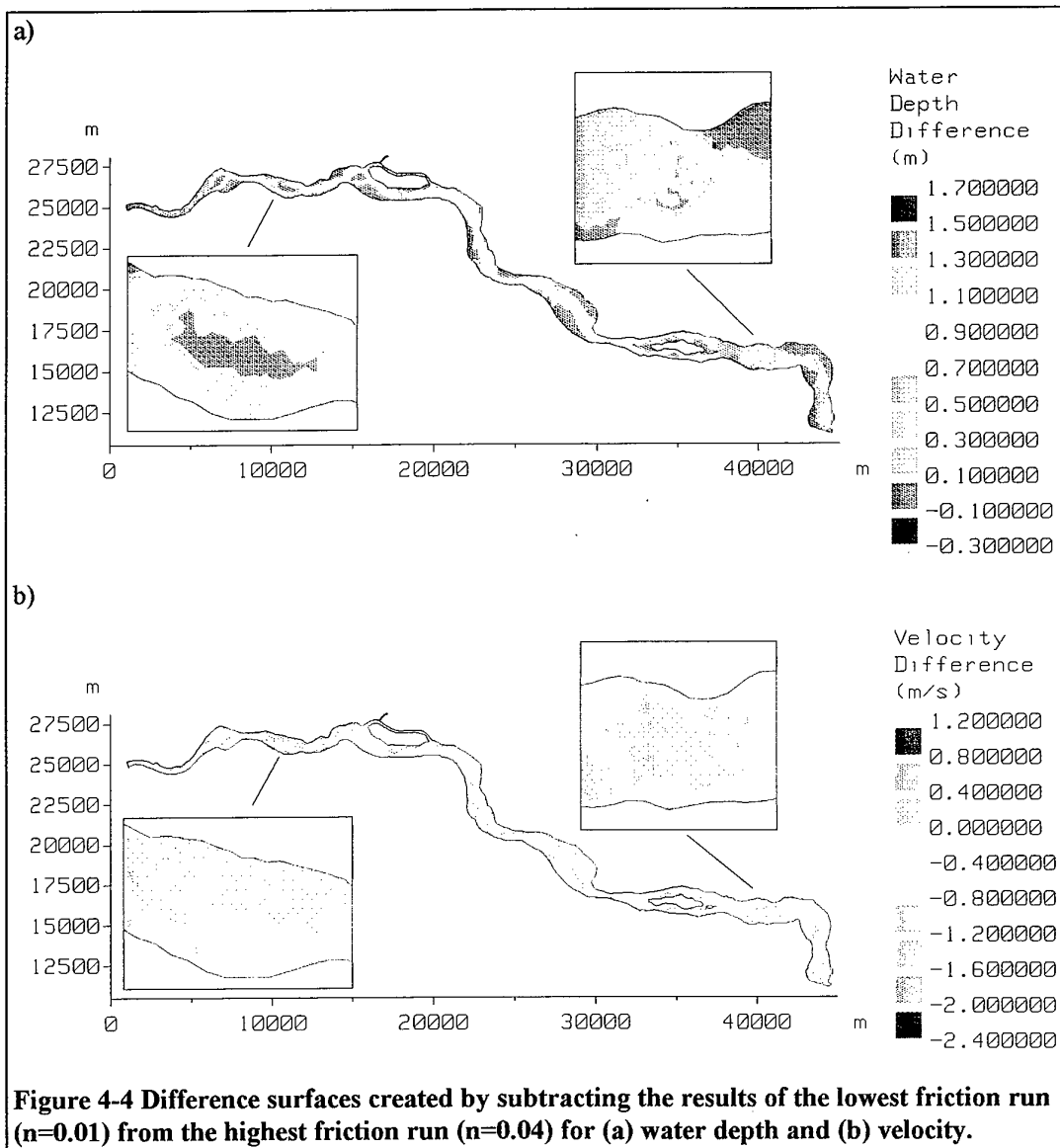
The impact of parameter variation on velocity at a point, in this case at Gayville, is shown in Figure 4.3. Bed friction is again dominant but the response is not linear.



From the above three diagrams it is clear that the bed friction is clearly the most influential parameter having a far greater impact than velocity diffusivity on all the model results. The mesh resolution has a consistent impact on the model predictions. The greater the resolution of the mesh the lower the prediction for an equivalent parameter set for all model results. This is a slightly unusual result and shows that the model structure does have an important impact on the model predictions.

Having determined that the bed friction is by far the dominant parameter in the Missouri River model the further analysis is carried varying only this parameter. Using the argument of Troutman (1985), the velocity diffusivity can only introduce a small error into the results and varying it produces only small changes, hence it can reasonably be overlooked. The difference in velocity and water depth were calculated at all node points between the highest friction run ( $n = 0.04$ ) and the lowest friction run ( $n = 0.01$ ) on the Mesh 1. The results are then plotted up as a spatial plot of the domain.

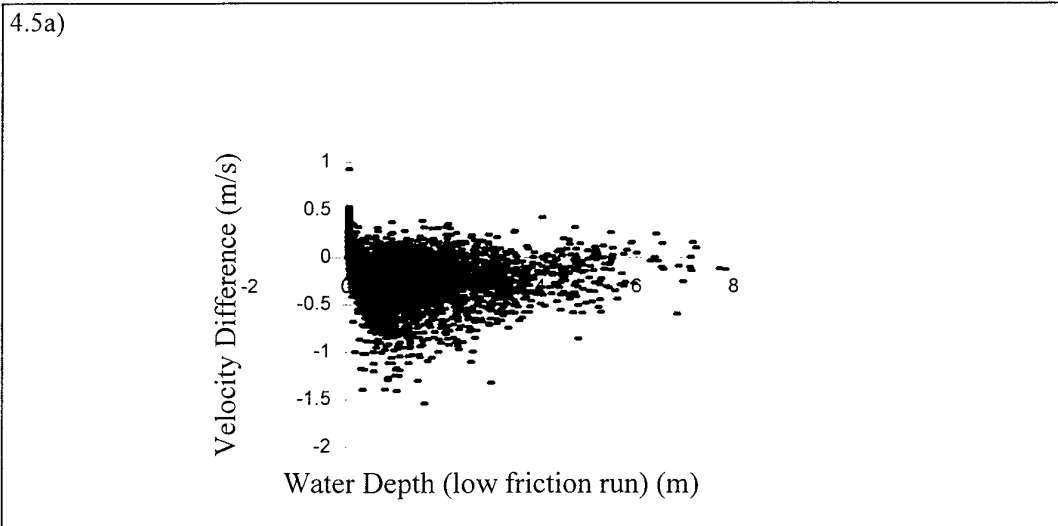
The water depth difference plot (Figure 4.4a) clearly shows that along the thalweg the model behaviour is expected in that the water depth is greater with higher friction (positive difference values). On areas with very little or no water, such as sand banks in the channel or out of channel regions in the model, the behaviour is very much less marked with only very small changes being present, as would be expected. There are however areas in the model domain where the behaviour looks to be more complex and perhaps unexpected.



The velocity difference plot (Figure 4.4b) looks to more complex in structure than the water depth one. Along the thalweg the velocity is generally lower with the higher friction (negative difference values) but in the shallower regions the opposite is true. This is due to the water depth increase in these shallow areas facilitating an increase in velocity despite the increased bed friction. There are however many areas in the model where the behaviour is unexplained.



Further analysis of these plots has been carried out to find out more about the complex model behaviour at all the nodes. The nodal values of velocity difference, water depth difference, and the water depth for the low friction run were extracted from TELEMAC-2D results files. The velocity difference was then plotted against the two water depth variables mentioned. The results are of great interest (Figure 4.5) and show that unexpected model behaviour is much more frequent than anticipated. Figure 4.5a shows the velocity difference plotted against the water depth in the low friction run and in this case, from the above discussion, it would be expected that at all nodes but those of very shallow depth the velocity difference should be negative. This is however clearly not the whole story. Although the majority of velocity differences are negative there are, across the whole depth spectrum, nodes that show the opposite behaviour. At very low (near zero) depths the majority of nodes do show an increase in velocity but this is not complete. The magnitude of the velocity differences seems to be greater at smallish depths (around 1m) possibly caused by bed friction having a greater influence on flow hydraulics at such depths than at greater depths. Although with the limited number of points at greater depths this could just be a random effect.



4.5b)

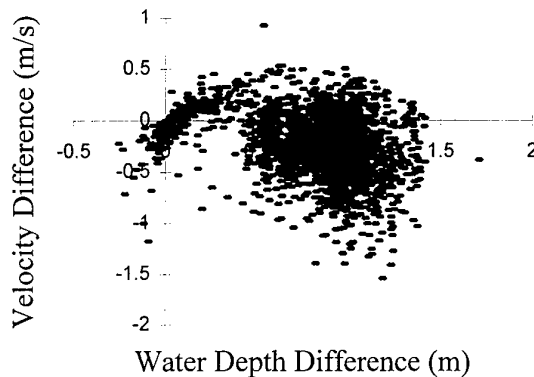


**Figure 4-5 Sensitivity analysis plots showing results for all node points for differences between high and low friction runs for (a) velocity difference against water depth in the low friction run and (b) velocity difference against water depth difference.**

Figure 4.5b shows the velocity difference against the water depth difference. The first point to note is that there are points that unexpectedly show a decrease in water depth as friction increases. All these points also show a decrease in velocity. Between water depth changes of approximately 0 to 0.5m there is predominantly an increase in velocity as friction increase, probably corresponding to the nodes with shallow water depths initially. At greater water depth differences the majority of the behaviour is as expected, decreasing velocity as friction increases but there is a significant proportion of nodes revealing the opposite, though not to the same magnitude.

These results have shown the complexity of the model response to very simple changes in parameter values. Some of the unusual results can be explained by physical reasoning, others are perhaps artefacts generated by the model specification.

### **4.3 Conclusions of the sensitivity analysis**

The sensitivity analysis has shown that the bed friction is by far the most influential parameter on all outputs in this model application. The strategy for calibrating the model must therefore be based on varying this parameter. At present the parameters are distributed evenly over the entire model domain but although this is perhaps simplistic there is no case, or data, to change them at the moment. The mesh resolution has a consistent influence on the model predictions showing the model structure is an important factor in the determining the model predictions and thus diminishes the physical basis of the model. The sensitivity analysis also highlighted some strange and unexpected non-linear responses in some areas of the model domain.

## 5. Comparison of model predictions to observed data

The TELEMAC-2D modelling system has now been shown to be a high quality hydraulic model capable of simulating flows in a variety of situations. The setting up of the model and its subsequent sensitivity analysis have shown the Missouri River application to be a highly specified and physically based hydraulic model. The final tests for the model are the comparison of model predictions to observed data. The observed data for the Missouri model is of very high quality and quantity. The available data sets are of special value because they allow both detailed point comparisons using the stage data at two sites, Yankton and Gayville, and spatially distributed comparisons using the satellite imagery. Using this data the performance of the Missouri River model can be comprehensively analysed.

The comparison of model predictions to field data is a common task in all hydrologic modelling, as such a broad literature exists on this subject. It is still however a very difficult area. The latest theories on this are that models can never be completely validated for two reasons. Firstly hydrological models are essentially complex hypotheses and can therefore never be proved correct only supported or disproved (Konikow and Bredehoeft, 1992; Beven, 1993). Secondly models can be considered as a series of equations with more variables influencing the behaviour than equations to account for them. The models cannot therefore account for all possible behaviour and hence cannot be validated. Instead of complete validation it is now the task to look for partial or achievable validation of the model (Samper *et al.*, 1990). As such the strength of the partial validation can be gauged depending on which aspect of model performance the data validates. As was indicated in the introduction the determination of the strength of validation of the 2-D hydraulic model with the novel data sources is one of the objectives of this project.

The observed data used must be comparable to a model prediction. These can therefore be water depth (free surface elevation) and its two dimensional extension inundation extent, flow velocity and the outflow hydrograph. The strength of these can be ranked according to three criteria, where > indicates greater strength of validation:

- internal > external - whether the validation data is internal or external to the modelled domain.
- 2D > 1D - whether the validation data is 1- or 2-dimensional. For a 2-D model the 2-D data is the more powerful as it cannot be simulated by a simpler model and is more difficult to match.
- process > numerical - process validation is matching the processes occurring in the field with those in the model, this is usually considered more powerful than simple numerical matching of results that could have been reached by incorrect processes (Fawcett *et al.*, 1995).

The data available for this study is stage data at two sites within the model domain which can be considered internal but 1-D and numerical. The satellite images are also internal but 2-D and numerical (except for example of process validation that shall be shown later). The satellite imagery is therefore the more powerful validation data type. How well the observed and predicted match shall be shown in the following sections and at the end this idea of strength of validation shall be revisited in the light of the results. Firstly however the methods of model application used in this study and elsewhere are reviewed.

Usually when hydrological models are applied to actual scenarios a two stage process of model calibration and validation is carried out. Calibration is the process by which parameter values are varied within reasonable ranges until the differences between observed and computed values are minimised (Konikow and Bredehoeft, 1992). Theoretically speaking, physically

based model should not need calibrating. The estimation and application of physically realistic parameter values for the model should enable the model to perform well without any further manipulation. However the numerous simplifications involved in modelling and problems in parameter estimation mean that such a notion is unrealistic. Calibration is therefore performed on virtually all physically based hydrologic models. Following the calibration phase the model must then be validated. In most cases the calibrated parameter values are used again on a different portion of the flow record to see if they enable a good match between observed and predicted variables. If they do then the model and parameters are considered validated and can be used with confidence for prediction of future events. If not then calibration and possibly some stage of model formulation must be repeated until the model is validated. It should be noted at this point that validation is used here to mean that a reasonable comparison is obtained between observed and predicted data rather than that the model has been shown to be an accurate representation of the system.

With this application of TELEMAT-2D the highly structured methodology for calibration and validation outlined above is not entirely appropriate for several reasons:

- this study is for research of model behaviour,
- the number and variety of data sources make its application difficult,
- there is no need to produce a model capable of predicting future events at this stage,

The two processes are therefore not used as distinct entities in the following investigation. Instead a hybrid of the two forms is used enabling all benefits of the calibration-validation procedure to be accrued but also much more. The model shall be run using a wide range of bed friction values over several sections of the flow record. This shall enable the calibrated parameter values to be found for:

- each comparison data set (2 internal stage gauges and possibly some areas on a satellite image)
- each portion of the flow record utilised.

Cross comparison of parameter values and the assessment of errors when the model is calibrated onto one data source allow an assessment of the model/parameter performance more complete and powerful than with the traditional calibration-validation procedure.

The sections of the flow record to be utilised have very different flow conditions and occur over a decade meaning that bed morphology changes could have occurred. Three of the sections of record coincide with satellite images of the reach. The flow records around the dates of the images showed very little (<5%) variation in the data set enabling the runs to remain as steady state simulations, ideal for comparing to the snapshot images. One other period of steady state flow shall be utilised, being shortly after an image but with different flowrates it should enable a comparison between the two sections of the flow record without any impact of bed morphology change. Finally one dynamic section of the flow record shall be simulated. Table 5.1 shows all the flow records to be simulated and the available data for comparisons.

**Table 5-1 The flow records to be simulated.**

Event Number	Dates	Type	Inflows - Gavins Point : James River (m <sup>3</sup> /s)	Satellite Image
Event 1	6th June 1994	Steady State	905 : 45	LANDSAT-TM
Event 2	25th June 1994	Steady State	795 : 52	None available
Event 3	26th June 1984	Steady State	285 : 500	LANDSAT-TM
Event 4	8th February 1991	Steady State	255 : 0.2	SPOT
Event 5	13th - 14th June 1994	Dynamic	905 - 765 : 45	None available

The following analysis is split between the different portions of the flow record. Each is dealt with separately, comparing the available data and finding the calibrated parameter values before all the data is brought together again for an overall comparison. The analysis of the first event contains details of the background and methods used in that and all the other cases.

### 5.1 Event 1 (6th June 1994)

The time period being simulated for this comparison is around 6th June 1994 synchronous to the satellite image of the area that will be used in the following section. The flow record around this date showed very little (<2%) variation in the data set. The simulation was therefore taken as a simple steady state computation, simplifying the analysis of results. All the following comparisons are therefore done on a single point in time basis, e.g. a single water level for each point in the domain for each parameter set.

#### 5.1.1 Internal Stage Data

Two internal gauges for water level are available for the reach of the Missouri River described in section 1. The gauges are at Yankton, 7.5 km down the reach, and Gayville, 21.5 km down the reach (Figure 1.1). Hourly stage records are available for these gauges.

The sensitivity of the model prediction of the water depth at these two locations has been shown to be dependant predominantly on the bed friction parameter. This is the only parameter varied in the following analysis. Other parameters would have only minimal effect but increase complexity greatly. The sensitivity of water depth to friction is virtually linear at both internal gauge sites (Figure 5.1) and in the expected direction, i.e. water depth increasing as friction increases.

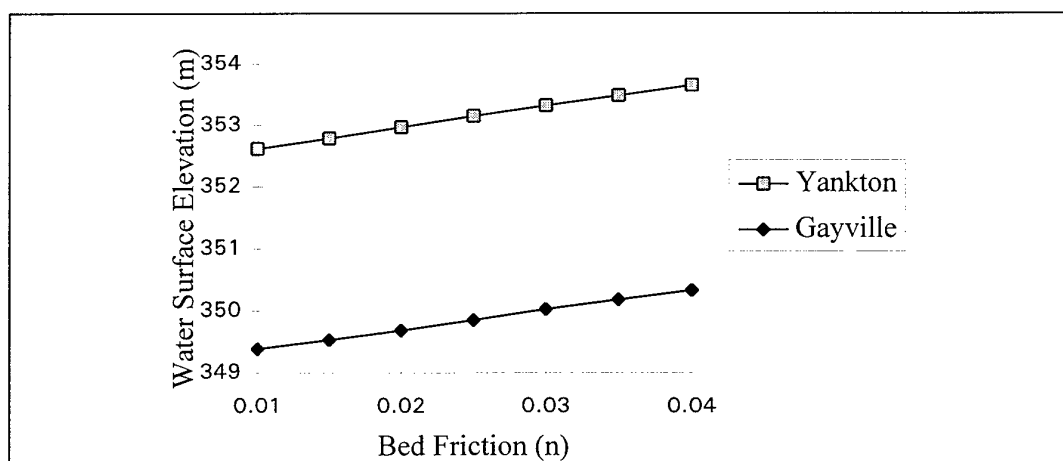


**Figure 5-1 Linear sensitivity of water surface elevation to bed friction at the two gauge sites, Yankton and Gayville.**

This finding allows the use of McCuen's (1973) linearized sensitivity equation seen in section 4 but a simple regression equation is more useful for applying the results in this analysis and is therefore used here. Equations were produced for the model behaviour at both sites, Yankton and Gayville, relating the error in water level prediction to the bed friction (Manning's 'n')

parameter. The equations, calculated using the statistical computing package MINITAB, can be written thus:

$$\text{Yankton Error} = -0.410 + 34.72 n$$

$$\text{Gayville Error} = -0.976 + 31.93 n$$

Alternatively they can relate the water depth to the bed friction thus:

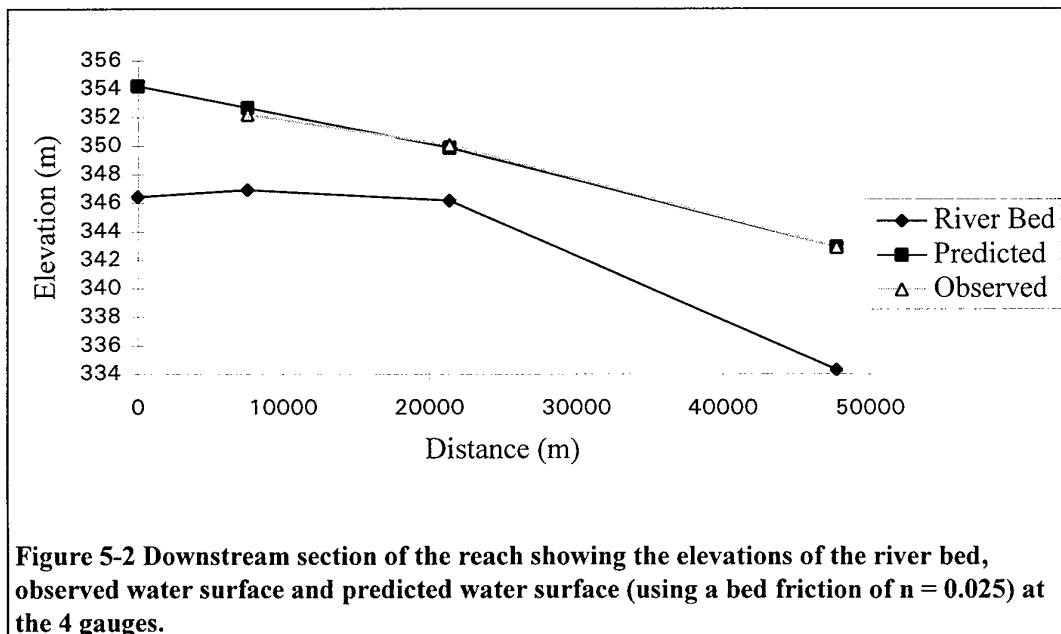
$$\text{Yankton Water Depth} = 4.87 + 34.72 n$$

$$\text{Gayville Water Depth} = 2.91 + 31.93 n$$

The confidence in these regression lines is huge with tiny residuals ( $<0.015\text{m}$ ) in all cases. These equations can therefore be used as a very powerful tool for estimating model predictions for 'n' values at which the model has not been run, although it should not be extrapolated beyond the range of 'n' values used to make the relationship (i.e. 0.01 to 0.04). At present this is only shown at two points but could perhaps be applied at every node.

It can easily be calculated from the above equations that the 'n' value to eliminate the error in water surface elevation at Yankton is 0.0118 whereas at Gayville it is 0.0306. The power of the above regression equations can now be utilised to calculate the error in the other observation whilst one is correct. Whilst the stage at Yankton is predicted correctly at Gayville the prediction is 0.60m too low. Reversing this, whilst Gayville is predicted correctly the prediction at Yankton is 0.65m too high. In percentage terms these errors are 18.26% and 10.96% of the expected water depth at the two points respectively.

Taking the value central to the above two estimates of Manning's 'n' should enable the approximate calculation of the joint minimum errors in the predictions. This value of 'n' is 0.0212 and produces an error at Yankton of 0.33m and at Gayville of -0.30m. Slight adjustment of 'n' could equalise these errors but would be irrelevant. These errors can be expressed again as percentages of the water depth such that the error at Yankton is 5.89% and at Gayville is 8.37%. Figure 5.2 shows a downstream section of the comparison between observed and predicted water surface values.



Interestingly the value of rate of change of the water surface (error term or water depth) is different at the two gauging stations. Thus a fixed change in the bed friction produces a different change in the water surface elevation at the two stations. Investigation into how this type of behaviour occurs over the whole reach would be useful in determining more about model behaviour or what causes this phenomenon.

The comparison between observed and predicted stage values has shown that the model is capable of predicting this variable to about 0.3m at two sites simultaneously. This is a good result given the simplicity of the model set up. Given further work on the parameterization this could no doubt be reduced significantly.

### 5.1.2 Satellite Imagery

Many types of satellite imagery have been used widely in studies of fluvial and coastal hydraulics. The wide coverage, ease of use and wealth of information contained in the images makes them ideal for many uses in this field. Redfern and Williams (1996) review the available sensors and their applications in (primarily coastal) hydraulics. Previously a lot of work has been carried out on the remote sensing of flood extent because of the immense hazard and mitigation costs on floodplain developments. Rango and Salomonson (1974) show that the areal extent of flooding can be mapped using near-infrared sensors on ERTS 1 (Earth Resources Technology Satellite - later renamed Landsat). More recently Imhoff *et al.* (1987) use SAR (Synthetic Aperture Radar) and Landsat MSS (Multispectral Scanner) for mapping flood extent and damage in Bangladesh. SAR has been shown to be very accurate for flood boundary delineation by Biggin and Blythe (1996) on the River Thames in the UK. Satellite remote sensing of the 1993 floods on the Mississippi and Missouri Rivers in the USA with both SAR (Brackenridge *et al.*, 1994) and Landsat TM (Thematic Mapper) have further shown the potential of such methodology.

Satellite data has also been used to measure flood stages as illustrated by Koblinksky *et al.* (1993) using the U.S. Navy's Geosat radar altimeter on the Amazon basin and Brackenridge *et al.* (1994) using SAR data and topographic maps on the Mississippi. Both methods have quite large errors associated with them at present.

Plumes of sediment rich water can also be identified as they have a higher reflectance than clear water in the visible region of the spectrum (Lillesand and Kiefer 1987). Brackenridge *et al.* (1994) use this factor to highlight levee breaches along the Mississippi River during the 1993 floods, the breaches acting as a sediment sources, and explain sediment deposition patterns. Other forms of pollution and thermal emissions can also be traced (Lillesand and Kiefer, 1987).

The availability of satellite imagery for the modelled reach of the Missouri River synchronous to the flow records has enabled several fundamental research objectives to be addressed. Data from satellite images is ideal for use with 2-D fluvial hydraulic models being of a scale commensurate to the model resolution and being widely spatially distributed. In this study such data has the potential to be used for:

- validation of inundation extent predictions,
- identify regions of error,
- calibration data,
- process validation.

Remotely sensed data has the potential to be used more widely in hydraulic modelling for topographic and physical parameterization (Bates *et al.*, 1997) but these are ongoing research themes.

The images available for this study are Landsat TM for events 1 and 3 and SPOT (Système Probatoire pour l'Observation de la Terre) for event 4. The resolution of Landsat TM is 30m and SPOT is 10m, both higher than the resolution of the model so they are both more than adequate to supply the quality of data needed to achieve the above objectives.

Six sites have been chosen to be looked at along the modelled reach. They have been chosen specifically because of their complex bathymetry and topography, involving mud flats, permanent and temporary islands. The location of the six sites are shown on Figure 5.3. Side by side comparisons of the observed and predicted inundation are to be made using different friction values at all six sites followed by an overlay of the two showing the geo-referencing that can be done to the results.

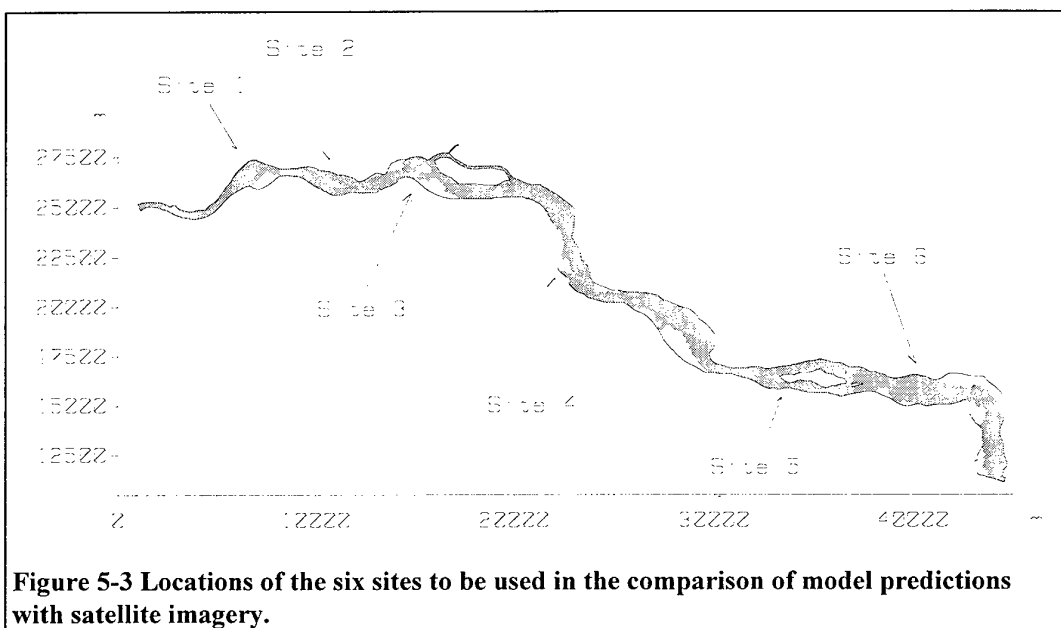


**Figure 5-3 Locations of the six sites to be used in the comparison of model predictions with satellite imagery.**

The side by side comparisons of the model predictions against the Landsat TM image, using bed friction values of 0.01, 0.02, 0.03 and 0.04, are shown in Figure 5.4a-f for the six sites. These figures plot the satellite image against the predicted flow field boundary as this is the model result that can be directly compared to the image. From these it can be seen that the model predictions are generally good, producing a close spatial match against the observed data. There are some obvious areas where the bathymetry/topography in the model is inadequate such as around the right hand end of the permanent islands in site 5 (Figure 5.4e). Potentially this type of information allows specific improvements in the model's bathymetry/topography to be made. The effect of varying the friction values on the spatial predictions varies from site to site. For example at sites 1 and 3 there is very little variation in inundated area but at sites 2 and 6 the size of the island(s) decreases substantially as the friction increases, i.e. as the water level rises. This allows calibration of the model to be carried out with such data by varying bed friction until there is a close spatial match between observed and predicted. This variable behaviour is caused by the gradient of the topography around the water surface. If the topography has a shallow gradient then changes in the bed friction, changing the water depth, causes changes in the inundated areas. Where the topographic gradient is steeper then the same changes in water depth shall have virtually no impact on inundated area. A problem arises in this specific case, as far as calibrating the model on this data, because the topography above the water surface was only estimated from US Department of the Interior



maps and is therefore probably not of the accuracy required to enable much confidence to be placed in the predictions of inundated area on islands. However estimated parameter values to calibrate the inundated area at sites 2 and 6 are 0.025 and 0.02.

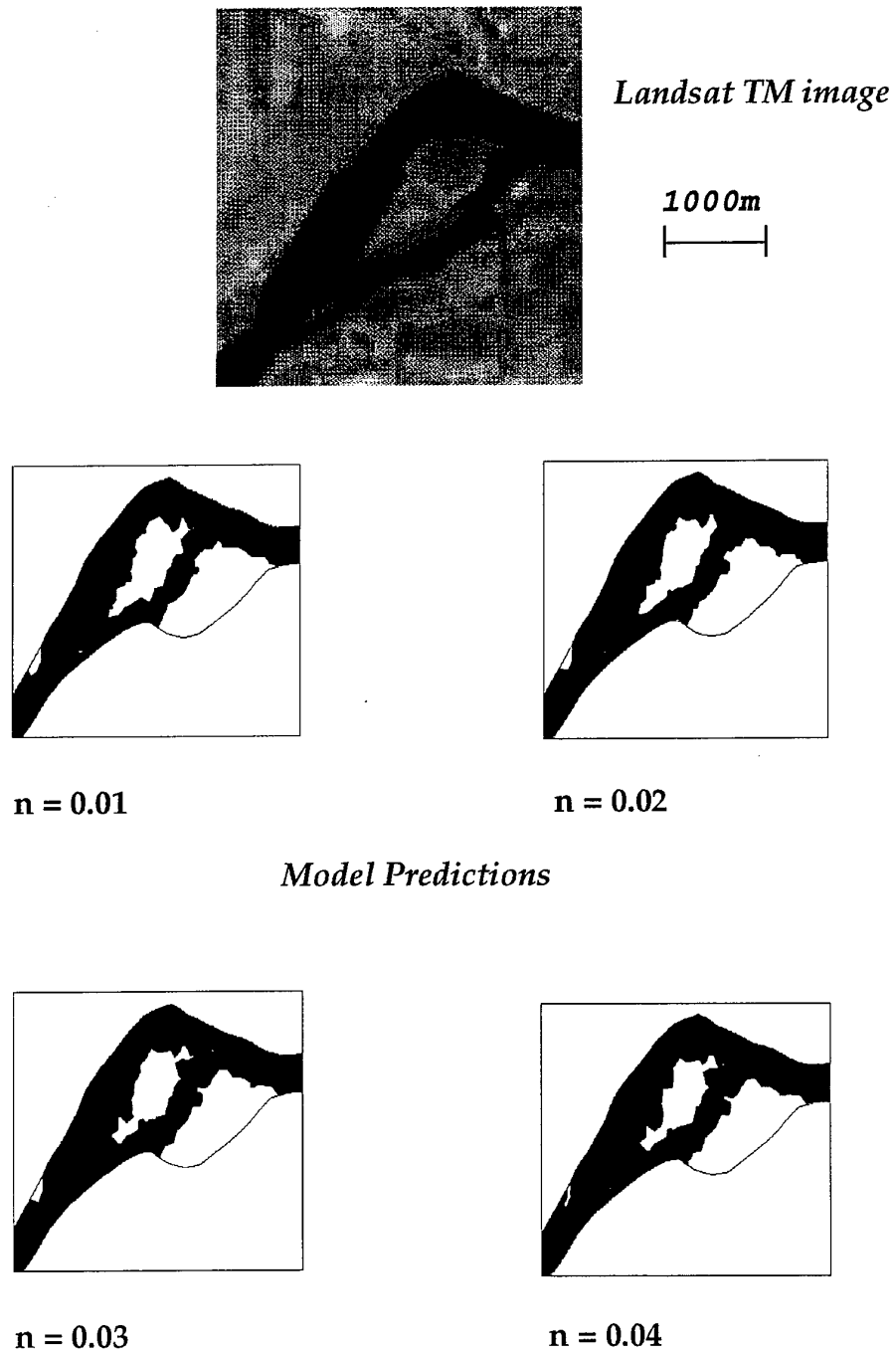


Figure 5-4a Comparison of Landsat TM image and 4 alternative model predictions with different bed friction (Manning's 'n') values at site 1 for event 1.

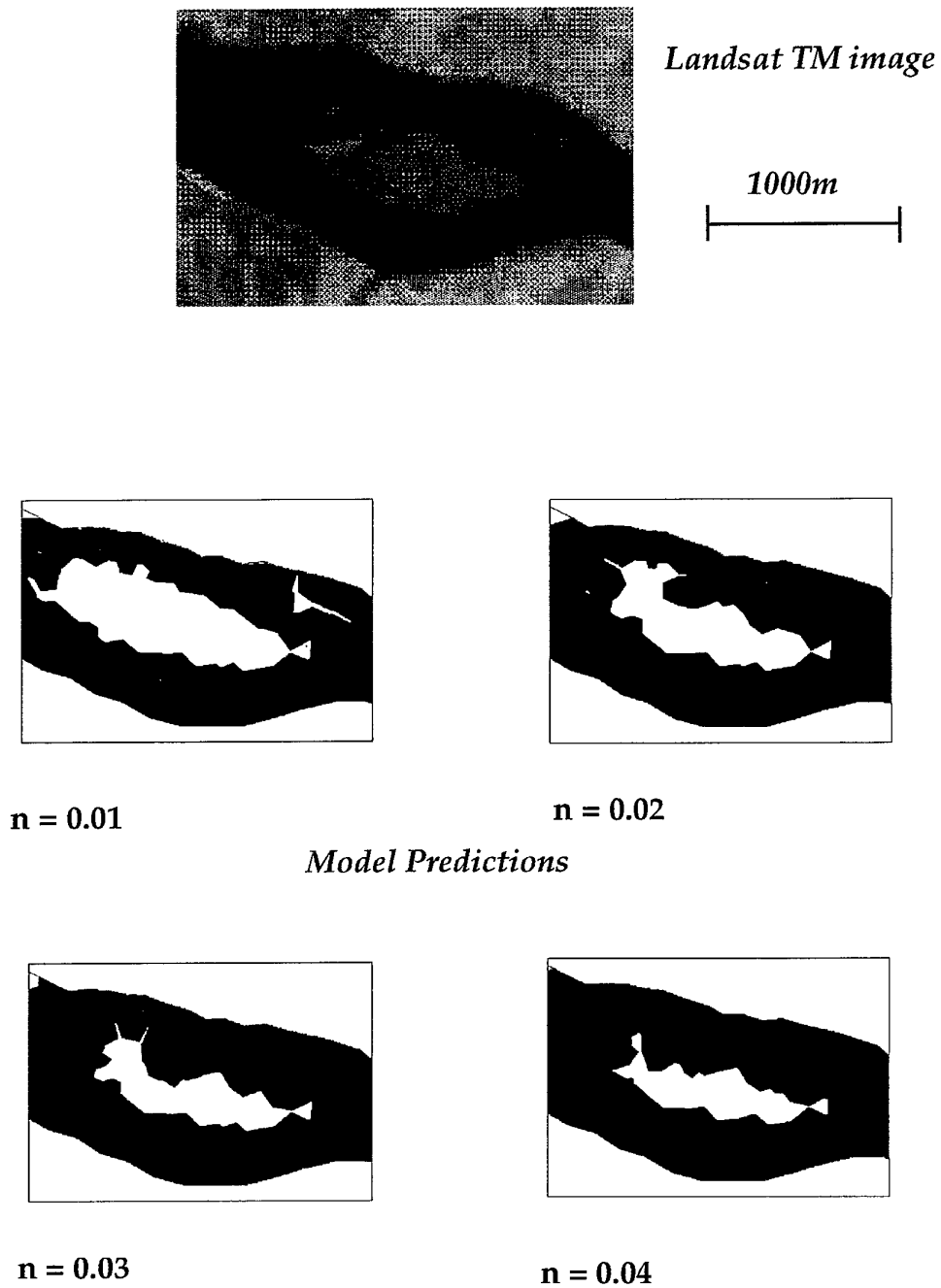


Figure 5-4b Comparison of Landsat TM image and 4 alternative model predictions with different bed friction (Manning's 'n') values at site 2 for event 1.

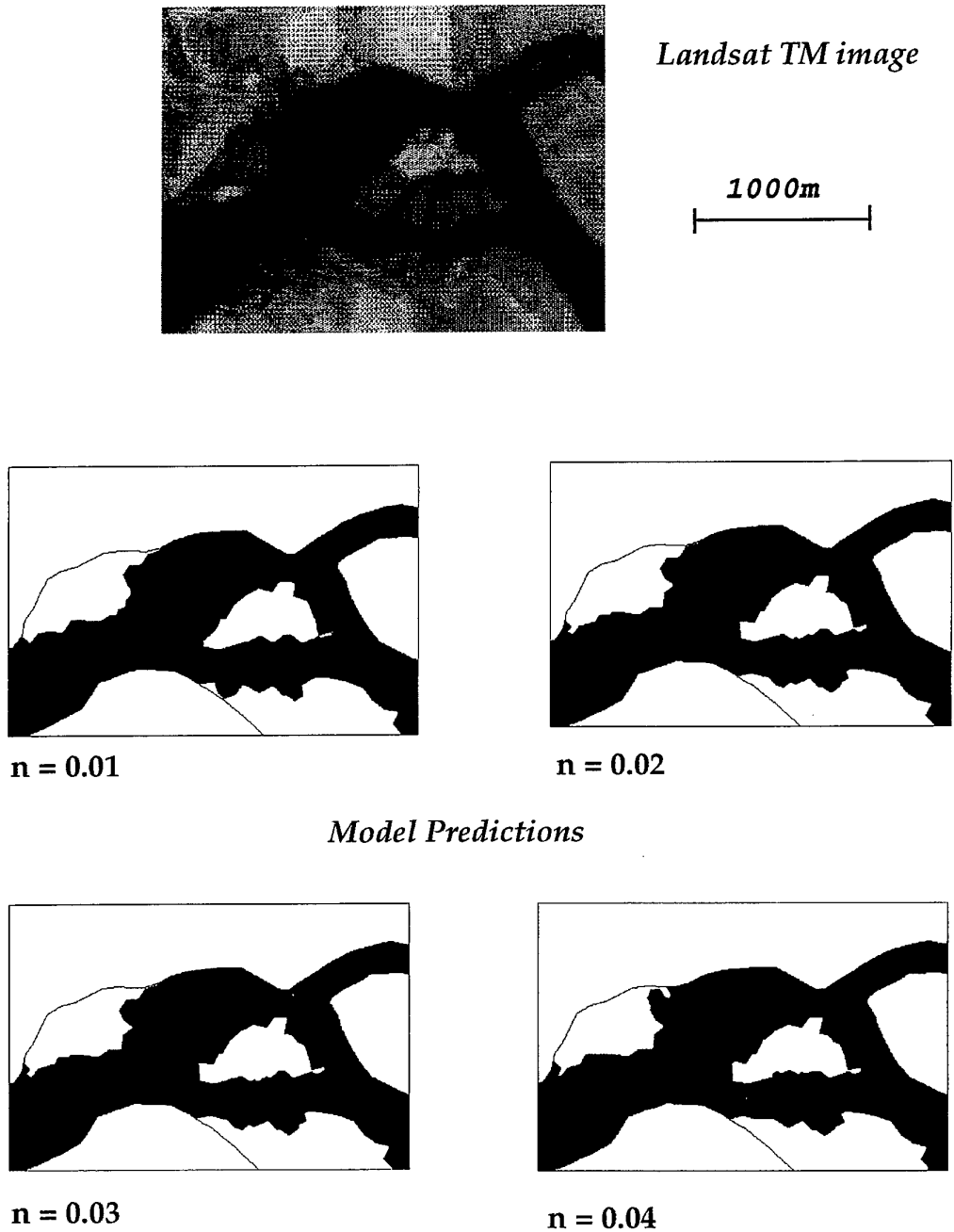


Figure 5-4c Comparison of Landsat TM image and 4 alternative model predictions with different bed friction (Manning's 'n') values at site 3 for event 1.

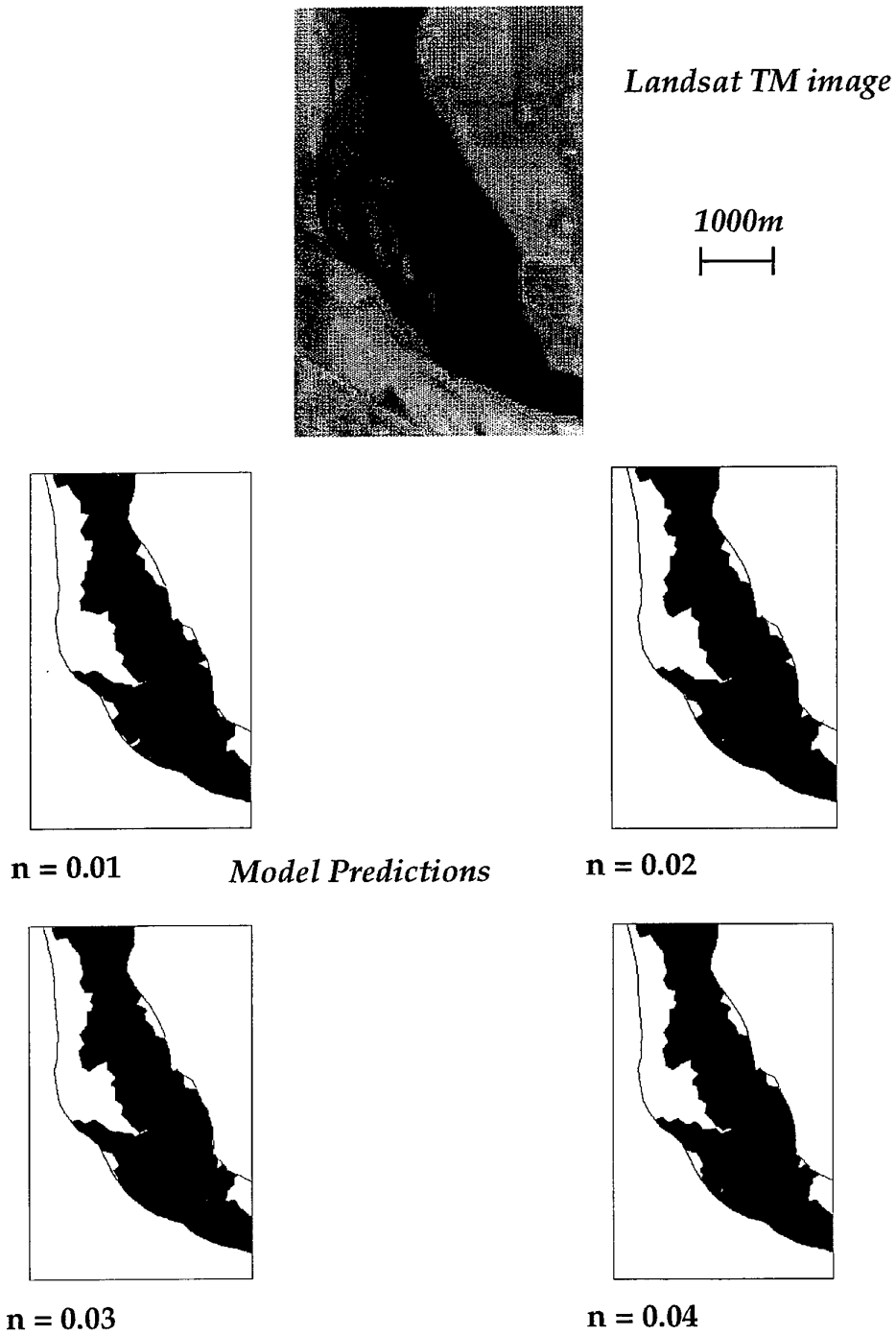
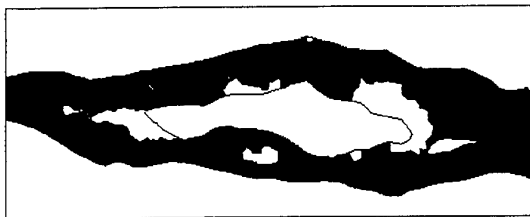


Figure 5-4d Comparison of Landsat TM image and 4 alternative model predictions with different bed friction (Manning's 'n') values at site 4 for event 1.

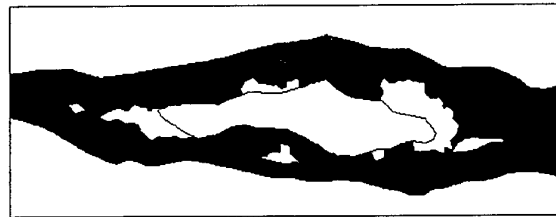


*Landsat TM image*

1000m

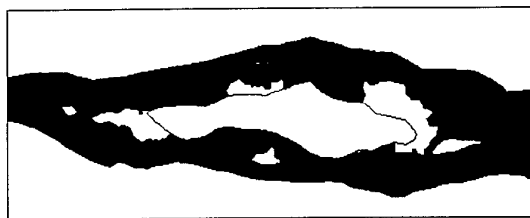


$n = 0.01$

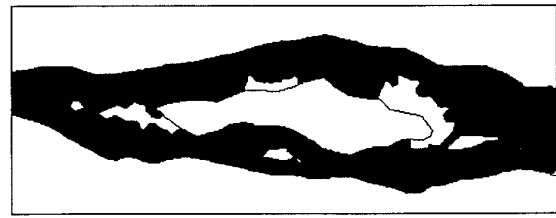


$n = 0.02$

*Model Predictions*



$n = 0.03$



$n = 0.04$

Figure 5-4e Comparison of Landsat TM image and 4 alternative model predictions with different bed friction (Manning's 'n') values at site 5 for event 1.

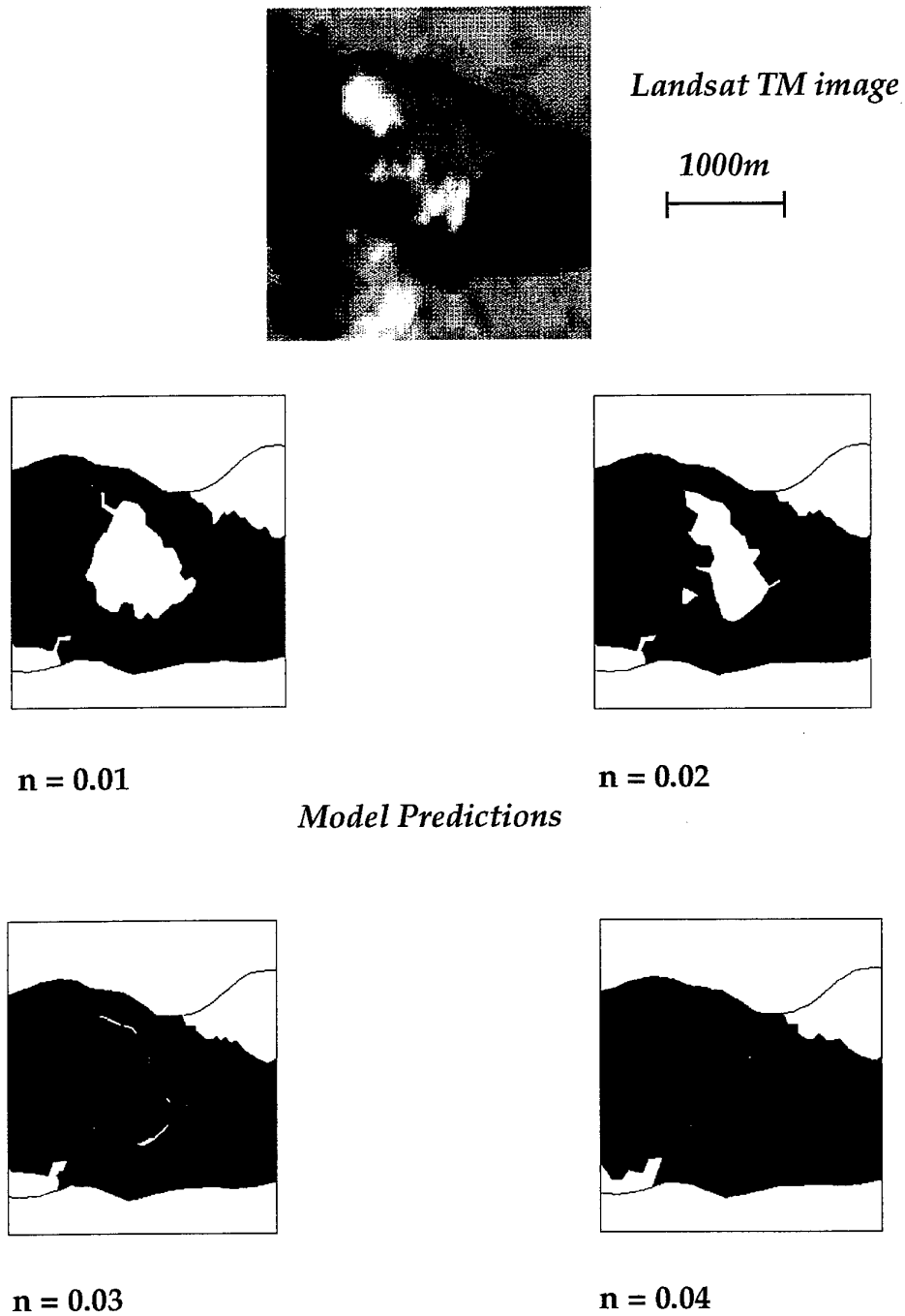


Figure 5-4f Comparison of Landsat TM image and 4 alternative model predictions with different bed friction (Manning's 'n') values at site 6 for event 1.

By geo-referencing the model results and satellite image an overlay of the two can be made. An example of such is shown in Figure 5.5 for a section of this reach. This detailed comparison between observed and predicted flow field boundary enables problem areas to be pinpointed and further model development to proceed by further data collection or adjustments to the model in these areas.



Figure 5-5 An overlay of the model prediction of flow field boundary onto the Landsat TM image for a region around Goat Island (including sites 5 and 6) for event 1.

### 5.1.3 Summary of Event 1

These first simulated flow conditions have shown the both the excellent predictions of the 2-D hydraulic model and the utility of the data sources to validate its performance. The internal stage data was matched at single points but not so closely at both points simultaneously. The inundation extent was validated against the satellite images very well. Some areas showed up problems in the models bathymetry/topography. Given possible future refinements in the model set-up the internal stage data should be able to be matched simultaneously at both sites quite easily. Matching all the flow field boundaries shall be more difficult given their dependence on the model bathymetry. This is however expected given the relative strength of the two validation types as discussed earlier.

## 5.2 Event 2 (25th June 1994)

This section of the 1994 flow record was chosen to be another period of steady state flow but with different flowrates than those in the previous event and temporally close to the previous event to eliminate potential effects of changing bed morphology. A section of the record around June 25th 1994 was identified as fitting these criteria. The inflow from Gavins Point Dam and the James River were virtually constant at 795m<sup>3</sup>/s and 52m<sup>3</sup>/s respectively (and the outflow stage at Maskell constant at 342.73m). The internal stage data was available at both sites for this time but unfortunately no satellite image could be obtained.

For these flow conditions the same series of seven runs with varying friction were carried out as for the calibration period. Again the results showed strong linear tendencies and have been treated in the same manner. In this case the equations relating water surface error to Manning's 'n' are:

$$\text{Yankton Error} = -0.327 + 32.44 n$$



$$\text{Gayville Error} = -0.981 + 30.00 n$$

Alternatively relating water depth to bed roughness (n) thus:

$$\text{Yankton Water Depth} = 4.77 + 32.44 n$$

$$\text{Gayville Water Depth} = 2.81 + 30.00 n$$

As with the regression lines for the previous case the residuals with these are very small indicating a high degree of confidence in the relationships within the range tested.

Again the values of bed roughness were calculated that eliminated the error at the two gauging stations in turn. These turned out to be 0.0101 to eliminate the error at Yankton and 0.0327 to eliminate the error at Gayville. Whilst the stage at Yankton is predicted correctly the prediction at Gayville is 0.68m too low (21.84% of the expected water depth) and conversely whilst the stage at Gayville is predicted correctly the prediction at Yankton is 0.73m too high (12.52%). Again a central value of bed roughness can be found that approximately equalises the errors at the two stations. In this case that value is 0.0214 and the error at Yankton and Gayville are 0.36m and -0.34m (6.59% and 9.85%) respectively.

The results from this flow event are very similar to those for event 1 despite the different flow conditions. This shows that the model has the potential to be robustly calibrated so that the a single parameter set could be used for any flow event if the bed morphology remains unchanged as it did between these first two flow events.

### 5.3 Event 3 (26th June 1984)

This event is during a period of very high flows in all the tributaries of the Missouri River, such as the James River. The volume of water being released from Gavins Point Dam is therefore very much reduced to counteract this and limit downstream flooding. No out of bank flow occurs along the modelled reach. A Landsat TM image of the reach on 26th June 1984 confirms this. Again this is a steady state run but several problems exist with the flow data:

- The James River gauge at Scotland stops recording as the flowrate tops 500m<sup>3</sup>/s just before the date of this simulation.
- No data is available for the downstream boundary at Maskell
- No internal stage data is available at Yankton and only daily values at Gayville.

The simulations are therefore more of an approximation than usual but the comparison to the satellite image makes them worthwhile. Again a full suite of seven simulations has been carried out with varying friction values.

The predicted water level at Gayville again showed a very strong linear tendency across the full range of bed friction values used. The regression equations for this can be written thus:

$$\text{Gayville Error} = -1.384 + 29.45 n$$

$$\text{Gayville Water Depth} = 2.73 + 29.45 n$$

The residuals with these regression equations are very small once again showing that a high degree of confidence can be placed in the predictions. The value of bed friction needed to eliminate the error in the prediction is however 0.0471 outside the range used to formulate the relationship. The model was therefore run at this value to confirm that this extrapolated prediction holds. The result from this simulation shows that the error is 0.025m at Gayville, indeed a very low error but not perfect, hence the relationship might be starting to break down

but it is unclear. This calibrated 'n' value is far higher than any other in any of the simulations. Two possible reasons for this are:

- Uncertainties in flow data mean that the model could be simulating a non-physical system hence needing an unrealistically large bed friction to compensate.
- This event was 10 years before the bathymetric data was collected hence substantial changes in the bathymetry over this period could have occurred again causing the substantial re-calibration to be necessary.

These two and other factors probably combined to cause this effect. It does however illustrate the way that model parameters can be used to overcome deficiencies in the model set up.

The model predictions are again compared to the satellite image at the 6 sites of interest (Figure 5.6a-f). At the first two sites, where the flow is very low, the bathymetric representation in the model is shown to be inadequate except with very high bed friction. A friction value of about 0.04 or higher is needed to calibrate the model at these sites. At sites 3,4 and 5 the comparison is quite close and varies very little with bed friction. At site 6 the inundation does vary considerably with friction, the closest match being at 0.03, but the positioning of the island could be much better. The model can therefore be said to predict the inundation well considering the time elapsed between this event and the collection of the bathymetric data. Some problems were apparent with the very low flow at the top of the reach.

Furthermore the conditions of the flow in this simulation, the channel geometry and the satellite image combine to allow an unrivalled degree of process validation to be performed. Process validation is, as the name suggests, simply comparing the processes in the field and the model. Potentially it is the most powerful form of model validation as it addresses the fundamentals of physically based modelling rather than simply the end results. The three factors allowing this form of validation to be carried out in this specific case are:

- The flow in the main stem is low but in the James River it is very high, more than likely out of bank further up the reach.
- The flood flows in the James River carry a large sediment load compared to the clear water released from Gavins Point Dam on the Missouri main stem. This facilitates the differentiation of the two water sources as water carrying large quantities of sediment has a higher reflectance than clear water in the visible region of the spectrum (Lillesand and Kiefer, 1987). The Landsat TM image used for this comparison has two wave bands in the visible spectrum allowing this difference to be picked up.
- The confluence of the two rivers occurs at the James River Island. The flow from the James River, under normal conditions, flows around the north of the island in a narrow channel before joining the main flow. Under flood conditions the possibility does exist for some of the flow to go round the Island the other way, joining the main stem much sooner.

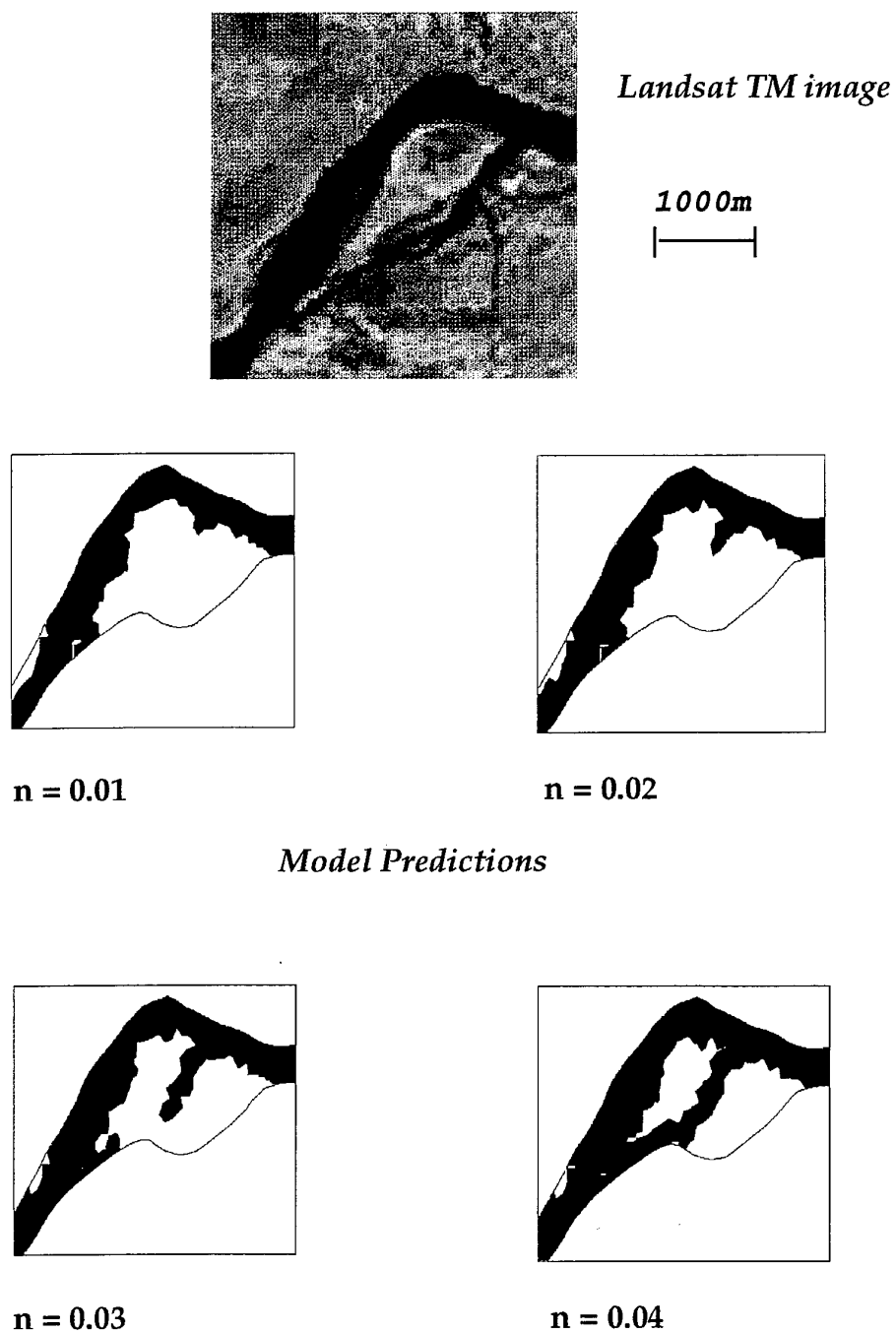
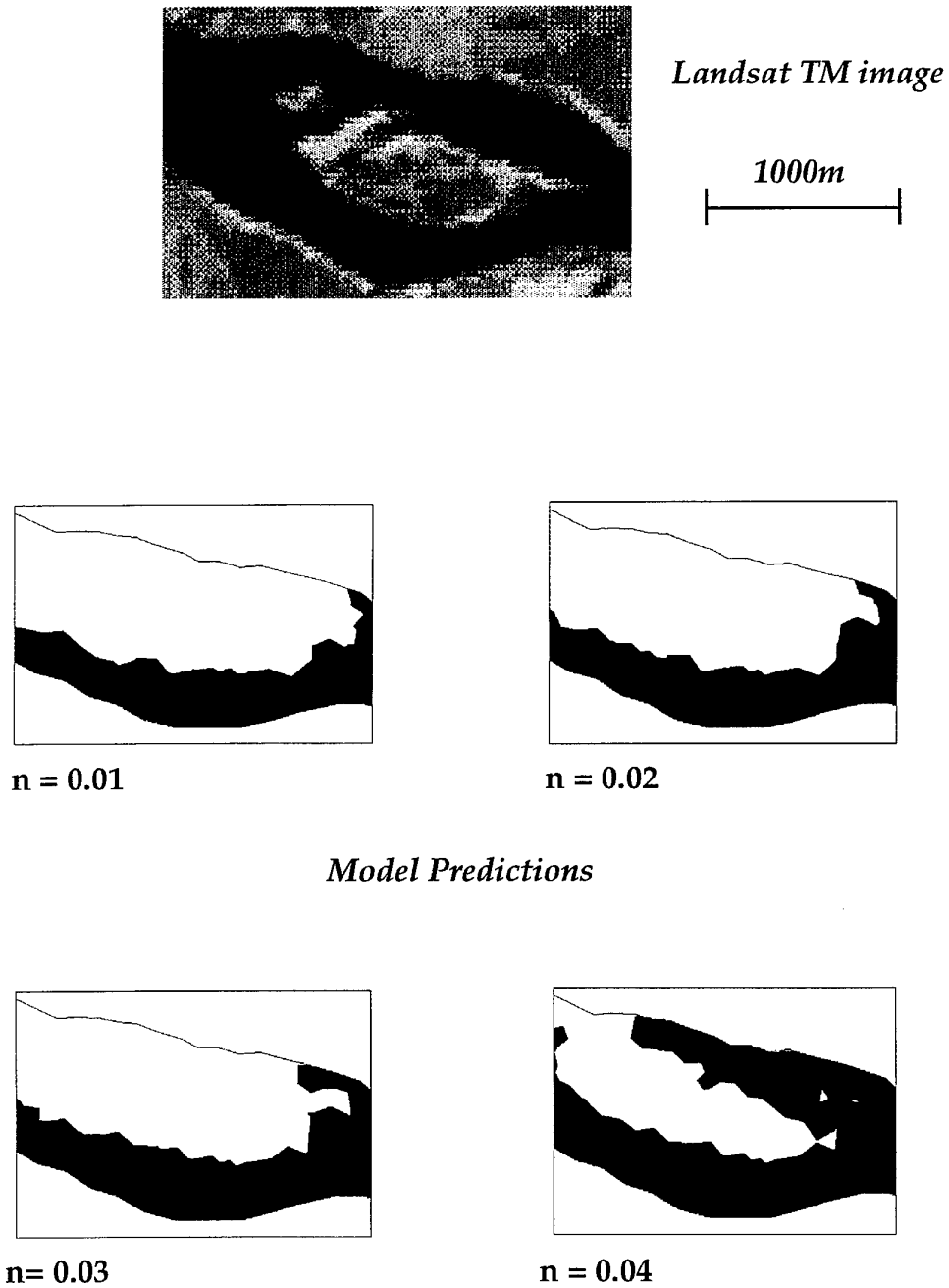
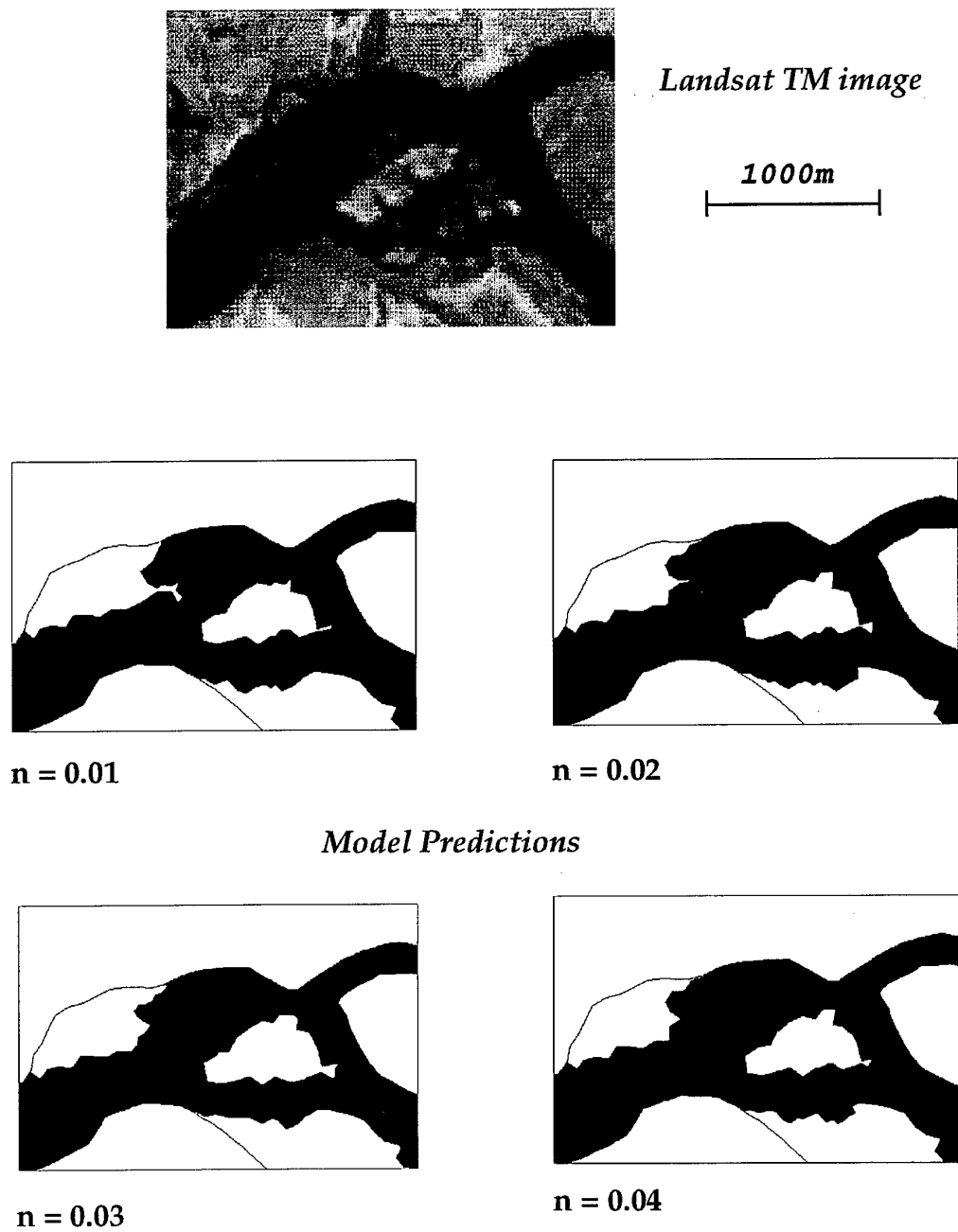


Figure 5-6a Comparison of Landsat TM image and 4 alternative model predictions with different bed friction (Manning's 'n') values at site 1 for event 3.



**Figure 5.6b Comparison of Landsat TM image and 4 alternative model predictions with different bed friction (Manning's 'n') values at site 2 for event 3.**



**Figure 5.6c Comparison of Landsat TM image and 4 alternative model predictions with different bed friction (Manning's 'n') values at site 3 for event 3.**

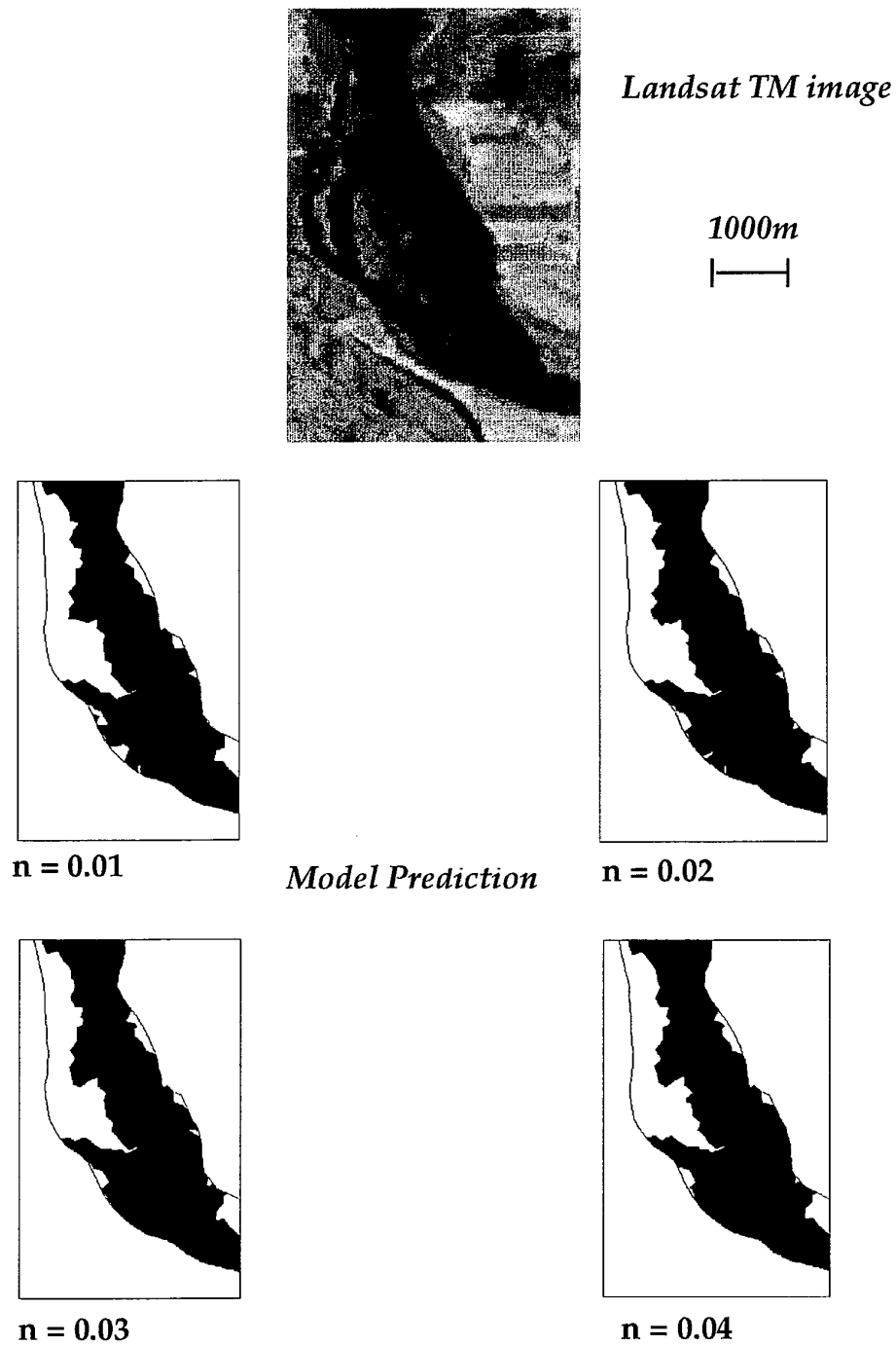
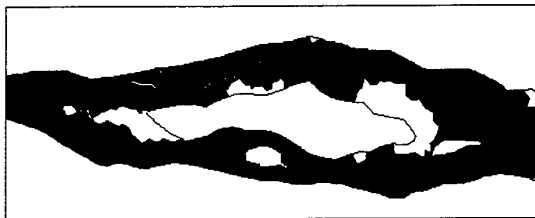


Figure 5.6d Comparison of Landsat TM image and 4 alternative model predictions with different bed friction (Manning's 'n') values at site 4 for event 3.

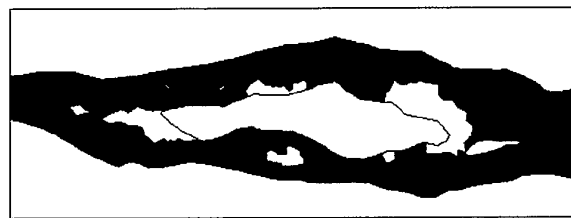


*Landsat TM image*

1000m

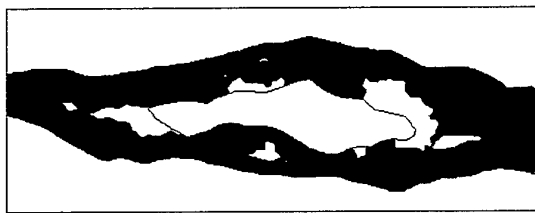


$n = 0.01$

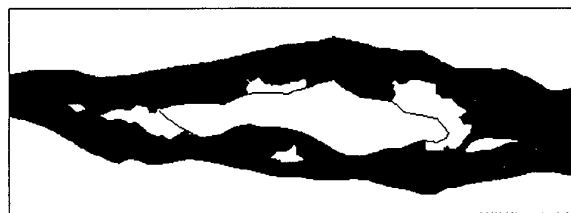


$n = 0.02$

*Model Predictions*



$n = 0.03$



$n = 0.04$

Figure 5.6e Comparison of Landsat TM image and 4 alternative model predictions with different bed friction (Manning's 'n') values at site 5 for event 3.

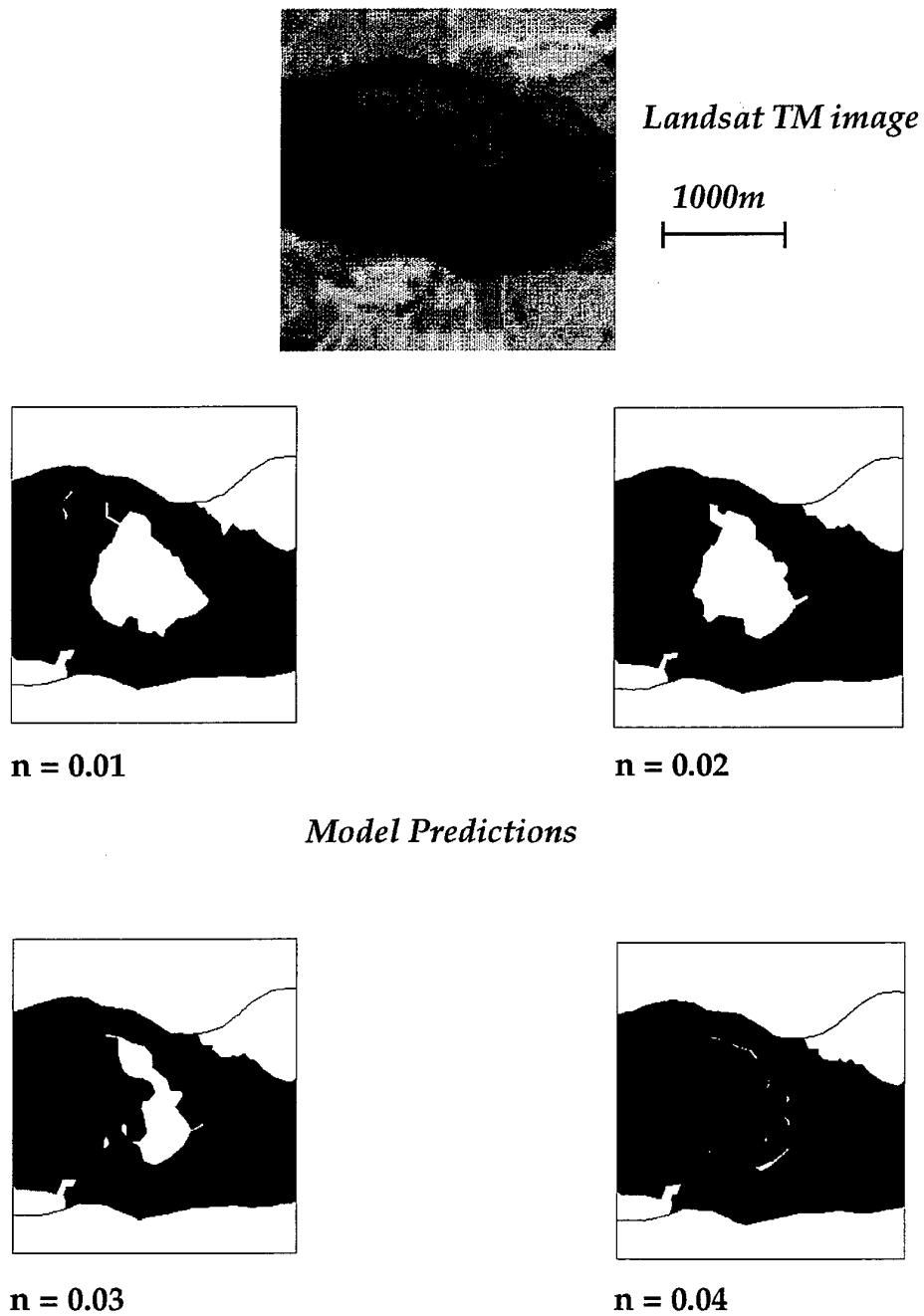
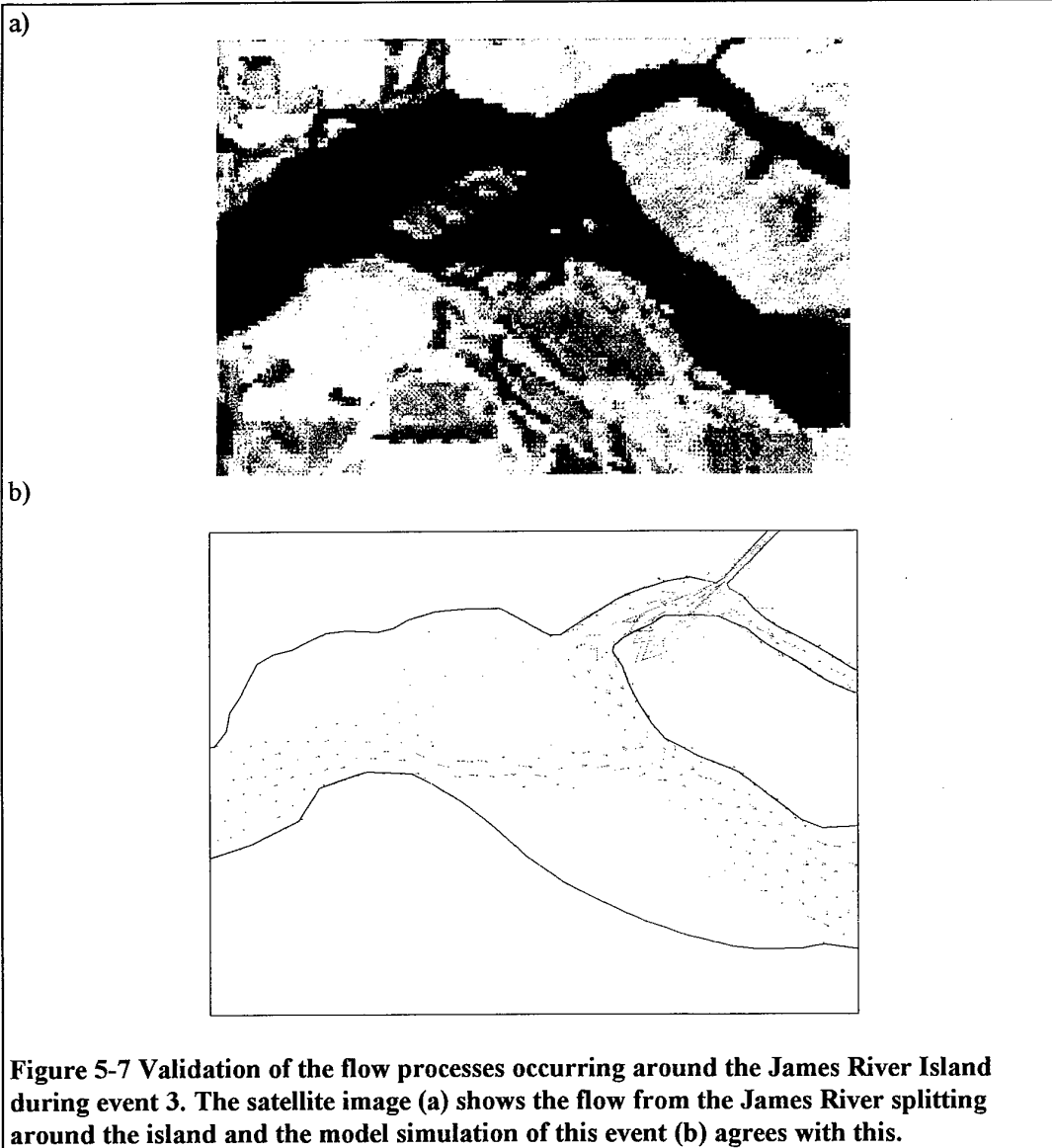


Figure 5.6f Comparison of Landsat TM image and 4 alternative model predictions with different bed friction (Manning's 'n') values at site 6 for event 3.



Looking first at the satellite image of the confluence (Figure 5.7a) it can clearly be seen that the flow does split around the James River Island as was hypothesised as occurring in flood conditions. This flow pattern, around the island, compares very well to the model prediction (Figure 5.7b). The model can therefore be said to represent the flow processes occurring under these novel conditions.



This flow event had substantial problems in its set-up but despite this valuable results have been achieved. Firstly the internal stage data was shown that it could be matched even if outside the range of parameter values expected. Secondly, flow field validation against satellite data was shown to be good but some problems exist perhaps because of channel morphology changes between when the image was taken in 1984 and when the bathymetric data was collected in 1995. Finally an example of the most powerful form of validation, process validation is shown. This is a very limited example of this but does illustrate that the model simulates the essential flow processes occurring in the reach.

#### 5.4 Event 4 (8th February 1991)

Contrary to the previous event this one is under conditions of very low flows from both the Missouri main stem and virtually non-existent flow in the James River. This creates a new set of problems for the model. A full set of internal data and a high resolution SPOT image taken on 8th February 1991 of most of the reach are available.

A brief inspection of the image shows that the low flows cause the channel to become braided, the flow filling only a tiny portion of its usual channel. Comparison of this to the first model run ( $n = 0.025$ ) shows instantly that the model is not highly resolved enough or containing great enough bathymetric data to allow the simulation of the braided channel (Figure 5.8). Further runs would therefore be irrelevant.

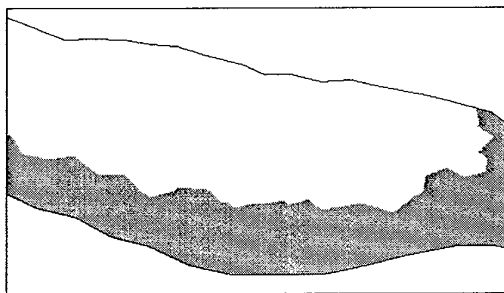
A quick comparison of the predicted to observed stage values at Yankton and Gayville is shown in Table 5.2. The match is reasonable but could no doubt be calibrated to be much closer but again this is pointless given the evidence showing the model is failing to represent the processes under these flow conditions.

**Table 5-2 Comparison of observed and predicted water surface elevations at Yankton and Gayville on 8th February 1991.**

	Yankton	Gayville
Observed (m)	351.13	348.24
Predicted (m)	351.58	348.84

Simulating this flow event has highlighted problems in the model performance under very low flow conditions. The model bathymetry is not refined enough to simulate the braided channel that forms under these conditions as shown on the satellite image.

*a)*



*b)*

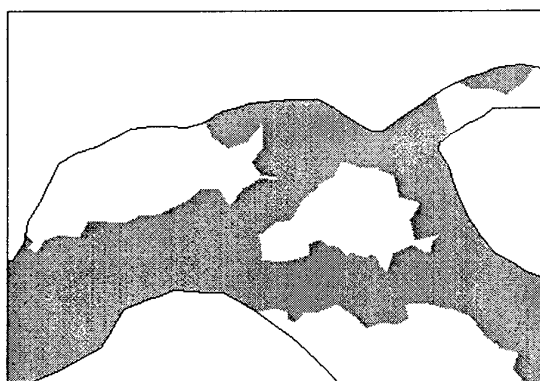
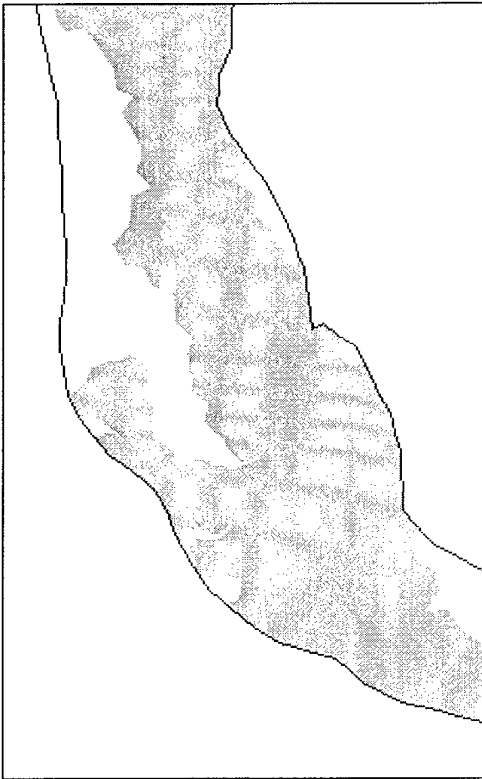


**Figure 5-8 Comparison of SPOT image to model predictions for event 4 at (a) site 2 and (b) site 3.**

c)



d)

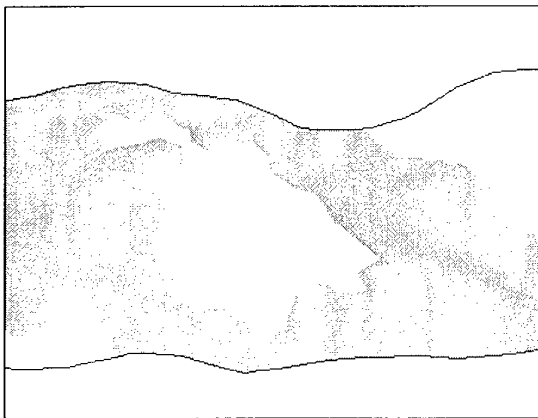


**Figure 5.8** Comparison of SPOT image to model predictions for event 4 at (c) site 4 and (b) site 6.

e)

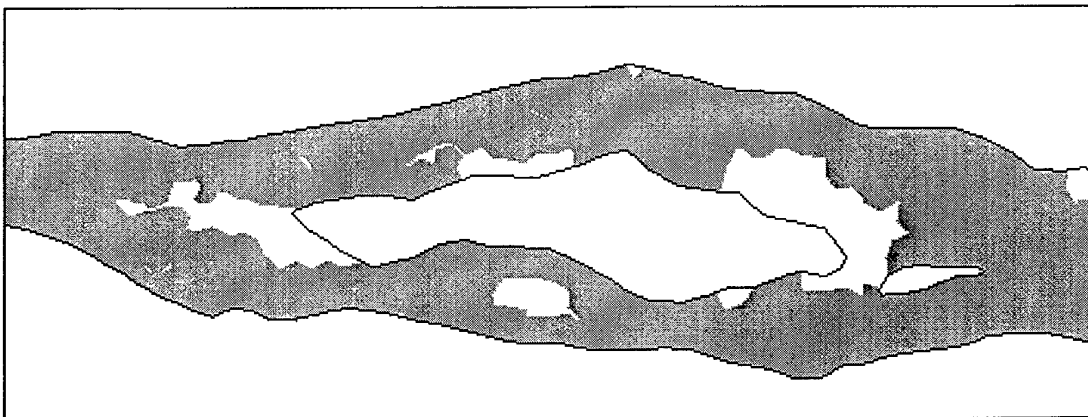


**Figure 5.8 Comparison of SPOT image to model predictions for event 4 at (e) site 5.**

### 5.5 Event 5 (13th - 14th June 1994)

Previous events have all been modelled under steady state conditions but this event is the one dynamic section of the flow record that has been simulated. Hence simulation of this event is the first step in analysing the performance of Missouri River application of TELEMAC-2D with conditions varying with time. The event covers a twelve hour period from 13.00 hrs on the 13th June 1994 until 01.00 hrs on the 14th. During this period the inflow from the James River remains constant at  $45\text{m}^3/\text{s}$  but the inflow from Gavins Point Dam decreases from  $905\text{m}^3/\text{s}$  to  $765\text{m}^3/\text{s}$  between 14.00 hrs and 15.00 hrs on the 13th. The outflow elevation at Maskell decreases from 342.9m to 342.8m during the final 6 hours of the simulation. Initial conditions for the simulation are the steady state using these starting values, which are that exact conditions for event 1. No satellite image is available for this event but stage elevations at both Yankton and Gayville are available hourly throughout. Performance can therefore be analysed through time but only at two points in space.

Simulations of this event were carried out for Manning's 'n' values from 0.01 to 0.04 in increments of 0.005, the predicted and observed results at Yankton and Gayville are plotted in Figure 5.9. Looking first at the behaviour of the model over this dynamic event shows that the bed friction influences not only the water surface elevation, as seen before, but also the timing of the changes at the gauge stations. This has potential implications to the calibration of the model. Now the predicted and observed data are compared at the two stations.

With the initial conditions of these simulations being identical to those in event 1 the calibrated 'n' values from that event can be used here. Hence initially the calibrated value at Yankton is 0.0118 and Gayville is 0.0306. Figure 5.9(a and b) confirms this. At the end of the simulations the stage values (observed and predicted) at Yankton have returned to a steady state. At Gayville, further down the reach, they are still changing. Immediately noticeable from Figure 5.9a is that at the end of the simulation the calibrated 'n' value at Yankton is different than at the start. The same is likely true at Gayville if Figure 5.9b is extrapolated. At Yankton the ideal parameter value decreases over the simulation but at Gayville it seems to increase. This is consistent with event 2 where the flow conditions are similar to those at the end of this event. In effect this shows that at Yankton the model predicts a larger change in water surface elevation than is observed and at Gayville the opposite occurs (Table 5.3). The nature of the change of the stage values is slightly awkward to analyse given the relative low density of the observed data. Figure 5.9a shows that the predicted decline in water surface elevation at Yankton is earlier and quicker but not as great as the observed. At Gayville (Figure 5.9b) the predicted reduction is later, slower and larger than the observed.

**Table 5-3 Observed and predicted changes in water surface elevation over dynamic event 5.**

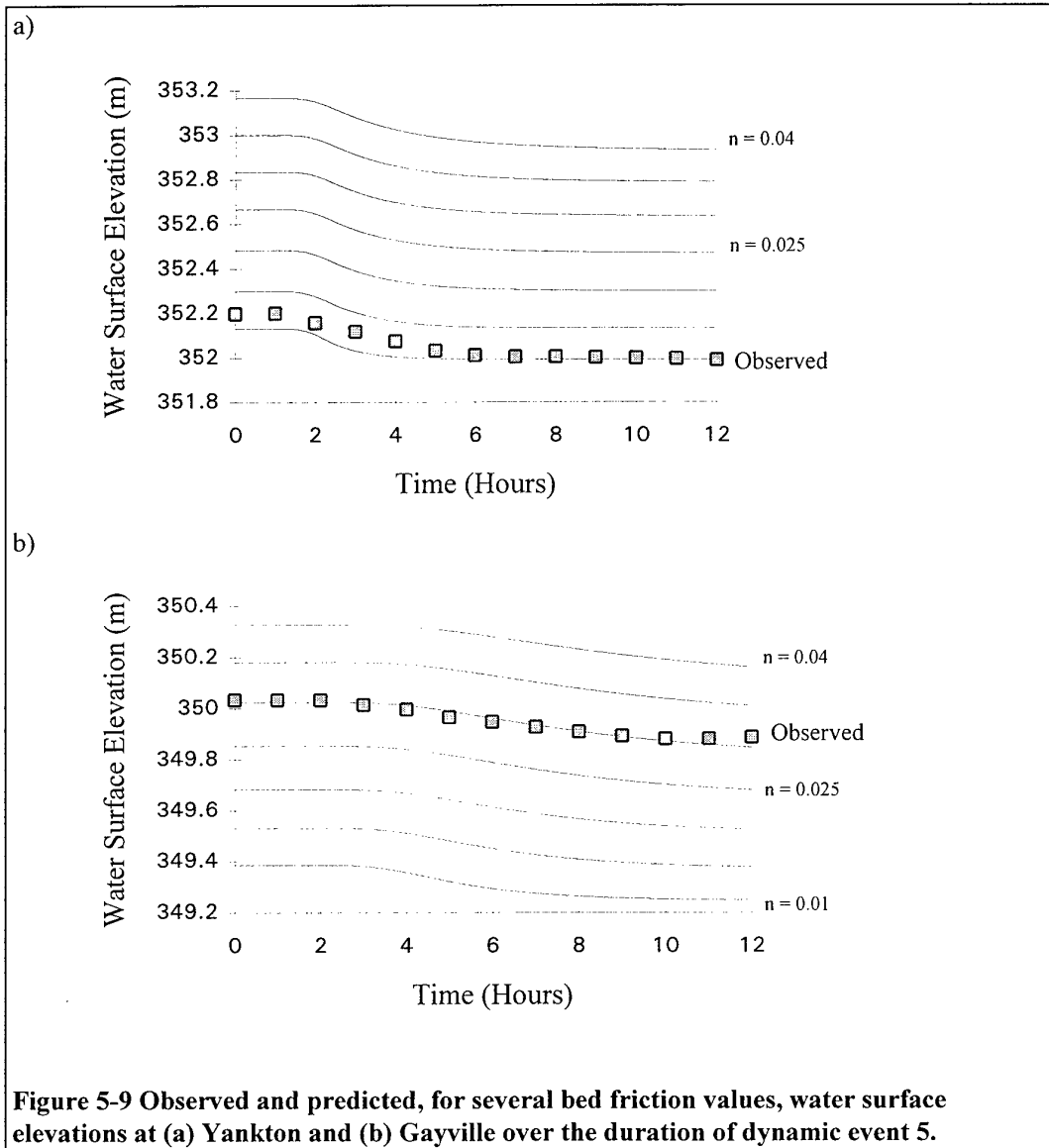
	Yankton	Gayville
Observed Change (m)	0.207	0.146
Predicted Change (m)	0.140	0.177

These simulations on the Missouri River application of TELEMAC-2D show that the model does predict the change in water surface elevation at two points fairly accurately under dynamic stresses, the timing and magnitude of the changes being broadly comparable with the observed given the overall uncertainties involved. Two problems do however stand out:

- The continuing different behaviour at the two gauge stations, this time extending over the full dynamic event.

- Only having a single parameter to vary means that the water surface elevation and timing cannot be varied separately but change together with friction.

Overall however this initial test shows that this model is capable of simulating dynamic flow events with a high degree of accuracy within the model domain. Further tests, preferably with spatially distributed comparison data, would be necessary to make a more comprehensive case for the models application in such events.



### **5.6 Summary of the comparison to observed data**

The model has been tested over widely varying flow conditions and compared to data through time and space. In general the model has been shown to be a good simulator of the river hydraulics under most conditions. The only serious problems occurred under exceptionally low flow conditions. The available data allowed detailed comparisons of observed and predicted giving an invaluable portrayal of model performance. The strength of the model validation has also been assessed. The weakest form of validation here is the internal stage data. This has been matched to about 0.3m at point sites on a first approximation of the model set-up. Further changes to the model parameters could reduce these errors significantly. The next step up in validation is the 2-D flow field boundary validation against the satellite imagery. Again this was shown to be good for a first attempt. Some areas in the model bathymetry were shown to be inadequate to meet this level of validation. Further data collection and model refinement would be necessary to meet this higher level of model validation. A simple example of process validation was also illustrated. The model was shown to represent the essential flow processes in this particular limited example.

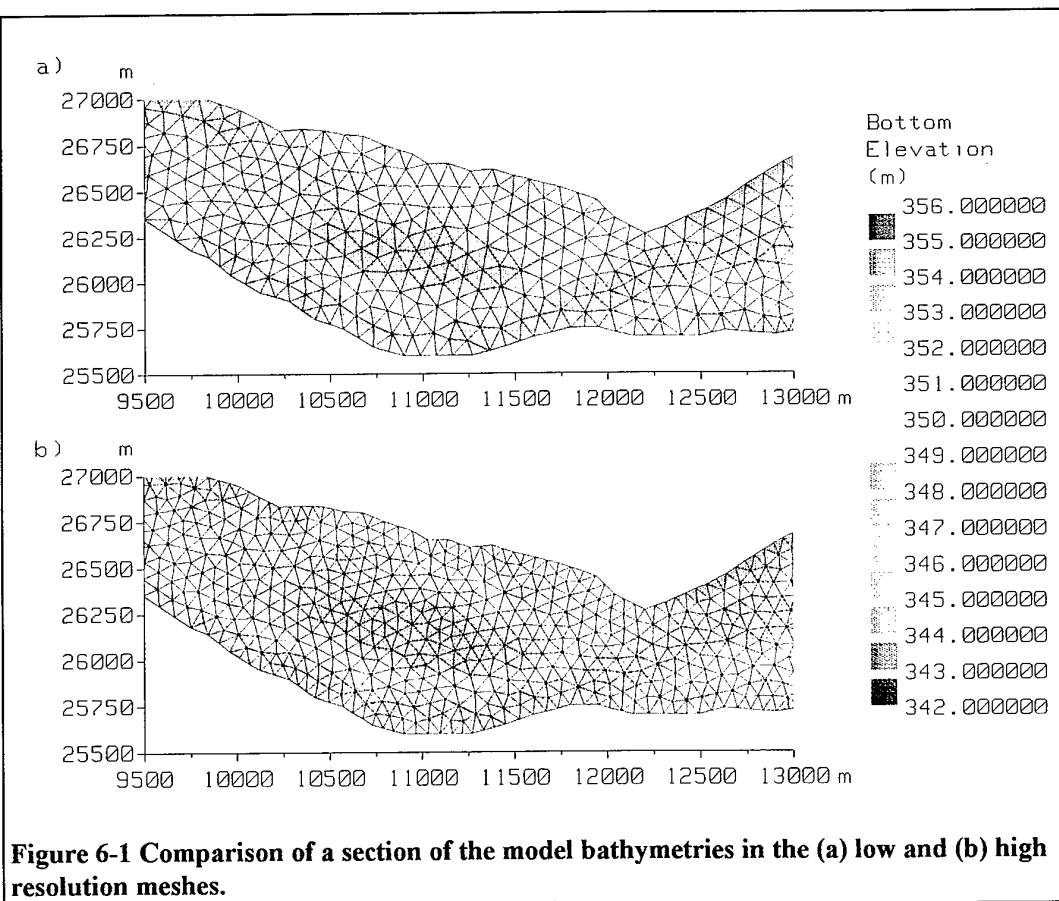
The first three objectives of this study have therefore now been achieved. A high-space time distributed model of river hydraulics has been produced and shown to be a good representation of the fluvial system. The validation data supplied by the Corps of Engineers has also been shown to be invaluable to the assessment of model behaviour and its effectiveness in achieving an improved partial validation of the model estimated.



## 6. Mesh Resolution Comparison

The two meshes and their relative sensitivities have been discussed previously. This section looks first at some aspects of the differing bathymetric representation between the two meshes and then the predictions of the high resolution mesh are compared to the observed data for the steady state event 1. Again simulations have been carried out for varying bed friction values from 0.01 to 0.04, incrementing by 0.005.

The higher resolution mesh allows a more detailed representation of the bathymetry of the river. However whether this representation is more accurate is unclear as the bathymetric data is more widely dispersed than even the low resolution mesh. Figure 6.1 shows an example bathymetric representation of the two meshes at one areas of the reach. Although the bathymetries are broadly similar, as would be expected, small differences do exist around potentially sensitive areas such as sand banks or channel boundaries. Whether they are improved in the high resolution mesh shall be explored later when predictions are compared to the satellite image.



### 6.1 Comparison to observed data

Firstly, however, the performance of the higher resolution model at the two internal gauge stations is examined. Regression equations have again been formulated as the models response is linear at both stations and can be written thus:

$$\text{Yankton Water Depth} = 4.39 + 32.63 n$$

$$\text{Gayville Water Depth} = 2.24 + 33.00 n$$

The results from applying these equations and the comparison with the lower resolution mesh can be seen in Table 6.1. From this table of results it can be seen that the bed friction values are consistently larger with the higher resolution mesh and the errors are also greater in every case. Using the more highly specified model cannot therefore be justified on this evidence.

**Table 6-1 Comparison of the calibrated results from the two meshes.**

	Mesh 1	Mesh 2
'n' value for zero error at Yankton	0.0118	0.0124
Corresponding error at Gayville (m)	-0.60 (18.26%)	-0.76 (28.69%)
'n' value for zero error at Gayville	0.0306	0.0354
Corresponding error at Yankton (m)	0.65 (10.96%)	0.75 (13.53%)
Intermediate value of 'n'	0.0212	0.0239
Corresponding error at Yankton (m)	0.33 (5.89%)	0.37 (7.16%)
Corresponding error at Gayville (m)	-0.30 (8.37%)	-0.38 (12.55%)

The same six sites have been chosen for the spatial comparison of model results from the high resolution mesh to the Landsat TM image as were used earlier with the lower resolution mesh. Again the images are compared side by side to four model predictions with varying bed friction (Figure 6.2). It is immediately evident that the resolution of the predictions is higher, than for the low resolution mesh (Figure 5.4) but whether this offers an improvement in prediction is however not so clear. Closer inspection of the figures suggest that in some areas the new predictions do have a closer spatial match, such as at sites 3 and 4, but this is by no means conclusive.

Compared to the low resolution mesh, figure 6.2 shows that to attain the same amount of inundation the friction values must be higher with the high resolution mesh. This is evident at sites 1,2,4 and 6 and concurs with the results for the stage values. Therefore it can be said that to achieve the same water surface elevation requires a higher friction value in the high resolution mesh. Why this should be so is unclear but could be a result of differing topographic or parameter representations.

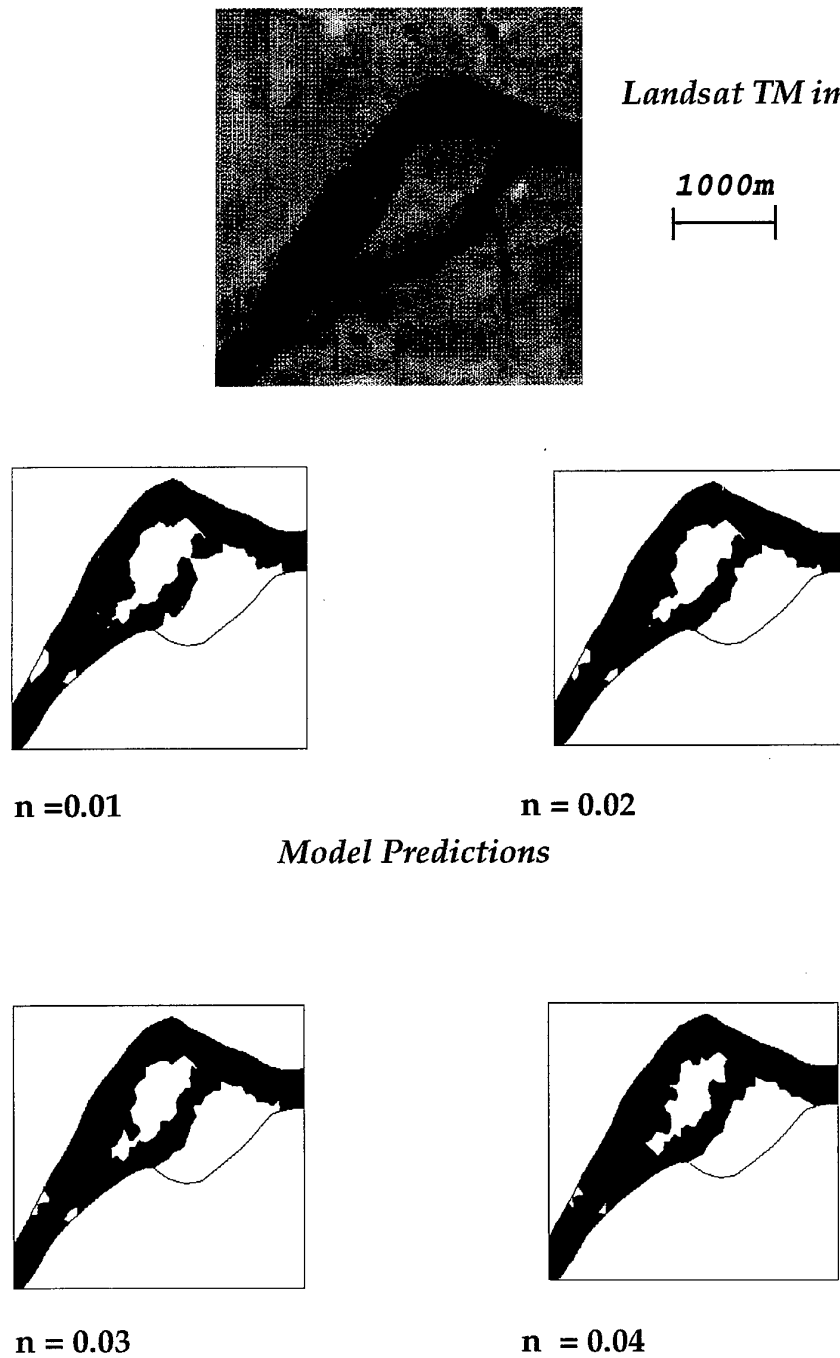


Figure 6-2a Comparison of Landsat TM image to 4 alternative model predictions with different values of bed friction (Manning's 'n') on the high resolution mesh (mesh 2) for event 1 at site 1.

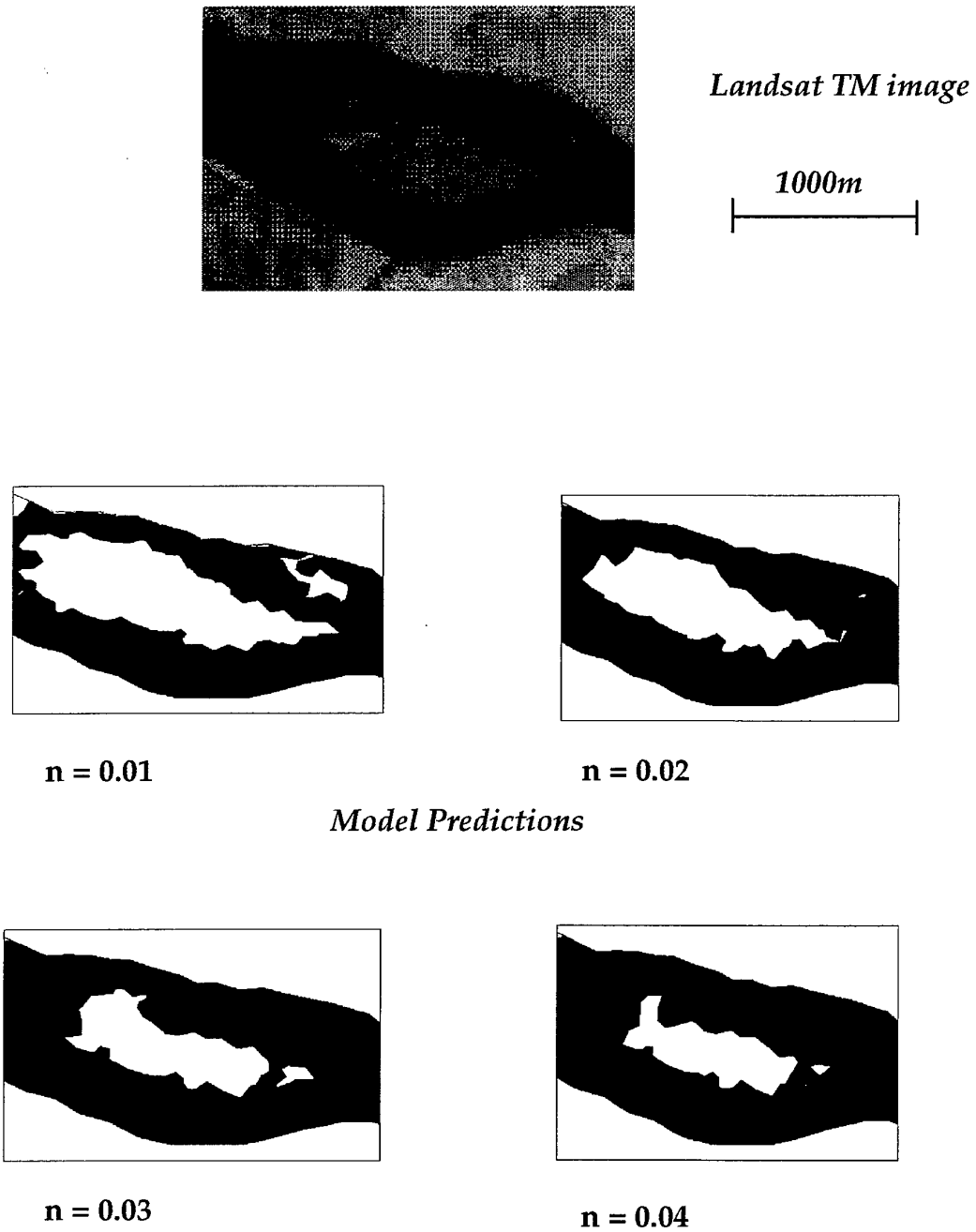


Figure 6-2b Comparison of Landsat TM image to 4 alternative model predictions with different values of bed friction (Manning's 'n') on the high resolution mesh (mesh 2) for event 1 at site 2.

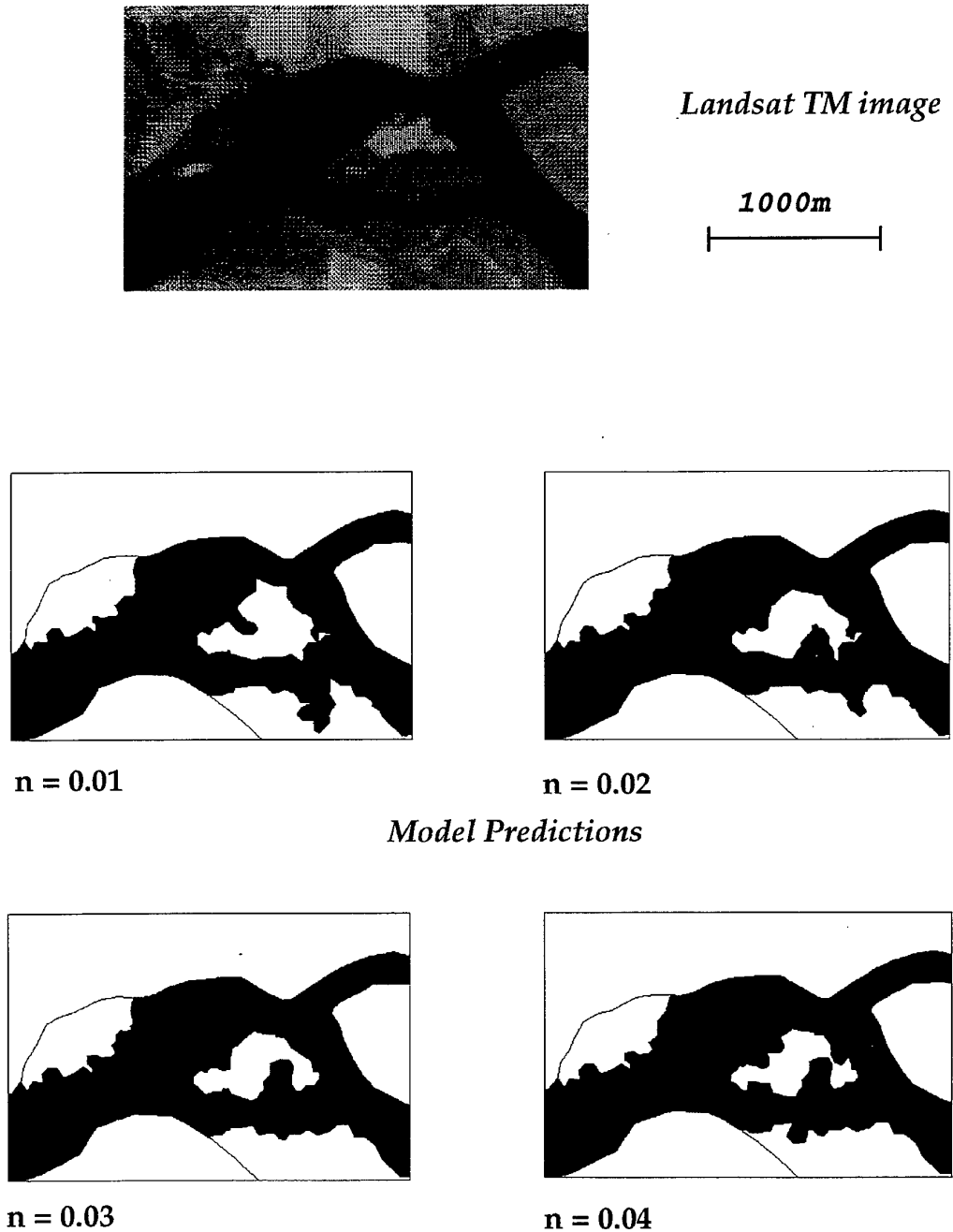


Figure 6-2c Comparison of Landsat TM image to 4 alternative model predictions with different values of bed friction (Manning's 'n') on the high resolution mesh (mesh 2) for event 1 at site 3.

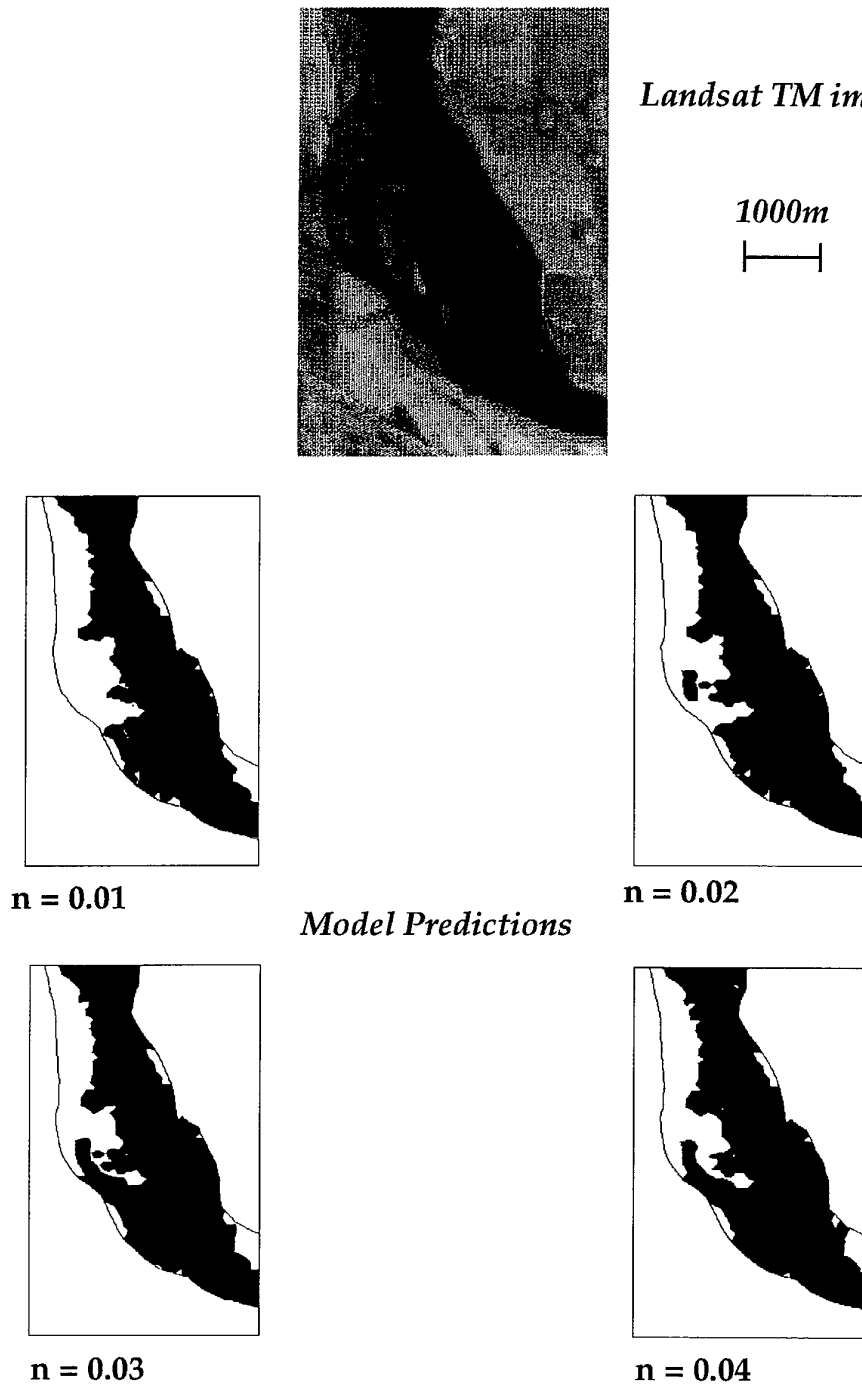
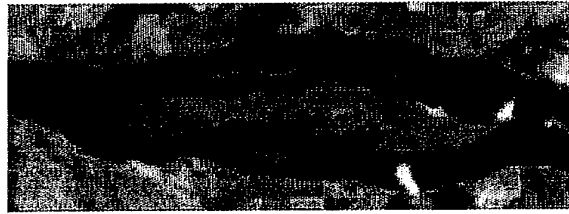
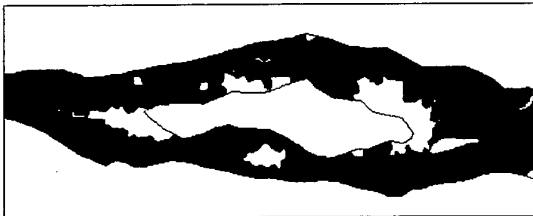


Figure 6-2d Comparison of Landsat TM image to 4 alternative model predictions with different values of bed friction (Manning's 'n') on the high resolution mesh (mesh 2) for event 1 at site 4.

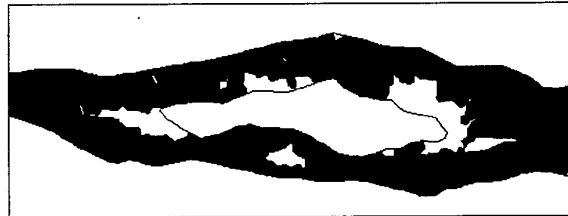


*Landsat TM image*

1000m

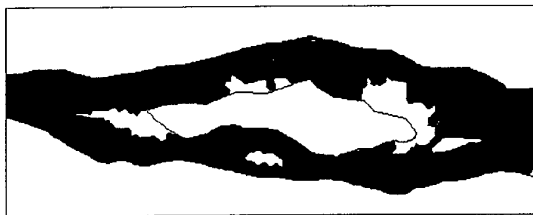


$n = 0.01$

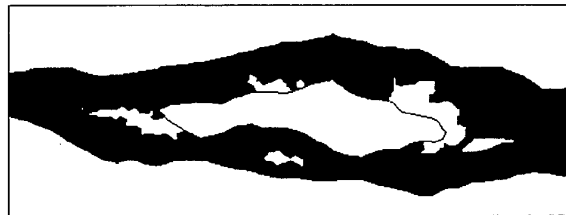


$n = 0.02$

*Model Predictions*



$n = 0.03$



$n = 0.04$

Figure 6-2e Comparison of Landsat TM image to 4 alternative model predictions with different values of bed friction (Manning's 'n') on the high resolution mesh (mesh 2) for event 1 at site 5.

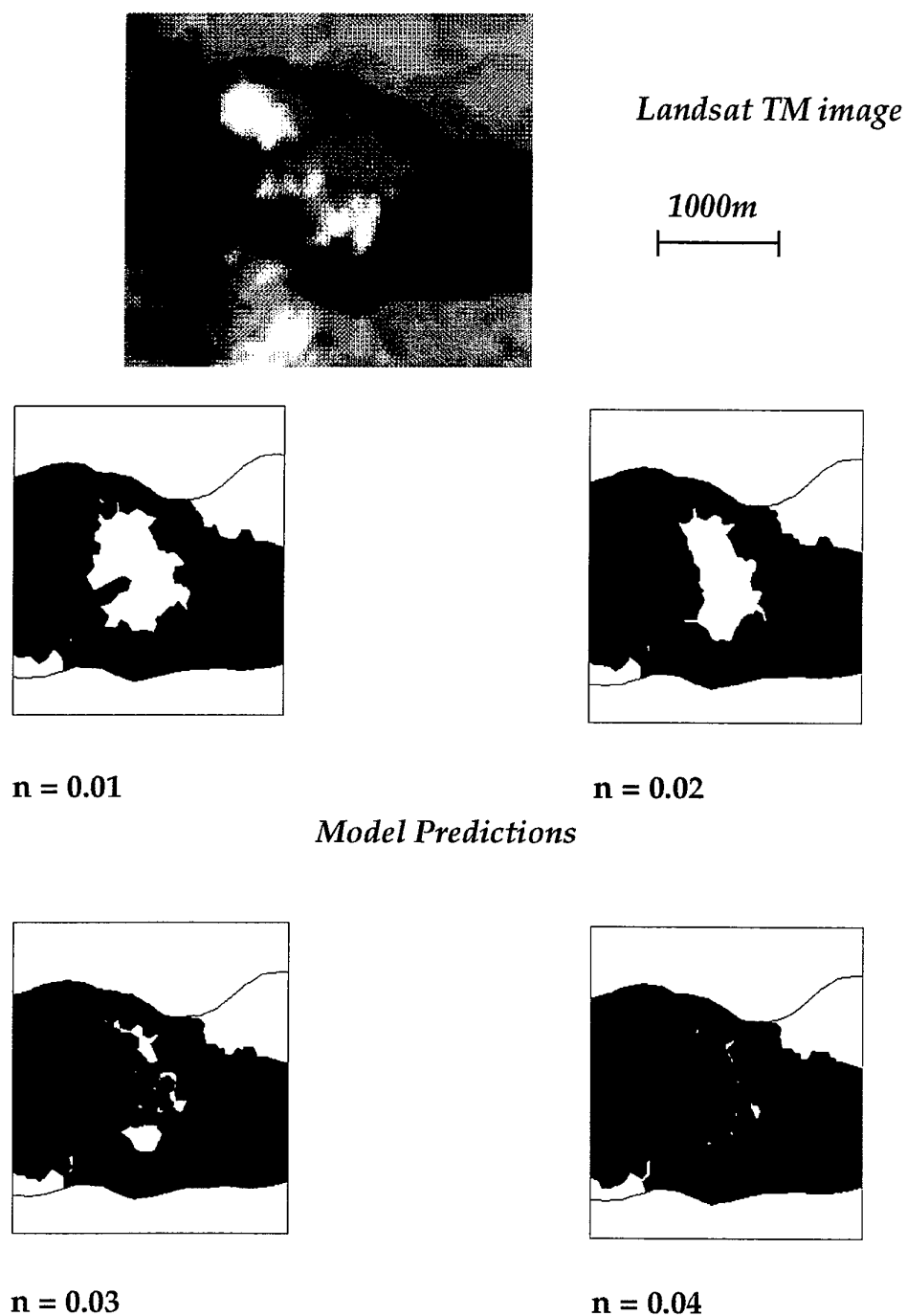


Figure 6-2f Comparison of Landsat TM image to 4 alternative model predictions with different values of bed friction (Manning's 'n') on the high resolution mesh (mesh 2) for event 1 at site 6.



## **6.2 Summary**

This brief look at the impact of mesh resolution on the model results has shown this to be an important factor. The bed friction values must be higher to achieve the same results than with the lower resolution mesh and the bathymetry is of a higher resolution, if not more accurate. Mesh resolution is a continual problem with no obvious solution except perhaps a compromise between increased representation with a high resolution mesh and reduced computational expense with a lower resolution mesh. Where this compromise lies is difficult to judge unless increased validation data is available to judge model performance in even more detail to justify increasing the representation in terms of model results improvements. From this study this would not seem to be the case given the limitations imposed by the data, particularly bathymetry. The following section continues to look at the bathymetric data in terms of its impact on model predictions.

## 7. Bathymetric Data Requirements

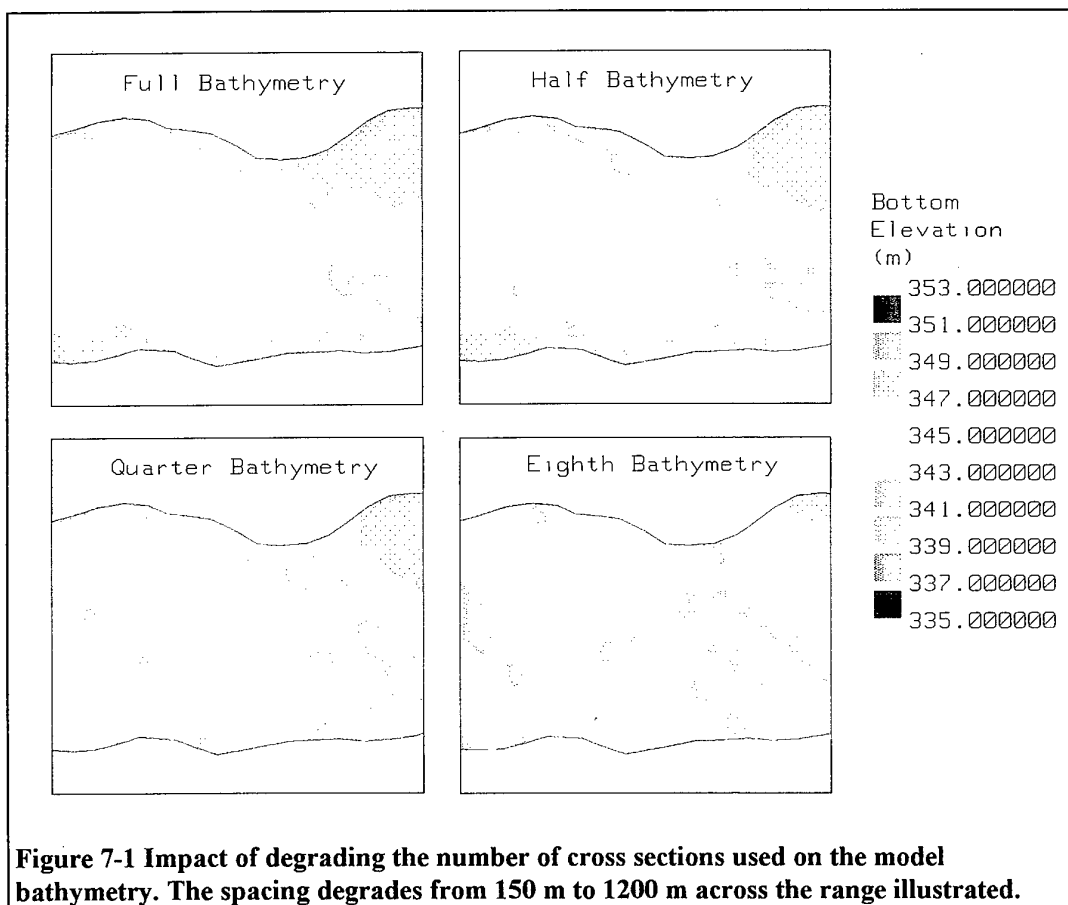
The high cost of collecting bathymetric and topographic data must be justified by attaining high quality model results that could not be accomplished with a more basic representation. The impact of the density of cross section on the models bathymetry and model predictions are investigated in this section.

Four realisations of the model bathymetry were created using:

- all the available cross sections (150 m spacing),
- alternate cross sections (300 m spacing),
- one in four cross sections (600 m spacing),
- one in eight cross sections (1200 m spacing).

From each of these data sets the model bathymetry was created at the node points on the low resolution mesh using the directional interpolator described in section 3.2. The model was then run once with each of these representations for the conditions of event 1 with a bed friction value of 0.025.

The impact of these changes on the model bathymetry was profound. Figure 7.1 shows the impacts in one example area (site 6). As can be clearly seen the detail of the bathymetric representation in the model degrades rapidly as the number of cross sections decrease.



## 7.1 Comparison to observed data

The influence of changing the level of bathymetric data on the water surface elevation predictions at Yankton and Gayville is shown in Table 7.1. From this table it can be seen that at Yankton the level of data provision has minimal effects on the predictions, varying them by only 0.1m compared to an actual error of approaching 0.5m. At Gayville, however, decreasing the bathymetric produces a continuous increase in water surface elevation. The magnitude of the change over the runs is 0.72m, spanning the observed value. The half data set run produces a prediction of water surface elevation at Gayville within 0.015m of the observed value.

**Table 7-1 Water surface elevations at Yankton and Gayville for simulations with the various levels of bathymetric data supplied to the model.**

Location	Full	Half	Quarter	Eighth	Observed
Yankton	352.667	352.751	352.665	352.721	352.196
Gayville	349.854	349.990	350.398	350.578	350.032

From these results there appears to be little benefit in using the highest density data set as the results are equally good using half the data. The quarter and eighth runs do however show decay in the quality of the results at Gayville. The more important results are however the spatially distributed ones that are now investigated.

Once more the side by side comparisons have been made for model predictions, this time with the 4 levels of bathymetric data, against the Landsat TM image at the 6 sites of interest (Figure 7.2). In each case the full bathymetry appears to give a favourable comparison against the observed data. Reducing the bathymetric data has a major influence on the spatial predictions. In some cases this manifests itself even when half the data is used such as at sites 1,3 and 6, where the spatial match degrades rapidly. As the data reduction continues huge errors are introduced at some of the sites, e.g. site 1, but not so in other, e.g. site 2.

## 7.2 Summary

The results from this section have shown the bathymetric data to have a profound influence on the spatial predictions of the 2-D hydraulic model and a lesser influence on the water surface elevation. This fits well with the rigour of validation discussed in section 5. There it was proposed that matching internal stage values was a weaker form of validation than matching 2-D inundation. These results show that a more poorly specified model, i.e. that with less bathymetric data, can match the internal stage values but not the inundation extent. Hence inundation extent validation is a more rigorous test of model performance.

From these results it would seem, as expected, that the highest density of bathymetric data produces the best results. More detailed simulations looking at the relationship between mesh resolution, bathymetric data density and distribution, and interpolation method must be carried out before more detailed guidelines on the optimum level of bathymetric data can be considered.

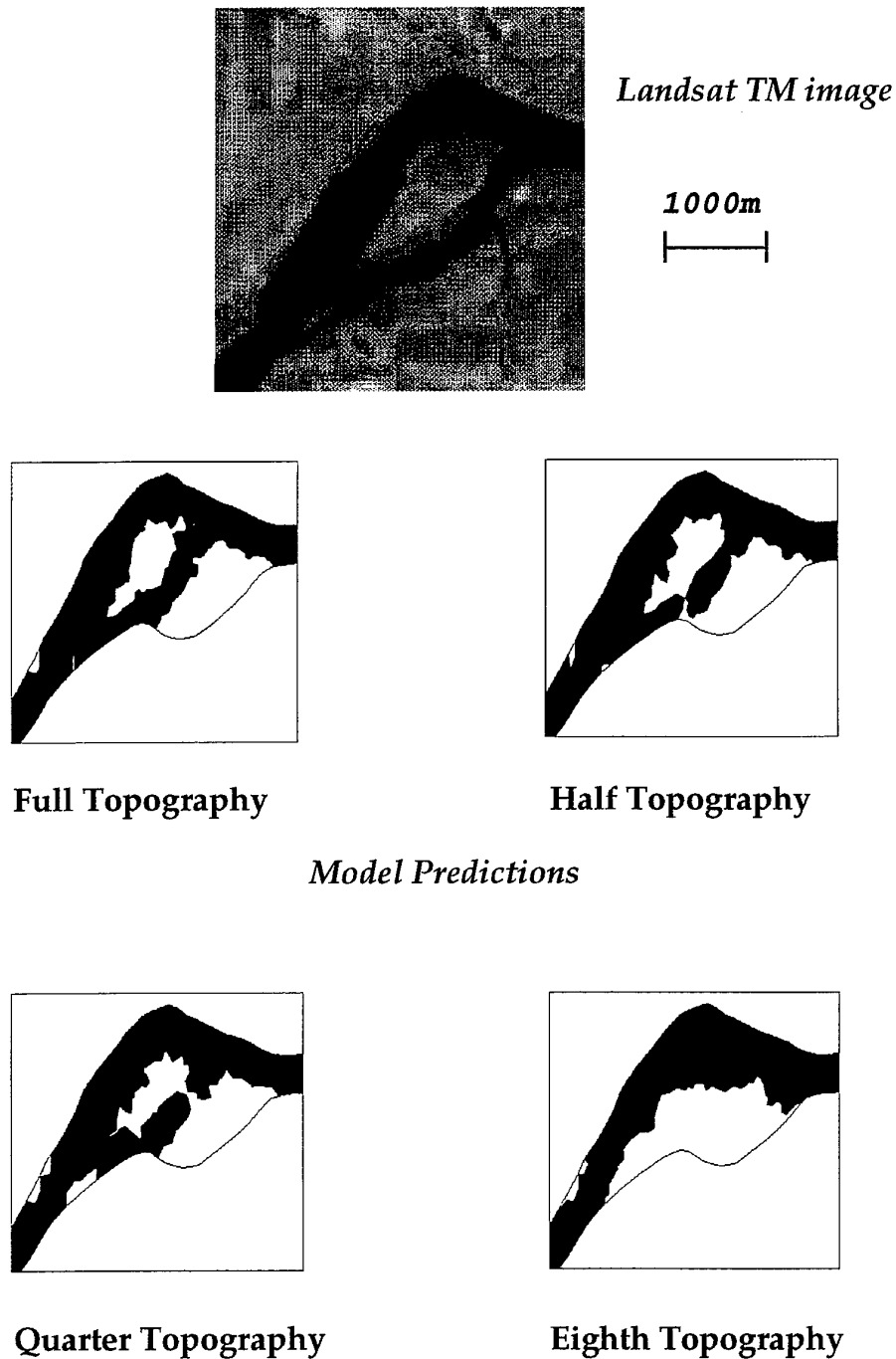


Figure 7-2a Comparison of the Landsat TM image to model predictions with the 4 levels of model bathymetry used for event 1 at site 1. The bathymetries were created by varying the spacing of cross sections used from 150 m to 1200 m.

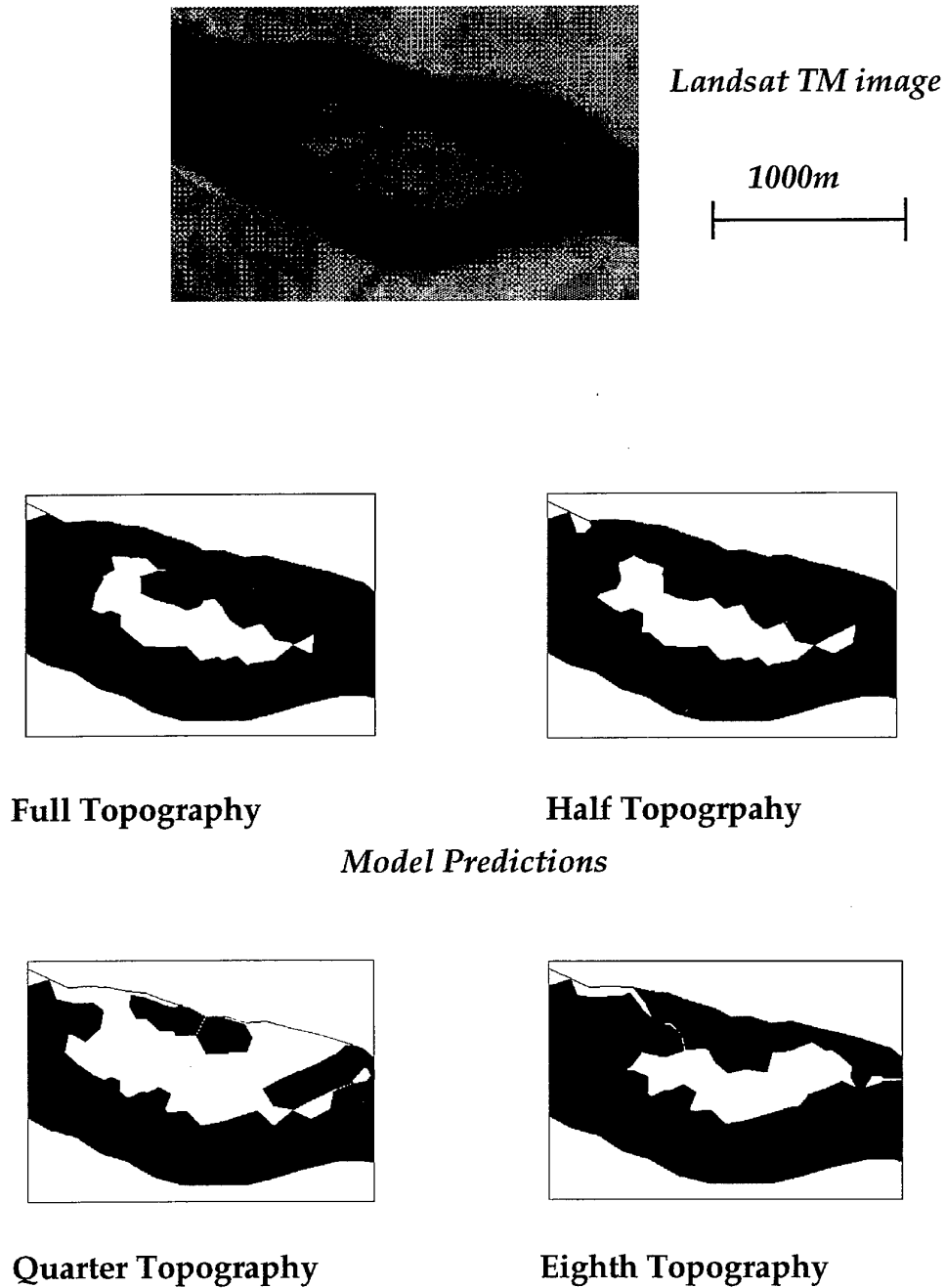


Figure 7-2b Comparison of the Landsat TM image to model predictions with the 4 levels of model bathymetry used for event 1 at site 2. The bathymetries were created by varying the spacing of cross sections used from 150 m to 1200 m.

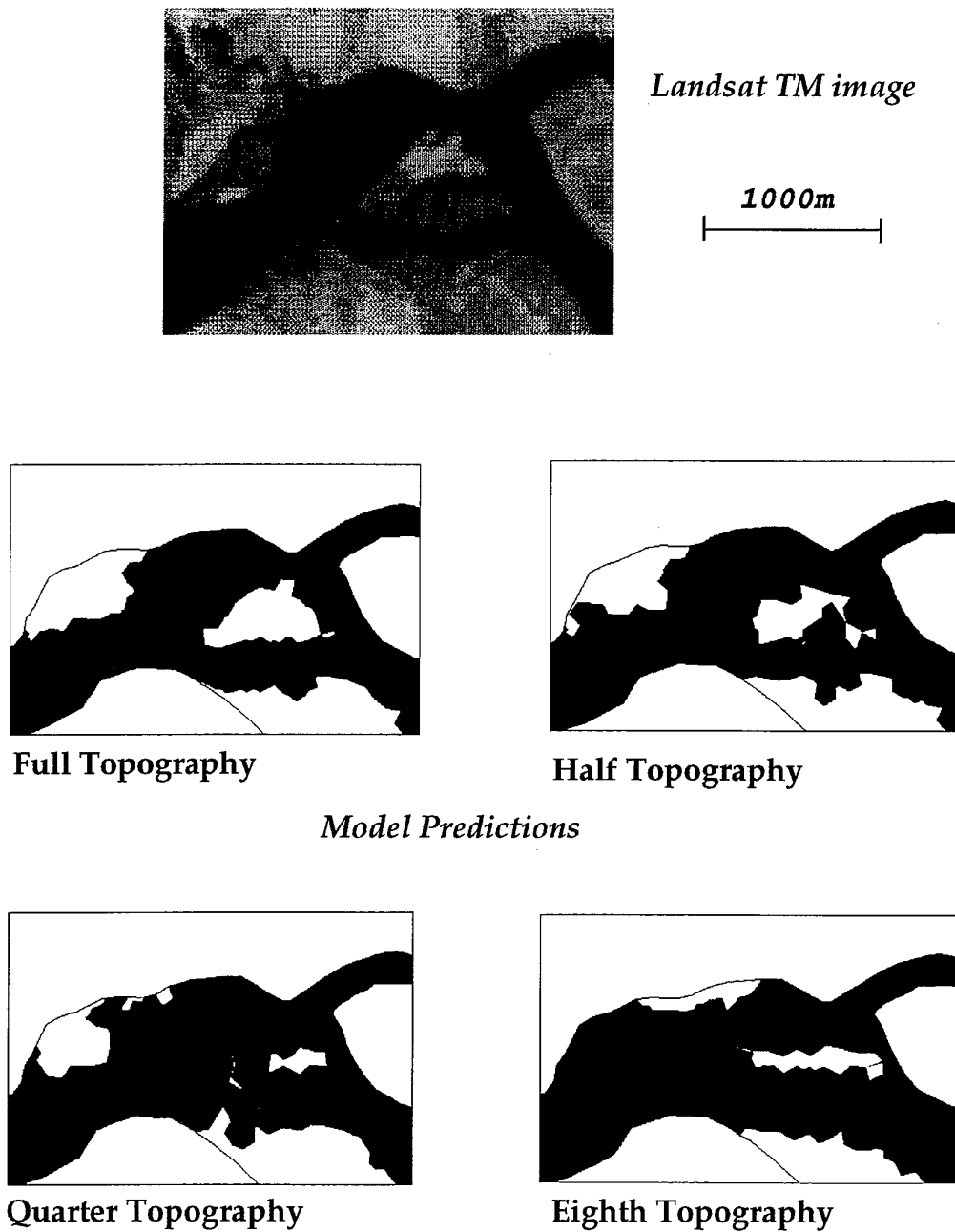


Figure 7-2c Comparison of the Landsat TM image to model predictions with the 4 levels of model bathymetry used for event 1 at site 3. The bathymetries were created by varying the spacing of cross sections used from 150 m to 1200 m.

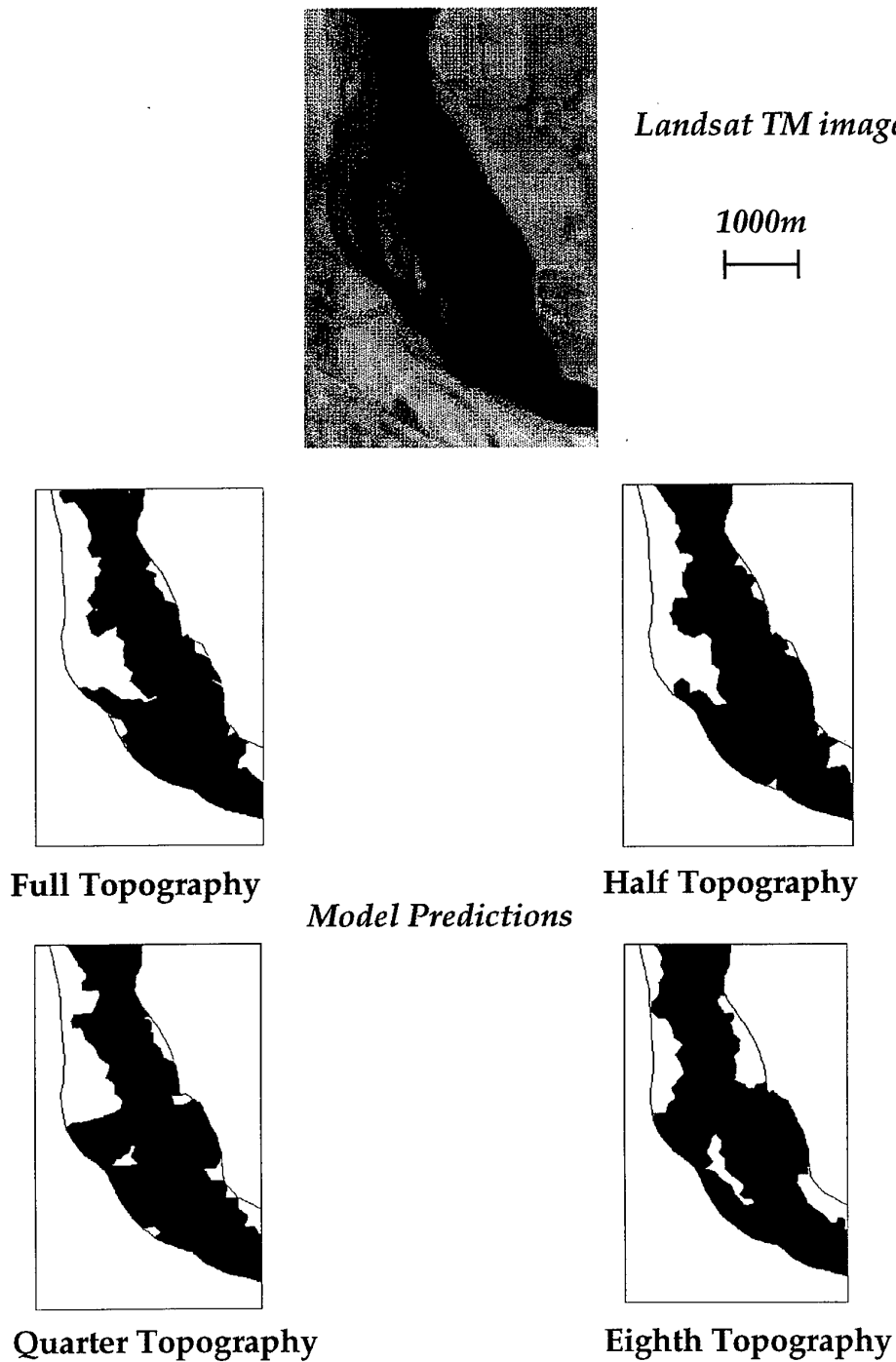
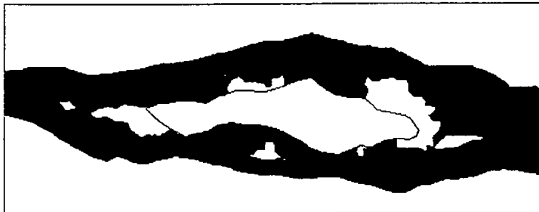


Figure 7-2d Comparison of the Landsat TM image to model predictions with the 4 levels of model bathymetry used for event 1 at site 4. The bathymetries were created by varying the spacing of cross sections used from 150 m to 1200 m.

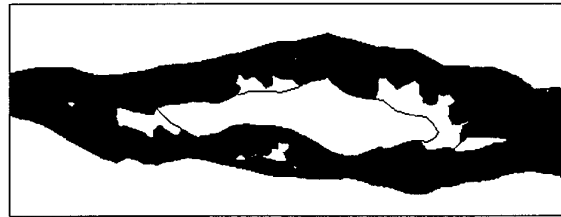


*Landsat TM image*

1000m

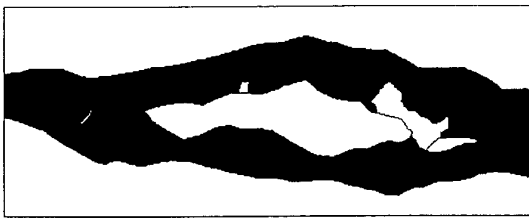


**Full Topography**

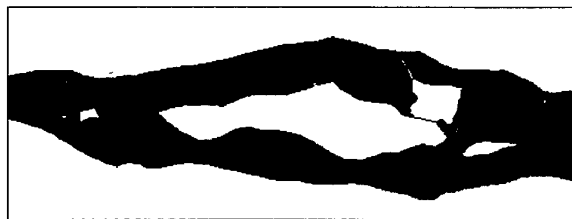


**Half Topography**

*Model Predictions*



**Quarter Topography**



**Eighth Topography**

**Figure 7-2e Comparison of the Landsat TM image to model predictions with the 4 levels of model bathymetry used for event 1 at site 5. The bathymetries were created by varying the spacing of cross sections used from 150 m to 1200 m.**



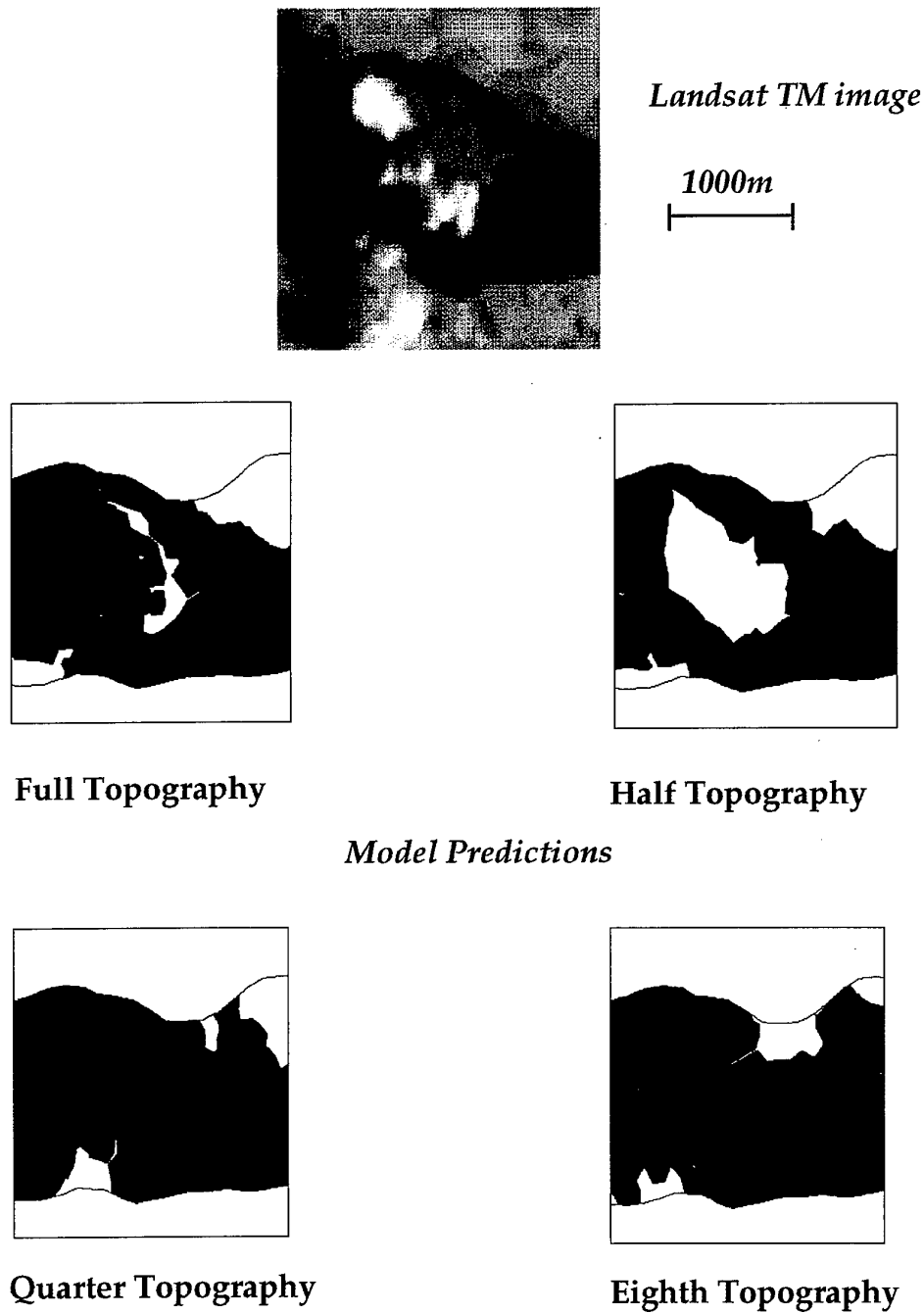


Figure 7-2f Comparison of the Landsat TM image to model predictions with the 4 levels of model bathymetry used for event 1 at site 6. The bathymetries were created by varying the spacing of cross sections used from 150 m to 1200 m.

## 8. Concluding Remarks

This modelling study of a 55 km reach of the Missouri River has illustrated the capability of high resolution, physically based fluvial hydraulic models for accurate flow representation. A hydraulic model was created for the reach of interest, between Gavins Point Dam and Maskell, using the TELEMAC-2D modelling system. A sensitivity analysis of the model showed bed friction to be the dominant parameter governing model performance. Extensive validation of the model predictions was carried out against both internal stage data and satellite imagery of flow field boundaries. Finally the impact of mesh resolution and bathymetric data provision was briefly examined.

The key findings of this study can be summarised thus:

- A state of the art two-dimensional hydraulic model can simulate fluvial hydraulics accurately on this scale in both steady state and dynamic conditions.
- Model predictions can be matched to stage data internal to the model domain with a high degree of accuracy for initial simulations (Figure 5.2). Improvements to the match could no doubt follow with further model developments.
- Spatial distribution of flow field boundaries has been shown to be accurate in most cases by comparison to satellite imagery (Landsat TM and SPOT) (Figure 5.4).
- Partial model validation has been graded by its rigour. Matching 2-D inundation data is considered more powerful than matching internal stage data, a hypothesis corroborated by model predictions with varying specifications of bathymetry (Figure 7.2 and Table 7.1).
- A degree of process validation was achieved against satellite imagery in a specific case (Figure 5.7).
- The relationship between mesh resolution and bathymetric data is vital to model specification but requires further study to quantify.

There remain however, many areas where further work could improve the model predictions.

- The fundamental complexity and connection of mesh and bathymetry is a limiting factor whilst a) only limited bathymetric data is available and b) computational expense must be considered when making meshes. Until meshes can be much more finely resolved and the bathymetric data available to apply to them at a commensurate scale then this problem of bathymetric representation and its impact on model predictions shall remain. Further data collection in specific problem areas could mitigate the problem in this specific case.
- The above problem is manifested predominantly under low flow conditions (Figure 5.8) where the bed representation is exposed more than usual.
- The model set-up used here in terms of parameters was extremely simple and as such model results were not as good as they could be following further modifications. With modification of the bed friction parameter, distributing it over time and/or space the errors particularly in internal stage could be reduced dramatically. The 2-D flow field boundaries are however more dependant on the bathymetry than the parameter distribution.
- With the knowledge gained from the simulations carried out already the model structure could be modified to include more permanent islands where they are evident and vary the mesh resolution over the domain where the gradient of predicted variables are greatest.
- Now that model validation has been somewhat structured the possibility exists for deliberate data collection in order to validate specific outputs of the model to produce as strong and complete a validation as possible. For example more 2-D process data could be collected in order to validate the most fundamental aspect of a 2-D hydraulic model.

The ever progressing capability of highly resolved 2-D fluvial hydraulic models, including flows over dry areas, opens up a wide range of potential applications that include:

- Predicting the impact of anthropogenic activity
- Flood hazard assessment
- Geomorphological and hydrological process studies
- River management schemes

This report has shown that the capability now exists for high resolution fluvial hydraulic modelling to be applied over long (>50 km) reaches with a high degree of accuracy. The use of wetting and drying algorithms allows the simulation of dynamic flows over initially dry areas and their retreat. This capability opens up a wide range of potential applications especially for the “what if” type modelling vital for controlled management and development of river systems.

## 9. References

- Baird, L. and Anderson, M.G. (1990). "Flood inundation modelling using MILHY", US Army European Research Office, Final Technical Report, DAJA 45-87-c-0053, Volume 1, 337pp.
- Bates, P.D., Anderson, M.G., Baird, L. Walling, D.E. and Simm, D. (1992). "Modelling floodplain flows using a two-dimensional finite element model", *Earth Surface Processes and Landforms*, **17**, 575-588.
- Bates, P.D., Anderson, M.G., Price, D.A., Hardy, R.J. and Smith, C.N. (1996). "Analysis and developments of hydraulic models for floodplain flows". In M.G. Anderson, D.E. Walling and P.D. Bates (eds), "*Floodplain processes*", John Wiley and Sons, Chichester, 215-254.
- Bates, P.D., Horrit, M.S., Smith, C.N. and Mason, D. (1997) "Integrating remote sensing observations of flood hydrology and hydraulic modelling", *Hydrological Processes*, (in press).
- Bathurst, J.C. (1988). "Flow processes and data provision for channel flow models". In M.G. Anderson (ed), "*Modelling Geomorphological Systems*" John Wiley and Sons, Chichester, 127-152.
- Beven, K. (1979) "A sensitivity analysis of the Penman-Montieth actual evapotranspiration estimates", *Journal of Hydrology*, **44**, 169-190.
- Beven, K.J. (1993). "Prophecy, reality and uncertainty in distributed hydrological modelling", *Advances in Water Resources*, **16**, 41-51.
- Biggin, D.S. and Blyth, K. (1996) "A comparison of ERS-1 satellite radar and aerial photography for river flood mapping", *Journal of the Chartered Institution of Water and Environmental Management*, **10(1)**, 59-64.
- Brakenridge, G.R., Knpx, J.C., Paylor, E.D. II, and Magilligan, F.J. (1994) "Radar Remote Sensing Aids Study Of The Great Flood Of 1993", *EOS, Transactions, American Geophysical Union*, **75(45)**, November 8th 1994, 521 and 526-527.
- Brooks, A.N. and Hughes, T.J.R. (1982). "Streamline upwind/Petrov-Galerkin formulations for convection dominated flows with particular emphasis on the incompressible Navier-Stokes equations", *Computer Methods in Applied Mechanics and Engineering*, **32**, 199-259.
- Cooper, A.J. (1996). "TELEMAC-2D, version 3.0 Validation Document". *Report EDF HE-43/96/006/A*, 74pp.
- Fawcett, K.R., Anderson, M.G., Bates, P.D., Jordan, J-P. and Bathurst, J.C. (1995). "The importance of internal validation in the assessment of physically based distributed models", *Transactions of the Institute of British Geographers*, **20**, 248-265.
- Hardy, R.J. (1997), Unpublished Ph.D thesis, University of Bristol.
- Hervouet, J-M, Hubert, J-L, Janin, J-M, Lepeintre, F. and Peltier, E. (1994). "The computation of free surface flows with TELEMAC - An example of evolution towards hydroinformatics". *Report EDF-LNH HE-43/94/046/A*, 34pp.

- Hervouet, J-M and Janin, J-M (1994). "Finite element algorithms for modelling flood propagation". In P. Molinaro and L. Natale (eds.), *"Modelling of Flood Propagation Over Initially Dry Areas"*, American Society of Civil Engineers, New York, 102-113.
- Hervouet, J-M. and Lang, P. (1995) "TELEMAC-2D Version 3.0 User's Manual". *Report EDF-LNH HE-43/94/070B*, 195pp.
- Hervouet, J-M. and Van Haren, L. (1995). "TELEMAC-2D Version 3.0 Principle Note". *Report EDF-LNH HE-43/94/052/B*, 90pp.
- Hervouet, J-M. and Van Haren, L. (1996). "Recent advances In numerical methods for fluid flows". In M.G. Anderson, D.E. Walling and P.D. Bates (eds), *"Floodplain processes"*, John Wiley and Sons, Chichester, 183-214.
- Howes, S. and Anderson, M.G. (1988) "Computer Simulation In Geomorphology". In M.G. Anderson(ed), *"Modelling Geomorphological Systems"* John Wiley and Sons, Chichester, 421-440.
- Imhoff, M.L., Vermillion, C., Story, M.H., Choudhury, A.M., Gafoor, A. and Polcyn, F. (1987) "Monsoon flood boundary delineation and damage assessment using space borne imaging radar and landsat data", *Photogrammetric Engineering & Remote Sensing*, **53(4)**, 405-413.
- Koblinsky, C.J., Clarke, R.T., Brenner, A.C. and Frey, H. (1993) "Measurement of river level variations with satellite altimetry", *Water Resources Research*, **29(6)**, 1839-1848.
- Konikow, L.F. and Bredehoeft, J.D. (1992). "Ground-water models cannot be validated", *Advances in Water Resources*, **15**, 75-83.
- Lane, S.N., Chandler, J.H. and Richards, K.S. (1994). "Developments in monitoring and modelling small-scale river bed topography", *Earth Surface Processes and Landforms*, **19**, 349-368.
- LaVenue, M., Andrews, R.W. and RamaRao, B.S. (1989) "Groundwater travel time uncertainty analysis using sensitivity derivatives", *Water Resources Research*, **25(7)**, 1551-1566.
- Lillesand, T.M. and Kiefer, R.W. (1987). *"Remote sensing and image interpretation"*, John Wiley and Sons, New York, 721pp.
- Marchuk, G.I. (1975). *"Methods of numerical mathematics"*. Springer-Verlag, New York 316pp.
- McCuen R.H. (1973) "The Role Of Sensivity Analysis In Hydrologic Modelling", *Journal of Hydrology*, **18**, 37-53.
- Norton, W.R., King I.P. and Orlob, G.T. (1973). "A finite element model for Lower Granite Reservoir: a report prepared for the U.S. Army Corps of Engineers, Walla Walla District, Washington.". Water Resources Engineers, Walnut Creek, California, 105pp.
- Pinder G.F. and Gray, W.G. (1977). *"Finite element simulation in surface and subsurface hydrology"*. Academic Press, New York, 295pp.
- Piro, M. (1993). "RUBENS reference manual (version 2.0)". *Report EDF-LNH HE-45/93.02*, 65pp.

Price, D.A. (1997) "An integrated approach to modelling floodplain hydraulics, hydrology and nitrate chemistry", Unpublished Ph.D. thesis, University of Bristol, 242pp.

Rango, A. and Salomonson, V.V. (1974) "Regional Flood Mapping From Space", *Water Resources Research*, **10(3)**, 473-484.

Redfern, H. and Williams, R.G. (1996) "Remote sensing: latest developments and uses", *Journal of the Chartered Institution of Water and Environmental Management*, **10(6)**, 423-428.

Samper, J., Carrera, J., Galarza, G. and Medina, A. (1990) "Application of an automatic calibration technique to modelling an alluvial aquifer". In K. Kovar (ed), "*ModelCARE 90: Calibration and reliability in groundwater modelling (Proceedings of the conference held in The Hague, September 1990)*", IAHS Publication 195, D. Reidel, Dordrecht, 87-95.

Troutman, B.M. (1985) "Errors and parameter estimation in precipitation-runoff modelling 2. Case study", *Water Resources Research*, **21(8)**, 1214-1222.

Younis, B.A. (1996). "Progress in turbulence modelling for open-channel flows". In M.G. Anderson, D.E. Walling and P.D. Bates (eds), "*Floodplain processes*", John Wiley and Sons, Chichester, 299-332.